INVESTIGATING THE NEED FOR DRAINAGE LAYERS IN FLEXIBLE PAVEMENTS

by

Masoud Seyed Mohammad Ghavami

A Dissertation

Submitted to the Faculty of Purdue University

In Partial Fulfilment of the Requirements for the Degree of

Doctor of Philosophy

Lyles School of Civil Engineering West

Lafayette, Indiana

May 2019

THE PURDUE UNIVERSITY GRADUATE SCHOOL
STATEMENT OF COMMITTEE APPROVAL

Prof. John E Haddock, Chair
Lyle School of Civil Engineering
Prof. Pablo D. Zavattieri
Lyle School of Civil Engineering
Prof. Jan Olek
Lyle School of Civil Engineering
Dr. Tommy E. Nantung
Indiana Department of Transportation

Approved by:

Dr. Dulcy Abraham
Head of the Graduate Program

Dedicated to my lovely and beautiful wife, parents and family.

ACKNOWLEDGMENTS

First, the author would like to thank my absolute gentleman advisor, Prof. John E. Haddock, for his support, patience and valuable guidance throughout this project. I would also like to thank my thesis committee members: Prof. Pablo Zavattieri, Prof. Jan Olek and Dr. Tommy Nantang for their helpful discussions, ideas, and suggestions that encouraged me to widen my research from a different perspective. Additionally, I would like to thank Dr. Maryam Hosseini, for her knowledge and contribution to this project. I would like to acknowledge the financial support of the Indiana Department of Transportation under the SPR-3807 research project.

I would like to appreciate the help and support from my colleagues and friends, Reyhaneh Rahbar, and other graduate fellows from Purdue University. Additionally, I want to thank Dr. Reza Hosseini for his admirable supports. Last but not least, I would like to thank my family for their unconditional love, encouragement, support, and prayers.

TABLE OF CONTENTS

LIST OF TABLES

LIST OF FIGURES

NOMENCLATURE

AASHTO	American Association of State Highway and Transportation Officials
ATPB	Asphalt Treated Permeable Base
DPC	Drucker-Prager/Cap
DRIP	Drainage Requirements in Pavement
FE	Finite Element
FEA	Finite Element Analysis
HMA	Hot Mix Asphalt
INDOT	Indiana Department of Transportation
NCHRP	National Cooperative Highway Research Program
OG	Open Graded
VWC	Volumetric Water Content
WCC	Water Characteristic Curves
DPC	Drucker-Prager/Cap

ABSTRACT

Author: Seyed Mohammad Ghavami, Masoud. Ph.D.
Institution: Purdue University
Degree Received: May 2019
Title: Investigating the Need For Drainage Layers In Flexible Pavements
Major Professor: John E. Haddock.

Moisture can significantly affect flexible pavement performance. As such, it is crucial to remove moisture as quickly as possible from the pavements, mainly to avoid allowing moisture into the pavement subgrade. In the 1990s the Indiana Department of Transportation (INDOT) adopted an asphalt pavement drainage system consisting of an open-graded asphalt drainage layer connected to edge drains and collector pipes to remove moisture from the pavement system. However, over the intervening two decades, asphalt pavement materials and designs have dramatically changed in Indiana, and the effectiveness of the pavements drainage system may have changed. Today, in-place field densities achieved during construction make asphalt mixtures less susceptible to moisture intrusion than their 1990s counterparts. Additionally, there are challenges involved in producing and placing open-graded asphalt drainage layers, they can potentially increase costs, and they tend to have lower strength than traditional dense-graded asphalt pavement layers.

Given the potential difficulties, the overall objective of this research was to evaluate the effectiveness of INDOT's current flexible pavement drainage systems given the changes to pavement cross-sections and materials that have occurred since the open-graded drainage layer was adopted. Additionally, the effectiveness of the filter layer and edge drains were examined. Laboratory experiments were performed to obtain the hydraulic properties of field-produced asphalt mixture specimens meeting INDOT's current specifications and the results used in finite element modeling of moisture flow through pavement sections. Modeling was also performed to investigate the rutting performance of the drainage layer in flexible pavements under various traffic loads and subgrade moisture conditions in combination with typical Indiana subgrade soils. The results were used to develop design graphs to assist the pavement designer in more accurately assessing the need for a pavement drainage system in any given flexible pavement.

In general, the results indicate that drainage layers do effectively lower the subgrade moisture content and act to maintain subgrade moisture contents at native levels, while flexible pavements without drainage layers result in fully saturated subgrades. Also, while the results show that either a dense-graded aggregate or a dense-graded asphalt mixture can be used as a filter layer between the subgrade and the open-graded drainage layer, the subgrade tends to have lower moisture content when a granular filter is used. Moreover, the results indicate that edge drains have a positive effect on flexible pavement performance, especially those that do not contain a drainage layer. As expected, the modeling results showed an increase in pavement rutting whenever high moisture levels are present in the pavement system. Finally, a series of simple design graphs were developed to suggest when the flexible pavement drainage layers are needed, and when such a layer can be safely eliminated.

CHAPTER 1. INTRODUCTION

1.1 Introduction

Moisture intrusion into flexible pavements can reduce the strength and durability of the pavement layers, resulting in moisture damage and pavements distress. Excess moisture can also enter the pavement subgrade and thereby accelerate pavement damage as a result of subgrade softening or frost action. A properly designed drainage system may help prevent excess moisture from entering the pavement layers and subgrade and reduce the chance of moisture-related damage.

In 1993, the Indiana Department of Transportation (INDOT) began building new and reconstructed pavement sections that included a drainage layer in the pavement designed to more effectively move moisture to the edge drains. Hassan and White (1996) further refined this drainage system. They recommended a dense-graded asphalt mixture be placed on the prepared subgrade to act as a filter, thus reducing moisture migration both into the subgrade from the pavement and from the subgrade into the pavement. The study also concluded that surface infiltration is the largest source of moisture entering a pavement and so an open-graded asphalt mixture layer was recommended over the dense-graded asphalt layer to serve as a drainage layer for the pavement. Moisture entering the pavement, from any direction, could thus be quickly moved to the edge drain, preventing moisture from migrating towards the subgrade.

In addition to providing adequate drainage, it is also necessary that drainage layers be structurally sound. The open-graded asphalt mixtures as a drainage layer and trench may reduce the overall flexible pavement mechanical performance. Feng et al. (1999) continued the study “Locating the Drainage Layer for Flexible Pavements" by Hassan and White (1996) to evaluate the mechanical performance of the flexible pavement sections under repeated traffic loading. They

compared several pavement sections that each included a drainage layer over a different type of dense-graded filter layer (asphalt mixture or granular) placed on the prepared subgrade. They furthur confirmed the mechanical performance for the section that had a drainage layer over a dense-graded asphalt mixture as previously suggested by Hassan and White (1996). However, they indicated a higher amount of rutting occurred for the section with the dense-graded asphalt filter, as compared to the other sections.

Over the intervening two decades, INDOT has changed design specifications and construction practices for flexible pavements. Flexible pavement materials' properties have been modified due to changes in asphalt mixture design technology. Today's asphalt mixtures are designed using the Superpave mixture design method and have higher in-place densities than those designed in the early 1990's using the Marshall mixture design method, making them less susceptible to moisture intrusion. Using the older Marshall-designed mixture and construction specification, dense-graded asphalt mixtures could be placed at densities as low as 88% of maximum theoretical density (G_{mm}) and still pass specification. Today, with the newer mixture designs and construction specifications, in-place densities are routinely 93% of G_{mm} or higher.

Additionally, INDOT's flexible pavement cross-section design has been changed. For example, today, the 2.5 in. (6.4 cm) thick drainage layer is sandwiched between two layers of dense-graded asphalt base mixture, while in the 1990s the drainage layer was much thicker and not necessarily sandwiched between two dense-graded asphalt base layers. There is also some uncertainty about the idea of placing a drainage layer over a dense-graded asphalt mixture filter layer. In the event of capillary rise, moisture moving from the subgrade (subsurface moisture) toward the pavement could be trapped under the bound dense filter layer, preventing it from reaching the drainage layer and thereby reducing the drainage system effectiveness.

Moreover, the flexible pavement drainage mechanical performance study by Feng et al. (1999) did not consider the effect of the subgrade moisture condition beneath pavements. Therefore, concern developed over the rutting characteristics of the open-graded drainage layers in flexible pavements varying in the subgrade moisture and traffic loads conditions.

Finally, the open-graded asphalt mixtures may reduce the overall flexible pavement structural capacity thereby at least partially invalidating the benefit of using the newer mixture designs and construction specifications. Also, the construction of open-graded asphalt mixtures layers can be challenging. Open-graded asphalt mixtures can often be difficult to handle and compact. Additionally, current INDOT specifications require that a PG 76-22 asphalt binder be used in all open-graded asphalt mixtures. Typically, this is a modified binder that costs substantially more than a unmodified binder, thus increasing the overall pavement cost.

1.2 Background

Moisture can easily find its way into flexible pavements through cracks, shoulders, and groundwater sources. This moisture, accompanied by traffic loads and freezing temperatures, can have detrimental effects on flexible pavement performance (Diefenderfer et al., 2005). A properly designed drainage system can help prevent excess moisture from entering the subgrade and thereby reduce the damage that can be caused by subgrade softening and frost action. The effectiveness of the drainage system is a key element influencing long-term flexible pavement performance, as evidenced by many studies (Fleckenstein & Allen, 1996; Hall & Correa, 2003; Ji & Nantung, 2015; Liang, 2007; Smith et al., 1970). Research indicates that flexible pavements with adequate drainage systems have up to three times longer service lives than those without (Cedergren, 1988). A report by Harrigan (2002) presented the positive effect of an edge drain, even for undrained

pavements; installing edge drains in flexible pavements having no drainage layer led to decreased fatigue cracking and a more cost-effective design.

Conversely, several studies have reported the failures or disadvantages of pavement drainage systems (Ahmed et al. 1993; Wyatt & Macari, 2000). However, the failures reported in these works were mainly due to improperly designed or poorly constructed drainage systems or due to the contractors failing to follow the specifications (Ghavami, 2014). Additionally, improper drainage maintenance caused the systems to trap moisture inside the pavement structures, thereby accelerating pavement damage. In some cases the poor drainage systems caused more damage to the pavement than if no drainage system had been present (Hall & Correa, 2003).

The longer moisture remains in a flexible pavement structure, the more likely pavement failure will occur. The continuous presence of moisture in the pavement subgrade can significantly affect the subgrade moduli and reduce pavement performance. Work by Ji and Nantung (2015) found that increasing pavement subgrade moisture content 2 percent above optimum moisture content resulted in a subgrade resilient modulus reduction by as much as 25 percent. Arika et al. (2009) found that subgrade moisture contents 8 percent above optimum can result in a 50 percent decrease in pavement life, or a 32 percent increase in construction costs. Conversely, Zaghloul et al. (2004) found that reducing the moisture content in a flexible pavement base course from 45 to 16 percent can increase the flexible pavement service life from 7 to 13 years. Research has also indicated lower moisture in pavement subgrades when edge drains are used. Fleckenstein and Allen (1996) reported that pavements with edge drains had 28 percent less moisture in their subgrades when compared to similar pavements without edge drains. Pavements containing edge drains would, therefore, tend to have higher subgrade strengths and longer service lives.

1.3 Problem Statement and Objective

Given the importance of flexible pavement drainage layers, filter layers, and edge drains, along with changes to INDOT's standard flexible pavement cross section and material design over the past 20 years, this research sought to evaluate the effectiveness of the currently designed flexible pavement drainage system using the newer cross-sections and materials. Specifically, the effect of a pavement drainage layer was investigated to see if such a layer acts to reduce pavement subgrade moisture. Also, the effect of filter material type was examined to determine its effect on the pavement subgrade moisture. Moreover, the effectiveness of edge drains in flexible pavements without a drainage layer was studied. Finally, the rutting characteristics of the open-graded drainage layers were examined under various traffic loads and subgrade moisture conditions. Accordingly, the objectives of this research were:

1. Using finite element analyses, investigate moisture flow through flexible pavements to evaluate the subgrade moisture conditions after a specific rainfall event and how it affects pavement performance;
2. Evaluate the effectiveness of flexible pavement drainage systems containing currently specified materials to determine if the open-graded asphalt mixture drainage layer is still relevant in current flexible pavements;
3. Determine the combined effects of traffic loads coupled with moisture infiltration on flexible pavements placed over various subgrade soil types and having various saturation conditions;
4. Develop a simple design graph to suggest when the flexible pavement drainage layers are needed, and when such a layer can be safely eliminated.
5. Develop a field validation and long-term monitoring plan for flexible pavement drainage systems.

CHAPTER 2. LITERATURE REVIEW

2.1 Sources of Moisture

Moisture can infiltrate pavements through various sources such as surface infiltration, rising groundwater, seepage from higher ground, capillary action and vapor movement (Figure 2-1). Surface moisture infiltration through cracks is the primary and largest source of moisture infiltration in pavements (Hassan & White, 1996).

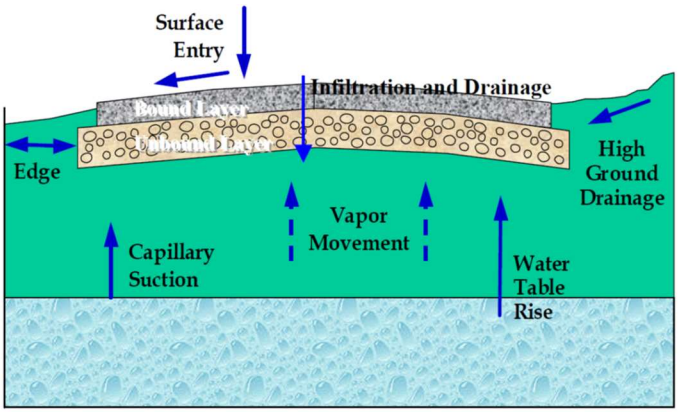

Figure 2-1 Sources of moisture in pavements (Apul et al., 2002)

2.2 Pavement Drainage Systems

Drainage systems in flexible pavements often include an open-graded layer (usually stabilized), a filter layer and a moisture collection system (underdrain) that may include outlet pipes to remove moisture from the pavement. The filter layer is placed under the drainage layer and acts as a separator to prevent fine subgrade particles from moving into the overlying drainage layer to avoid clogging (Diefenderfer et al., 2005). There are two common types of drainage layer systems in pavements, a permeable layer combined with longitudinal collectors (outlet pipe), and a daylighted permeable layer without outlet pipes (Figure 2-2). Huang recommended using a combination of

the two as the most efficient method to collect and remove moisture from pavement in the shortest possible drain time (Huang, 1993).

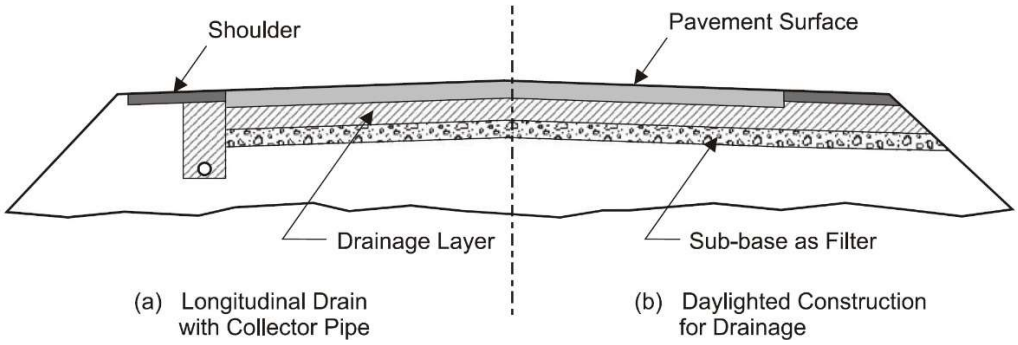

Figure 2-2 Typical pavement drainage system components (Huang, 1993)

2.3 INDOT Flexible Pavement Drainage Design

A typical INDOT full-depth asphalt pavement with a drainage layer and underdrain is shown in Figure 2-3. INDOT recommends placing an open-graded (OG) asphalt mixture drainage layer near the bottom of the pavement, sandwiched between two dense-graded base layers, or between intermediate and base layers. A new asphalt pavement usually has an asphalt surface course, on an asphalt intermediate course, on either an asphalt base or a compacted aggregate base layer, placed directly on a prepared subgrade. INDOT also recommends the thickness of 2.5 in. for an open-graded drainage layer with a typical lay rate of 250 lbs./yd^2 per inch. Additionally, a dense-graded base mixture is required under the open-graded layer, and underdrains must be included (Indiana Design Manual, 2016). This dense-graded mixture layer acts as a filter to prevent fine subgrade particles from moving into the overlying drainage layer, as well as to reduce moisture migration into the subgrade and to provide support for construction traffic when placing overlying layers (Hassan & White, 1996).

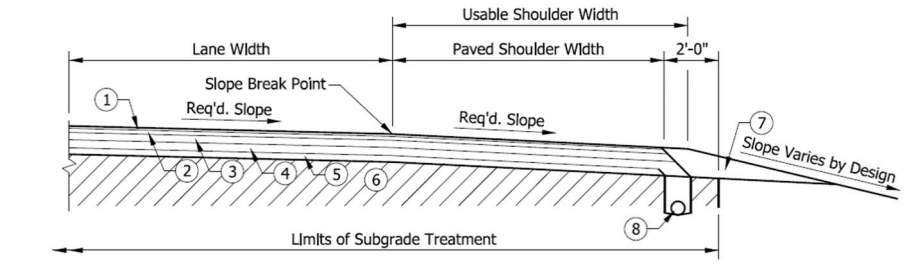

NOTES:

1. 165 lb/yd² HMA Surface 9.5 mm
2. ___ lb/yd² HMA Intermediate
3. ___ lb/yd² HMA Base
4. ___ lb/yd² QC/QA-HMA Intermediate OG
5. ___ lb/yd² HMA Base
6. Subgrade Treatment, Type _____
7. Variable-Depth Compacted Aggregate, No. 53
8. Underdrain. See Figure 304-21 I for detail.

* See Figure 304-21D for lay rate.

9. Safety edge as required for Surface and Intermediate layers. See Figure 304-21X for detail.
10. Longitudinal joint adhesive required for Surface and Intermediate layers.
11. Liquid Asphalt Sealant required on Surface layer over longitudinal joint, 24" width.
12. Base seal is required under all open-graded HMA layers.
13. Configuration for median shoulder is the same as for an outside shoulder except width and slope.

a)

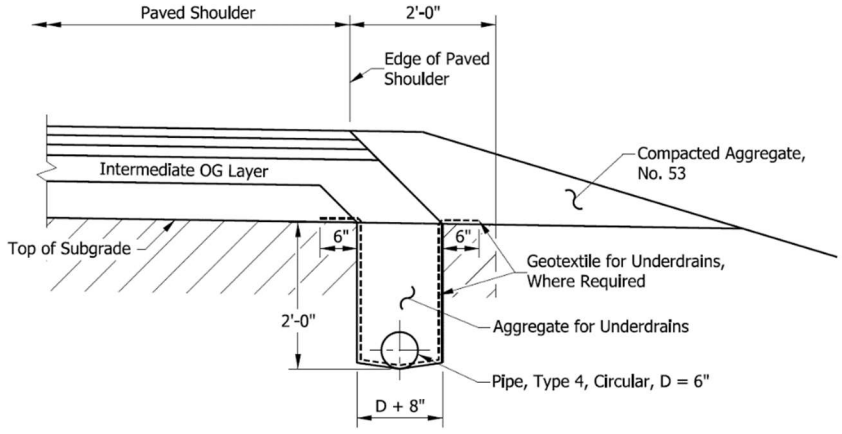

b)

Figure 2-3 a) Full-depth flexible pavement with drainage layer, and b) detailed underdrain view (Indiana Department of Transportation, 2013) – updated 2018

2.4 Assessing the Need for Pavement Drainage

As previously stated, pavement drainage system can vary in their effectiveness. Construction and life cycle costs can play a role; the drainage should be only used whenever it is expected to be cost-effective by reducing moisture-related pavement problems. Therefore, identifying the need for pavement drainage, while often complicated and dependant on many factors, becomes very important to successful pavement performance.

Indiana has a wet-freeze climate, defined as a climate having annual precipitation higher than 508 mm and experiencing freeze cycles. Such climates have a higher probability of moisture in the pavement structure throughout the year. The National Cooperative Highway Research Program (NCHRP) 1-37A report (NCHRP, 2004) suggests a drainage system be considered for any flexible pavement built in a wet-freeze climate condition with a subgrade permeability less than 3 m/day, a common condition in much of Indiana (Table 2-1).

In Table 2-1, “R” indicates that pavement drainage is recommended to prevent moisture-related problem. In this situation, the pavement drainage system will improve pavement performance to a degree that makes it cost-effective. Those cells marked with “F” indicate situations where providing drainage is feasible, but the cost-benefit analysis should be considered. Lastly, the “NR” rating implies that drainage is not recommended because it is likely not cost effective. While the recommendations in Table 2-1 are valuable, they should be calibrated to reflect local experience, in order to achieve the best result.

Table 2-1 Pavement drainage need assessment (NCHRP, 2004)

Climatic Condition	Greater than 12 million 20-yr design lane heavy trucks			Between 2.5 and 12 million 20-yr design lane heavy trucks			Less than 2.5 million 20-yr design lane heavy trucks		
	$k_{subgrade}$ (m/day)								
	< 3	3 to 30	> 30	< 3	3 to 30	> 30	< 3	3 to 30	> 30
Wet-Freeze	R	R	F	R	R	F	F	NR	NR
Wet-No Freeze	R	R	F	R	F	F	F	NR	NR
Dry-Freeze	F	F	NR	F	F	NR	NR	NR	NR
Dry-No Freeze	F	NR	NR	NR	NR	NR	NR	NR	NR

LEGEND:

$k_{subgrade}$ = Subgrade permeability.

R = Some form of subdrainage or other design features are recommended to combat potential moisture problems.

F = Providing subdrainage is feasible. The following additional factors need to be considered in the decision making:

1. Past pavement performance and experience in similar conditions, if any.
2. Cost differential and anticipated increase in service life through the use of various drainage alternatives.
3. Anticipated durability and/or erodibility of paving materials.

NR = Subsurface drainage is not required in these situations.

Wet Climate = Annual precipitation > 508 mm (20 in.)

Dry Climate = Annual precipitation < 508 mm (20 in.)

Freeze = Annual freezing index > 83 °C-days (150 °F-days)

No-Freeze = Annual freezing index < 83 °C-days (150 °F-days)

2.5 Drainage System Effectiveness in Flexible Pavements

A properly designed pavement drainage system will prevent excess moisture from entering the subgrade and thereby reduce the possibility of subgrade softening, or damage from frost action.

This can result in lower maintenance cost and longer pavement life. Conversely, the continuous presence of moisture in the pavement system, accompanied by heavy vehicle loads can result in major flexible pavement distresses, such as alligator cracking and potholes.

Open-graded drainage layers that rapidly drain excess moisture from pavement structures were introduced in the early 1970s. (Smith et al., 1970) performed field permeability tests to compare the drainage performance of two pavement sections. One section consisted of an asphalt pavement over a two-layer drainage blanket (asphalt treated permeable material over a well-graded aggregate layer), while the other was an asphalt pavement over a layer of permeable base course material. Results indicated both sections could successfully drain all subsurface water.

Pavement drainage effectiveness when edge-drains are used has also shown moisture reductions in the pavement subgrade. (Fleckenstein & Allen, 1996) reported that pavements with edge-drains had 28 percent lower moisture in their subgrades. Pavements with edge-drains would therefore tend to have higher subgrade strengths and longer service lives.

A visual survey performed on several drained and undrained flexible pavement sections in Indiana found few surface distresses in the drained pavements (Ji & Nantung, 2015). The study also performed a cost-benefit analysis to define the benefits of subsurface drainage on initial construction costs in Indiana. The results were based on the 2005 Indiana Department of Transportation Cost Index. It was concluded that with a properly designed and installed pavement drainage layer, approximately $40,000 to $60,000 per lane-mile could be saved over the pavement's life, for pavements with traffic levels of 10 to 30 million Equivalent Single Axle Loads (ESAL). This result shows the potentially substantial benefits of subsurface drainage on initial construction costs of asphalt pavements in Indiana (Ji & Nantung, 2015).

(Harrigan, 2002) reported on life-cycle cost analyses conducted on several flexible pavement sections to study the effectiveness of drainage systems. The pavement sections studied included a conventional, undrained asphalt layer over an undrained base layer (unbound dense aggregate base course) or a permeable aggregate base layer. A number of sections were designed with either edge-drains or day-lighted drainage systems. Results indicated the least cost-effective design was the one with an undrained base layer, due to increased fatigue cracking. Installing an edge-drain in this pavement decreased fatigue cracking and led to a more cost-effective design. The section with a permeable aggregate base layer resulted in a more cost-effective design while the most cost-effective design was the flexible pavement section with a day-lighted permeable aggregate base (Harrigan, 2002). These results indicate that flexible pavements with drainage systems tend to have longer lives and lower preservation costs.

In addition to providing adequate drainage, it is also necessary that drainage layers be structurally sound. Providing a flexible pavement with a drainage layer may reduce the pavement structural capacity. (Harrigan, 2002) stated that structural capacity and drainability of flexible pavements are two key elements in flexible pavement performance and that lack of either may lead to rutting and fatigue cracking. Therefore, both drainability performance and drainage structural capacity should be balanced to achieve the best flexible pavement performance for pavements with a drainage system. Pavement sections with asphalt-stabilized permeable bases and edge-drains showed the best rutting and fatigue performance in the study. Additionally, it was found that keeping edge-drain outlets open during the service life led to increased pavement performance. Clogged outlets result in increased pavement fatigue cracking and rutting (Harrigan, 2002).

In another study, Hall and Correa (2003) also found that drained pavement sections with permeable asphalt-treated bases had better performance than undrained pavement sections with

dense-graded aggregate bases. The results indicated that edge-drains in dense-graded base sections had minimal or no effect in improving rutting performance.

Liang (2007) evaluated different drainable base materials under flexible pavements in Ohio. Six types of bases (four unbound aggregate bases and two bound bases) were tested in the laboratory to define their mechanical properties including resilient modulus, strength and permanent deformation under cyclic loads, durability, and permeability. Additionally, for several asphalt pavement sections, field moisture monitoring was performed. The results showed no evidence of completely saturated subgrades under the drainable bases. Additionally, the bound base materials including Portland cement and asphalt treated bases showed better drainage efficiency than untreated bases. The cement treated base layer exhibited the best combination of drainability, resilient modulus, and resistance to permanent deformation.

While a good deal of the literature indicates the efficacy of drainage layers in flexible pavements, several studies have reported the failure and disadvantages of pavement drainage systems. Ahmed et al. (1993) evaluated the effect of edge-drains on pavement performance in Indiana and discovered poor edge-drain system performance, mainly due to poor construction practices and lack of proper inspection and maintenance.

Bejarano and Harvey (2002) used a heavy vehicle simulator (HVS) to apply traffic and investigate the performance of drained and undrained flexible pavements under wet conditions. They assigned an asphalt-treated permeable base (ATPB) as the drainage layer for the drained pavement sections. During the study, the ATPB had a short life due to asphalt stripping from the aggregate under the combined conditions of a wet base and heavy loading. The researchers found the ATPB layer clogged with fines from the underlying layer, thus trapping moisture in the layer and resulting in a saturated condition. However, similar service lives were found for both drained

and undrained pavement sections. The drainage layer ATBP pavement sections failed due to permanent deformation (rutting) resulting from the stripping; the undrained sections failed due to fatigue cracking.

The effectiveness of flexible pavement subsurface drainage systems depends on their design adequacy; the subsurface drainage of a drainable pavement must be designed based on an approved design methodology and be capable of handling the expected rate of moisture inflow to the pavement system. Wyatt and Macari (2000) reported several drainable pavement sections with edge drains that were not able to successfully drain moisture. The presence of a subsurface drainage system does not necessarily assure a drainable pavement system. Improperly designed or poorly constructed drainage systems, or those not properly maintained can often trap moisture inside the pavement structure thereby accelerating pavement damage, sometimes even more so than if no drainage system had been constructed. This excess water will reduce pavement life and result in increased pavement maintenance costs (Arika et al., 2009).

2.6 Flexible Pavement Rutting

Rutting (permanent deformation), a surface depression in the wheel paths, is one of the prevalent flexible pavement distresses. Rutting is the accumulation of the irretrievable strains due to the application of the repeated tire loads on flexible pavements. Excessive rutting can reduce the pavement service life and result in an unsafe driving condition particularly when water accumulates in the wheel path during freezing weather condition. Therefore, it is essential to examine the rutting behavior of flexible pavements, especially when the pavement has a drainage layer. In one study, White et al. (2002) considered the rutting failure limits to be 6.25 mm (0.25

in.) for asphalt layers and 12.5 mm (0.50 in.) for the total pavement rutting. INDOT currently specifies the maximum allowable total rutting of 10 mm (0.4 in.) for flexible pavements.

2.6.1 Cause of rutting

There are two primary causes of rutting in flexible pavements, one related to the asphalt materials, the other related to non-asphalt material layers. In the first case, poor asphalt mixture design or deficient construction practices may result in higher amounts of rutting. In the second scenario, rutting may result from an insufficient structural capacity of one or more pavement layers, such as the subgrade for example (Sivasubramaniam & Haddock, 2005; Tam & Tam, 2006).

Two types of rutting can occur in an asphalt pavement layer (Sivasubramaniam & Haddock, 2005), consolidation (densification), shear deformation (plastic flow), or both. Consolidation refers to the reduction of asphalt mixture air voids due to the application of traffic loads, resulting in the depression in the wheel path with no uplift of the asphalt layer (Figure 2-4). Shear deformation refers to the longitudinal depression in the wheel paths accompanied by uplift (upheavals) between and on the outsides of the wheel paths (Figure 2-5). Shear deformation causes about 90% of asphalt pavement rutting, while consolidation accounts for approximately 10% (Onyango, 2009). Shear deformation is the primary factor causing rutting on the surface of flexible pavements constructed with sufficient underlying support (Sivasubramaniam & Haddock, 2005).

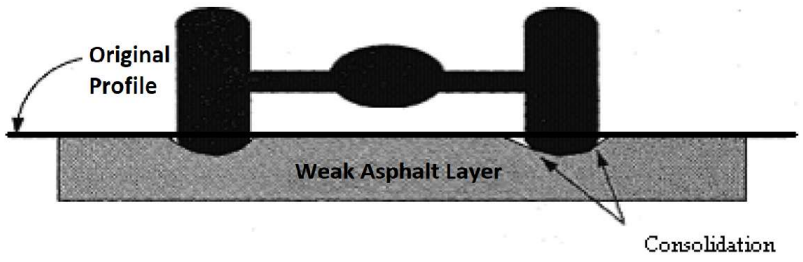

Figure 2-4 Permanent deformation from consolidation/densification (Onyango, 2009)

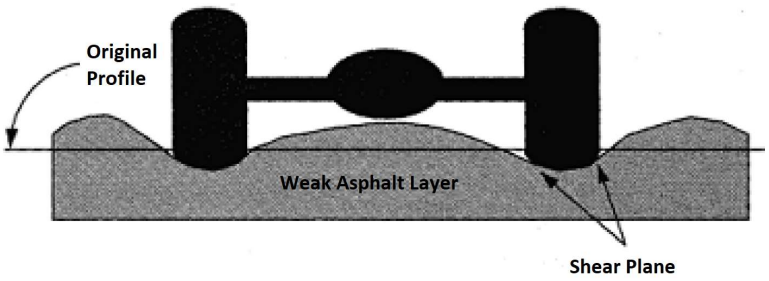

Figure 2-5 Pavement rutting from weak mixture, induced by traffic loading (Onyango, 2009)

The rutting that occurs from shear deformation indicates a low shear strength asphalt mixture resulting in a downward and lateral movement of the mixture. The Mohr-Coulomb equation (2.1), along with triaxial testing can successfully characterize the shear strength of asphalt materials (Feng et al., 1999; McGennis et al., 1995).

$$\tau = c + \sigma \tan\phi \tag{2.1}$$

where:

$\tau =$ shear strength of the mixture,

$c =$ mixture cohesion,

$\sigma =$ normal stress to which the mixture is subjected, and

$\phi =$ angle of internal friction.

2.7 Asphalt Mixture Mechanical Constitutive Models

Asphalt mixtures are visco-elasto-plastic materials (Quintus, 1994) that when repeatedly loaded exhibit elastic, plastic, visco-elastic and visco-plastic strain responses. Elastic and visco-elastic strains are recoverable, but plastic and visco-plastic strains are irrecoverable and result in

permanent deformation (rutting). Plastic strain is time independent while visco-plastic strain (creep) is time dependent; at a constant stress level, visco-plastic strain increases with time.

In finite element modeling using ABAQUS software, the extended Drucker-Prager yield surface defines the plastic strain, while the creep power-law constitutive model defines the creep strain, representing the time, temperature, and stress-dependent nature of asphalt mixture (Feng et al., 1999; Hua, 2000; Huang, 1995; Pan, 1997; Sivasubramaniam & Haddock, 2005). The quasi-static analysis procedure ("VISCO" step) can be used to analyze both the extended Drucker-Prager and the Power-law creep models. The extended Drucker-Prager yield surface (Figure 2-6) is defined as (ABAQUS, 2016):

$$F = t - p\,tan\,\beta - d = 0, \tag{2.5}$$

where:

$$t = \tfrac{1}{2} q\left[1 + \frac{1}{K} - \left(1 - \frac{1}{K}\right)\left(\frac{r}{q}\right)^3\right], \tag{2.3}$$

p = first stress invariant (equivalent pressure stress);

q = second stress invariant (Von Mises equivalent stress);

r = third stress invariant;

$d = [1 - \tfrac{1}{3}\tan\beta]\sigma_c^o$ (measure of cohesion, usually a function of plastic strain to provide isotropic hardening or softening);

$\sigma_c^o = 2c\dfrac{\cos\phi}{1-\sin\phi}$ (uniaxial compression yield stress);

c = cohesion (can be obtained directly from triaxial tests);

ϕ = friction angle from triaxial test (can be obtained directly from triaxial tests);

β = angle of internal friction: $\tan\beta = \frac{3\sin\phi}{3-\sin\phi}$; and

$K = \frac{3-\sin\phi}{3+\sin\phi}$, ratio of yield stress in triaxial tension to triaxial compression, $K \geq 0.778$ and $K < 1.0$ to ensure yield surface is convex (See Figure 2-7).

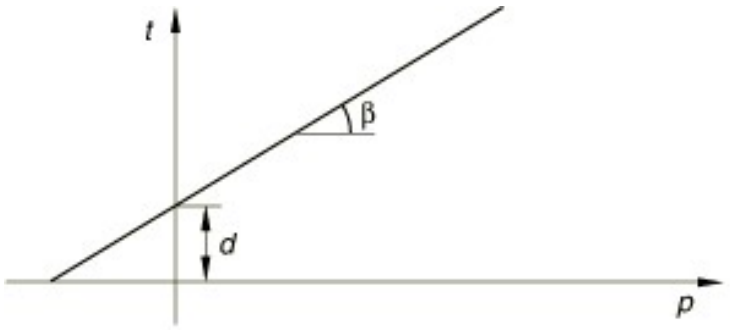

Figure 2-6 Extended Drucker-Prager model yield surfaces in the p–t plane (ABAQUS, 2016)

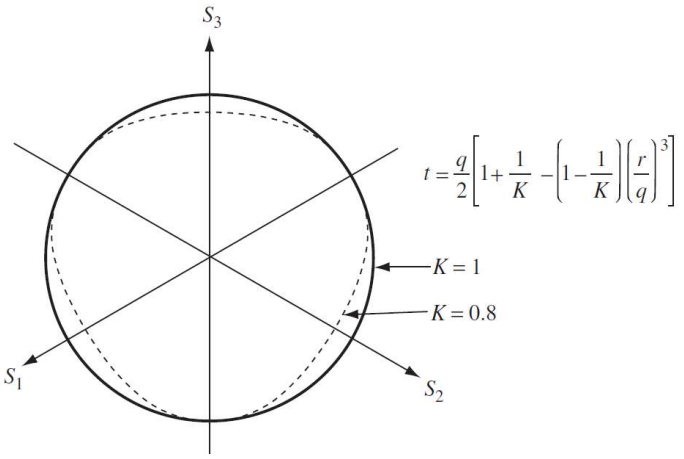

Figure 2-7 Typical yield/flow surfaces in the deviatoric plane (ABAQUS, 2016).

The creep power-law material model is defined as (Feng et al., 1999):

$$\varepsilon^{o} = A\sigma^{n}t^{m} \tag{2.4}$$

where:

ε^{o} = creep strain rate;

σ = uniaxial equivalent deviator stress;

t = time; and

A, n and m = temperature dependent constants.

2.8 Modified Drucker-Prager/Cap Model

The modified Drucker-Prager/Cap (DPC) plastisity model has been extensively used for a variety of geotechnical problem because it accounts for the effects of stress history, stress path, dilatancy, and intermediate principal stress. The DPC model adds an additional cap yield surface to the Extended Drucker-Prager plasticity model for two main reasons. First, the addition of the cap restricts the yield surface in hydrostatic compression, thus delivering an inelastic hardening mechanism to represent plastic compaction. Second, the cap controls volume dilatancy when the material yields in shear by providing softening as a function of the inelastic volume increase (ABAQUS, 2016; Helwany, 2007).

In the ABAQUS software, the DPC model is defined in the equivalent pressure stress–deviatoric stress plane (p-t plane) by three main parts: a Drucker‑Prager shear failure surface (F_s), an elliptical cap yield surface (F_c) that intersects the mean effective stress axis at a right angle, and a transition Surface (F_t) that is the region between the shear failure surface and the cap yield surface (see Figure 2-8).

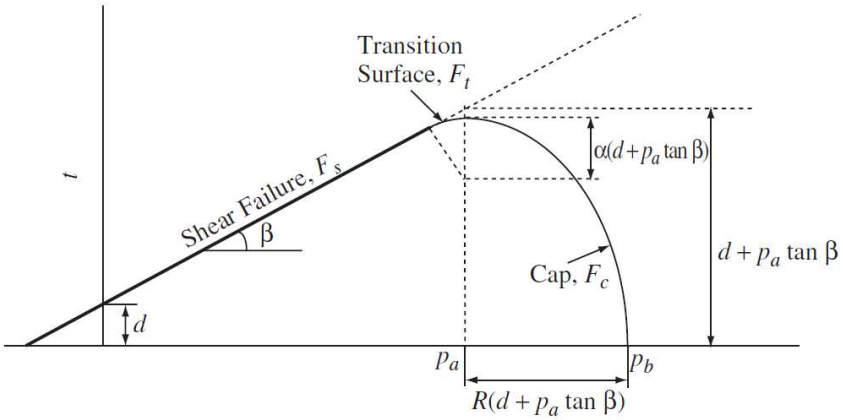

Figure 2-8 Modified Drucker-Prager/Cap model yield surfaces in the p–t plane (ABAQUS, 2016; Helwany, 2007)

$$F_s = t - p\tan\beta - d = 0 \tag{2.5}$$

$$F_c = \sqrt{(p - p_a)^2 + \left(\frac{Rt}{1+\alpha-\alpha/\cos\beta}\right)^2} - R(d + p_a \tan\beta) = 0, \tag{2.6}$$

where:

R = a material parameter that controls the shape of the cap;

α = numerical parameter (typically, 0.01 to 0.05) defining a smooth transition yield intersection between the cap and failure surface; and

p_a = an evolution parameter that controls the hardening/softening behavior as a function of the volumetric plastic strain;

The hardening/softening law is a user-defined piecewise linear function relating the hydrostatic compression yield stress (p_b) and volumetric inelastic strain as indicated in (2.7).

$$F_t = \sqrt{(p - p_a)^2 + \left[t - \left(1 - \frac{\alpha}{\cos\beta}\right)(d + p_a \tan\beta)\right]^2} - \alpha(d + p_a \tan\beta) = 0, \tag{2.7}$$

2.9 Moisture Flow Through Pavements

Figure 2-9 is a diagram indicating how moisture infiltrates and can be removed from flexible pavements with drainage systems (permeable base with edge drain). Two moisture flow conditions can occur (not simultaneously), saturated and unsaturated. Saturated flow condition refers to the situation when all pores in a layer are filled with moisture, resulting in a constant hydraulic conductivity (K). Unsaturated flow condition occurs when some, but not all pores in a layer medium are filled with moisture. This condition leads to a variable hydraulic conductivity that is a function of pore pressure. The unsaturated hydraulic conductivity decreases quickly as pore water content decreases (Tindall et al., 1999). The unsaturated hydraulic conductivity function and water characteristic curves are two key parameters for the unsaturated analysis of moisture flow through flexible pavements.

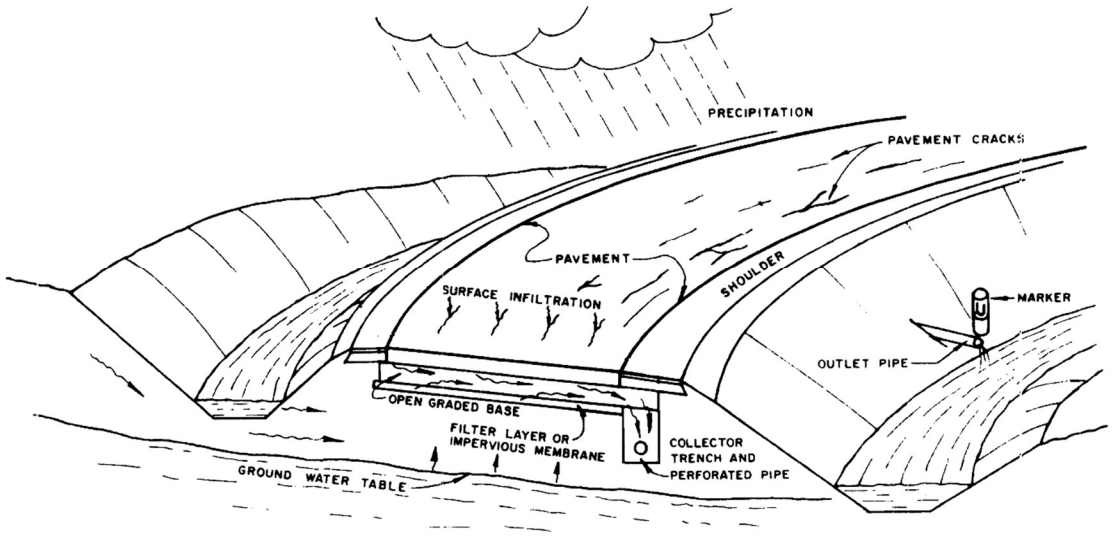

Figure 2-9 Moisture movement through a flexible pavement with drainage system (Cedergren, O'Brien, & Arman, 1972)

2.10 Saturated Hydraulic Conductivity (Saturated Permeability)

Hydraulic conductivity is the rate at which a porous material will convey or transport moisture under a hydraulic gradient (Kanitpong et al. 2001). Darcy introduced an equation that describes the flow during a saturated condition. Known as Darcy's Law, the equation (2.8) relates the moisture flow rate to the hydraulic gradient, permeability and the area of the material (Vivar & Haddock, 2006; FHWA, 1992):

$$Q = kiA \tag{2.8}$$

where:

Q = flow rate (cm^3/s);

k = coefficient of permeability (or simply permeability) (cm/s);

i = hydraulic gradient (cm/cm); and

A = total cross-sectional area (cm^2).

"The equation assumes a homogeneous material, with steady state, laminar, one-dimensional flow conditions, the fluid is incompressible, and the material completely saturated (Vivar & Haddock, 2006; FHWA, 1992)."

Permeability can be determined by theoretical design equations using laboratory and field test data. There are several equations for calculating the permeability of porous materials based on their grain size distribution. These include Hazen's equation (2.9a), Sherard's equation (2.9b), and the Moulton equation (2.9c) (Vivar and Haddock, 2006; FHWA, 1992)

$$\mathrm{K} = \mathrm{C}\mathrm{D}_{10}{}^{2} \tag{2.9a}$$

$$\mathrm{K} = 0.35\mathrm{C}\mathrm{D}_{15}{}^{2} \tag{2.9b}$$

$$\mathrm{K} = \frac{6.214*10^{5}(\frac{\mathrm{D}_{10}}{25.4})^{1.478}*\mathrm{n}^{6.654}}{(\mathrm{P}_{200})^{0.597}} \tag{2.9c}$$

These equations are dependent on effective size (D_x), porosity (n) and percent passing the 0.075 mm (No. 200) sieve (P_{200}). D_x represents the particle size (mm) than which x percent by dry mass of the sample is smaller, and C is an empirical coefficient ranging from 1 to 1.5.

2.11 Laboratory Determination of Saturated Permeability

Two common methods are available to determine permeability, a constant head permeability test used for coarse aggregates, and a falling-head permeability test used for fine aggregates. For compacted asphalt mixtures, the falling-head permeability test is preferred, and the Florida Department of Transportation (FDOT) developed a permeability test device to measure the saturated permeability of compacted asphalt mixture samples. According to this falling head method, the time required for a sample to lose a head of water is measured and used to determine the sample's permeability (Haddock and Vivar, 2006). The coefficient of permeability, k, can be determined using equation 2.10 which is based on Darcy's law. Initial head (h_1) and final head (h_2) are as shown in Figure 2-10.

$$K = \frac{aL}{At} \times \ln\frac{h_1}{h_2} \times t_c \tag{2.10}$$

where:

K = coefficient of permeability (cm/s);

L = average thickness of the test specimen (cm);

A = average cross-sectional area of the test specimen (cm^2);

t = elapsed time between h_1 and h_2 (s);

a = inside cross-sectional area of the buret (cm^2);

h_1= initial head across the test specimen (cm);

h_2= final head across the test specimen (cm); and

t_c = temperature correction for water viscosity.

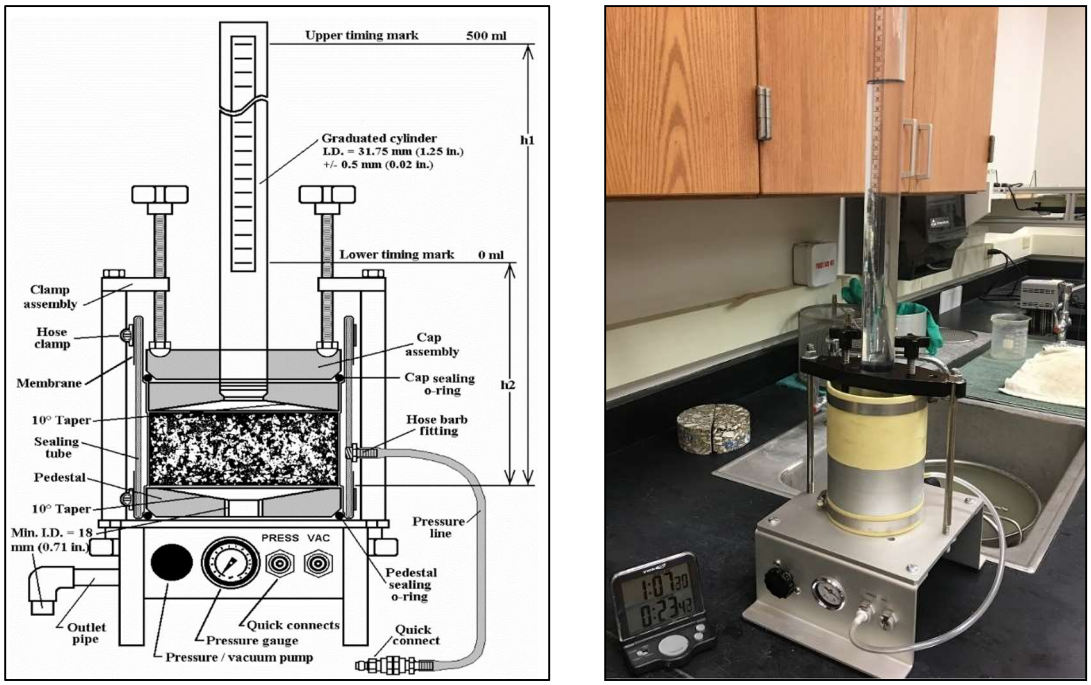

Figure 2-10 Permeability testing apparatus

2.12 Saturated and Unsaturated Pavement Drainage Design

The FHWA (1992) has recommended two approaches to design pavement drainage in fully saturated flow conditions, steady-state flow and time-to-drain. In the steady-state approach, a uniform flow condition in the pavement is assumed, and the permeable base continuously drains the rainfall into the edge drain system. For this approach, it is important to accurately estimate the design rainfall rate and the amount of rainfall that infiltrates the pavement.

In the time-to-drain approach, moisture begins to infiltrate the pavement when the rainfall event begins and continues infiltrating the pavement until the permeable base layer becomes saturated. Once this occurs, additional moisture is unable to enter the pavement system and instead will flow off the pavement surface. When the rainfall event ends, the permeable base immediately begins to drain by moving the infiltrated moisture to the edge drain system (FHWA, 1992). This

method specifies a specific time by which a given percentage of the moisture should be drained from the pavement system, thus the name, time-to-drain. The DRIP (Drainage Requirements in Pavement) software (Mallela et al. , 2002) for design and analysis of pavement subsurface drainage analyzes the water flow inside the pavement on the basis of the time-to-drain approach.

Unsaturated flow conditions can occur if one or more pavement layers become fully saturated while one or more other pavement layers remain partially saturated (unsaturated), a flow condition that is more realistic than the fully saturated condition. However, the FHWA and AASHTO pavement design methods do not consider unsaturated flow conditions in pavement drainage design; only a fully saturated flow condition is considered (Rabab'ah, 2007).

2.13 Water Characteristic Curves

To properly account for drainage conditions in the partially saturated condition it is necessary to estimate the unsaturated hydraulic conductivity function. This can be done using water characteristic curves (WCC), or the volumetric water content function. The WCC of a porous medium indicates the amount of water remaining in the media pores as a function of pore-water pressure (suction). This can be plotted as the media volumetric water content (VWC) as a function of the media suction. A typical WCC for soil is presented in Figure 2-11. The air-entry value of the soil is the pore pressure (matric suction) where air begins to enter the largest pores. The residual water content is the water content where a significant amount of suction is required to remove the extra water from the soil. Additionally, desorption and adsorption curves are shown that have the same format. Their differences are due to hysteresis (Fredlund & Xing, 1994).

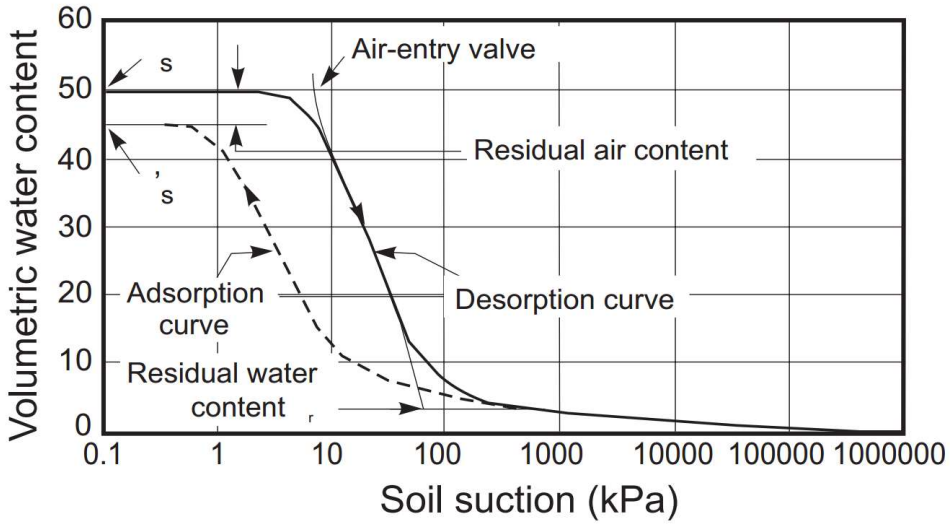

Figure 2-11 Typical soil water characteristic curve (Fredlund & Xing, 1994)

WCC can be determined in the laboratory by direct and indirect methods. In the direct measurement methods, a known air pressure higher than the atmospheric pressure (suction) is manually applied to a soil sample and the water content recorded (Kim et al., 2015). In geotechnical engineering practice, suction is defined as the negative difference between the pore-water pressure and atmospheric pressure. There are several direct laboratory methods to determine soil WCC. A particular method is selected for use based on the required suction range expected for the material. ASTM D6836, "Standard Test Methods for Determination of the Soil Water Characteristic Curve for Desorption Using Hanging Column, Pressure Extractor, Chilled Mirror Hygrometer, or Centrifuge," suggests a few methods, including hanging column for low range suctions (0 to 80 kPa), pressure plate (chamber) for mid-range suctions (0 to 1500 kPa) and chilled mirror hygrometer for high-range suctions (500 kPa to 100 MPa). Additional direct methods are available as described by (Klute & Klute, 1986). The data from various methods may be used in combination to form the entire water characteristic curve for a given material. Pease (2010)

combined hanging column, pressure plate and the relative humidity box methods to produce a WCC for a dense-graded asphalt mixture in the suction range of 0 to 83 MPa.

2.14 Indirect Methods of Measuring Soil Suction Using Filter Paper Method

The filter paper method is a simple, low-cost, experimental test method to indirectly determine VWC in the laboratory. It is an indirect technique used for suction measurement and has been used by geotechnical engineers since the 1980s (Chandler & Gutierrez, 1986; Ching & Fredlund, 1984; Daniel et al., 1981; Kim et al., 2015). The standard test method for measurement of soil suction using filter paper is ASTM D5298, "Standard Test Method for Measurement of Soil Potential (Suction) Using Filter Paper." The test can be used for the measurement of suction in the range of 0 to 1500 kPa (72.5 psi) (Kim et al., 2015) and can be performed simultaneously on any number of asphalt mixture specimens, something not possible with the direct methods.

The test method evaluates the soil matric and suction by measuring the free energy of the pore-water or tension stress applied on the pore-water by the soil matric. In this test method, the filter paper is in direct contact with the test specimen, which is in a tightly sealed plastic bag. The water content of the filter paper is measured when it is in equilibrium with the partial pressure of the water vapor inside the sealed plastic bag containing the specimen. In this condition, the partial pressure of the water vapor is in equilibrium with the vapor pressure of the pore-water in the test specimen. Once equilibrium is reached, the water content of the filter paper can be obtained by oven drying the paper. This value is used to determine the matric suction of the test specimen by reference to the available calibration curve (Figure 2-12), which relates filter paper water content and matric suction.

The result of the filter paper method test can be affected by various factors, such as the filter paper type and equilibration time. Whatman No. 42 filter paper (Table 2-2) and a minimum equilibration time of seven days are suggested to achieve the best result. It is also suggested that a small contact stress be applied to the filter paper to ensure good contact between the filter paper and the soil during the equilibration time (Kim et al., 2015).

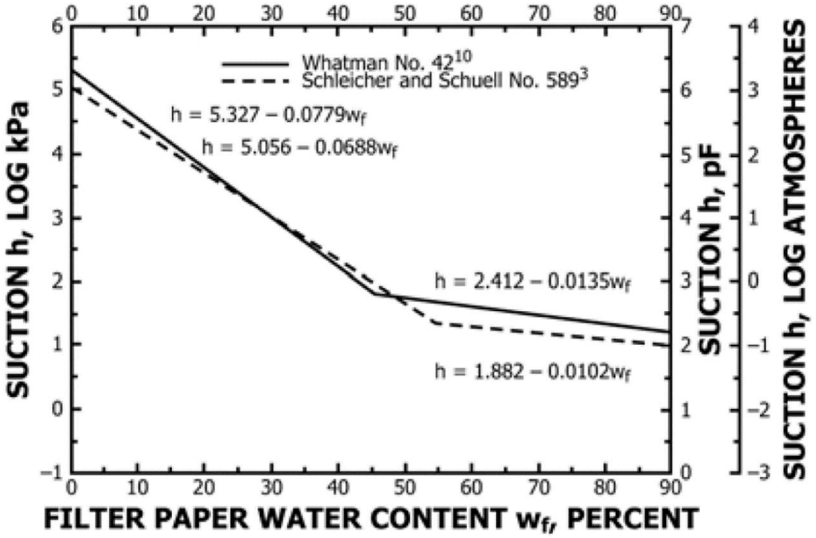

Figure 2-12 Calibration suction-water content curves (ASTM, 1995)

Table 2-2 Characteristics of Whatman. No 42 paper (Kim et al., 2015)

Grade	Diameter (mm)	Basis weight[a] (g/m^2)	Nominal particle retention in liquid[b] (μm)	Ash content[c] (%)	Nominal thickness (μm)
42	42.5–320	91–109	2.5	< 0.007	200

[a]The unit weight of the filter paper produced in Lot No. J11368905 was 95 g/m2 according to the certificate of analysis provided by GE Healthcare Co. Thus, the nominal weight of a 90-mm-diameter filter paper should be 0.6044 g; however, the average measured weight of three filter papers stored in a sealable plastic bag was 0.6089 g.
[b]Particle retention rating at 98% efficiency.
[c]Ash content determined by ignition of the cellulose filter at 900°C in air.

2.15 Unsaturated Hydraulic Conductivity Function

The unsaturated hydraulic conductivity (permeability) function can be determined by either direct experimental test or estimation methods. Experimental tests are time-consuming and complicated, while by using the estimation methods, the hydraulic conductivity function can be easily estimated from the volumetric water content function. The Fredlund (1994) and Van Genuchten (1980) estimation methods are two such estimation methods.

2.16 Finite Element Analysis of Water Flow Through Pavement By Using ABAQUS

Previous studies have indicated finite element (FE) methods can be a helpful tool in analyzing water flow (seepage) through pavements in either saturated or unsaturated conditions (Hassan & White, 1996; Rabab'ah, 2007; Ji et. al., 2013-1; Ji et. al., 2013-2; Ghavami et al., 2019). ABAQUS is an FE software package that can be used in the analysis of fully or partially saturated porous medium. The general governing equations used by the ABAQUS program are given by Equations 2.13 and 2.14 and can apply to the x-p system (x and p refer to the displacement and pore water pressure respectively) in the truncated space. The equations are derived based on the stress equilibrium law for the solid phase and the continuity law for the fluid phase. It should be noted that the stress tensor is in Voigt notation and the subscript I refers to the nodal space truncation index (ABAQUS, 2016; Saad, 2014).

$$F^{ext} = \int_{\upsilon} \left[B_I\right]^T \sigma' \, d\upsilon - C\, p_I, \qquad (2.13)$$

$$q_I = Hp_I + C\dot{x}_I + W\dot{p}_I, \qquad (2.14)$$

where, F^{ext} is the external mechanical force vector matrix, q_I is the external volumetric flux vector, $[B]$ is the strain displacement matrix given by $[B] = [\partial][N]^T$, σ' is the Bishop effective stress tensor that describes the stress state in the partially saturated medium given by $\sigma' = \sigma + \alpha\chi mp$,

σ is the total stress tensor; α is the Biot's coefficient (unity for incompressible soil particles) and χ is Bishop's parameter that equals to the degree of saturation, H is hydraulic conductivity matrix, C is fluid–solid coupling matrix, and W is hydraulic capacity matrix. H, C, and W are defined by Equations 2.15, 2.16, and 2.17.

$$H = \int_v ([\nabla][N_I^P])^T k^e [\nabla][N_I^P]\, dv, \quad (2.15)$$

$$C = \int_v \left([B_I\ ]\right)^T [m][N_I^P]^T\, dv, \quad (2.16)$$

$$W = \int_v \left(\frac{1}{Q}\right)\ [N_I^P]^T\, dv, \quad (2.17)$$

where, $[N]$ and $[N^P]$ are the shape function matrices used to truncate the *x* and *p* fields respectively, [m] is the Voigt representation of the Kronecker delta tensor m, k^e is the effective hydraulic conductivity matrix given by $k^e = k/\rho_w$ g, k is the permeability matrix, g is the gravitational acceleration, ρ_w is the mass density of the water, Q is the hydraulic capacity of the partially saturated mixture given for incompressible fluid and soil particles by $(1/Q) \equiv n(\partial S/\partial p)$, *n* is the porosity of the medium, and *S* is the degree of saturation.

CHAPTER 3. RESEARCH METHODOLOGY

The objectives of the research were accomplished through a literature review, laboratory testing, computer analyses using finite element modelling. Specifically, the following tasks were completed:

1. The hydraulic conductivity and moisture characteristics of asphalt mixtures meeting current INDOT specifications were determined in the laboratory. Laboratory testing included determining the saturated permeability and water characteristic curves of dense- and open-graded asphalt mixtures.
2. The Drainage Requirements in Pavements (DRIP) program was used to compare various pavement drainage scenarios. The program was able to evaluate the pavement drainage effectiveness of saturated pavements and identify the most drainable material for use in the drainage layer.
3. A finite element model of unsaturated moisture flow through flexible pavements was developed and used to:
    a) Investigate the effectiveness of pavement drainage systems by evaluating the moisture condition of flexible pavements and the underlying subgrades.
    b) Compare current and past flexible pavement drainage system approaches to see if current materials and construction specifications act to better protect flexible pavements from moisture, thus decreasing the need for a drainage layer.
    c) Investigate the need for a drainage layer in flexible pavements by comparing current as-designed and constructed flexible pavement sections both with and without a drainage layer.

4. Perform finite element analyses to evaluate the mechanical performance of the pavement drainage system.
5. Using the finite element program, couple the stress/pore-pressure analyses and traffic loading to investigate the effects of traffic loading on flexible pavements at various subgrade saturation levels (77 and 100% saturation).
6. Evaluate the pavement models using typical Indiana pavement subgrade soils subjected to various traffic loads application.
7. Develop a simple tool to determine the need for pavement drainage. This tool indicates when drainage is needed for flexible pavements, and when it can be safely eliminated.

An overview of the proposed research is shown in Figure 3-1.

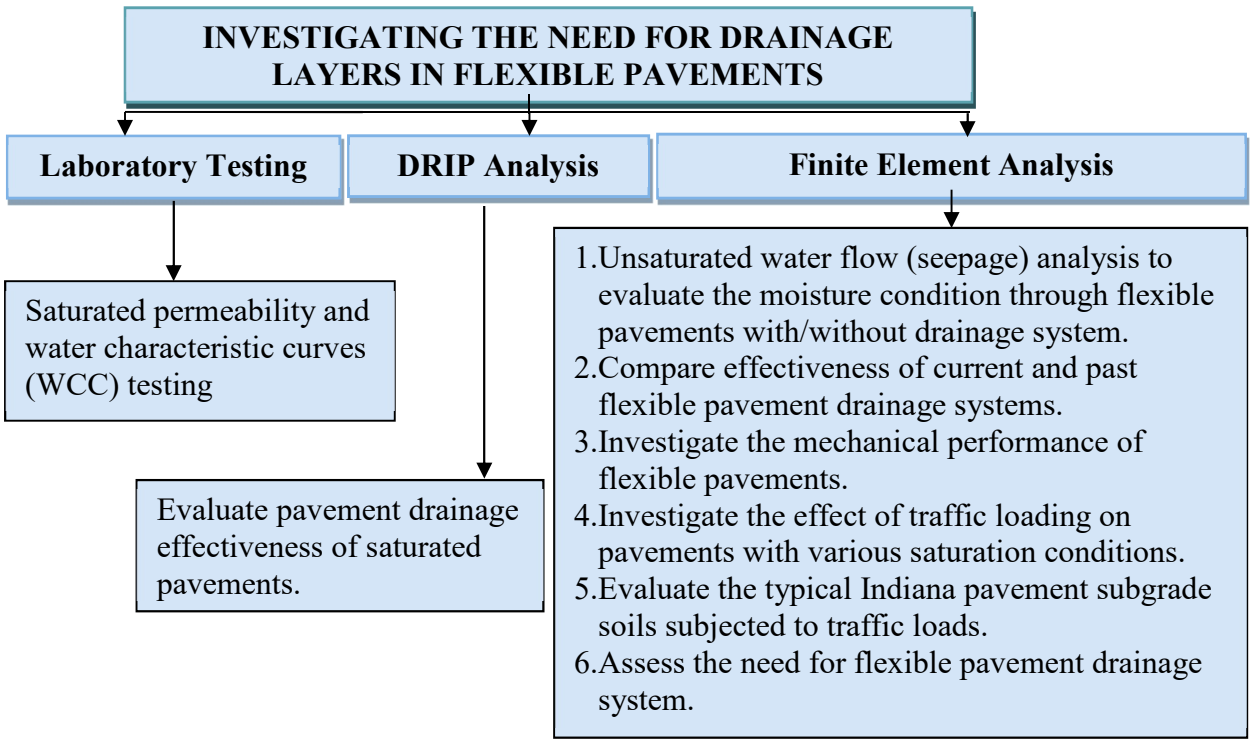

Figure 3-1 Research overview

CHAPTER 4. LABORATORY TESTS

4.1 Materials

The purpose of the laboratory testing was to determine the hydraulic properties of asphalt mixtures meeting current INDOT specifications to facilitate the numerical modeling of flexible pavement sections. This involved considering several asphalt mixture types utilized in a typical INDOT flexible pavement. Laboratory testing was performed to obtain the saturated permeability and the water characteristic curves (WCCs) of compacted asphalt mixtures.

Several cross-sectional cores were extracted from two different pavement sections containing asphalt mixtures meeting current INDOT specifications. The three asphalt mixtures tested were a 19.0-mm dense graded, a 19.0-mm open-graded, and a 9.5-mm dense graded mixture. The field cores were taken to the laboratory and the various pavement layers separated using a saw. This resulted in two, 100 mm (4-in.) diameter asphalt mixture specimens for each of the three mixture types. The bulk specific gravity (G_{mb}) and the theoretical maximum specific gravity (G_{mm}) were determined for each asphalt mixture specimen according to AASHTO T331, "Standard Method of Test for Bulk Specific Gravity (G_{mb}) and Density of Compacted HMA Using Automatic Vacuum Sealing Method," and AASHTO T209, "Standard Method of Test for Theoretical Maximum Specific Gravity (G_{mm}) and Density of Hot Mix Asphalt (HMA)," respectively, and the specimens' air voids contents calculated. The specific gravity and air voids results are shown in Table 4-1, while the mixture gradations are in Table 4-2 and shown graphically in Figure 4-1.

Table 4-1 Asphalt cores theoretical maximum specific gravity, bulk specific gravity, and air voids

Mixture Type	Sample No.	Theoretical Maximum Specific Gravity (G_{mm})	Bulk Specific Gravity (G_{mb})	Air Voids, %
9.5-mm dense-graded	1	2.756	2.571	6.7
	2		2.601	5.6
19.0-mm open-graded	3	2.574	2.25	12.6
	4		2.22	13.8
19.0-mm dense-graded	5	2.512	2.327	7.4
	6		2.35	6.4

Table 4-2 Asphalt mixture gradations

Sieve Size, mm	9.5-mm dense-graded	19.0-mm open-graded	19.0-mm dense-graded
	Percent Passing		
25	100.0	100.0	100.0
19	100.0	92.7	95.8
12.5	100.0	64.3	81.5
9.5	90.0	43.2	73.5
4.75	61.1	21.9	50.9
2.37	40.1	16.2	33.8
0.6	19.5	9.6	15.4
0.3	11.0	5.8	10.2
0.075	4.4	2.2	5.2

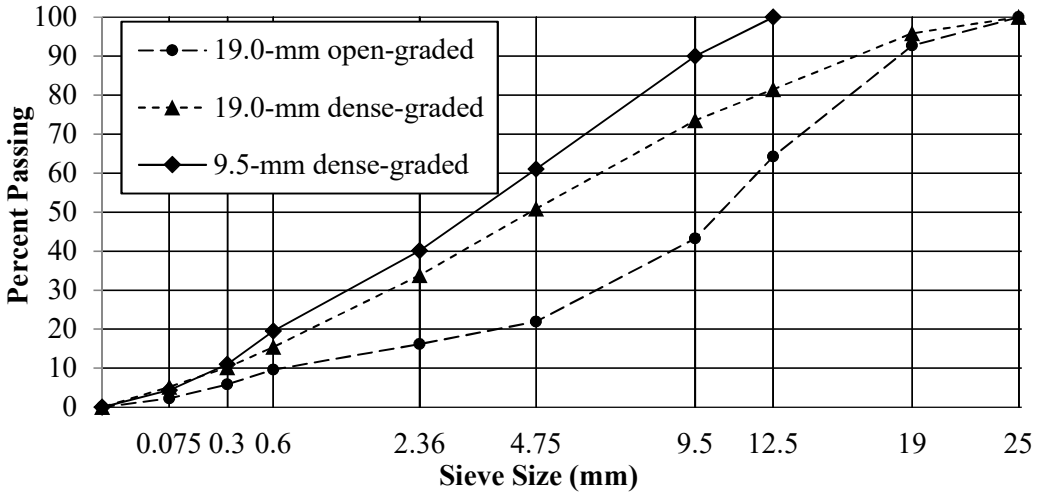

Figure 4-1 Asphalt mixture gradations

4.2 Laboratory Saturated Permeability Testing

Saturated permeability testing was performed using the falling head permeameter developed by the FDOT in 2002 according to the standard test method developed by the Virginia Department of Transportation, Test Method–120, "Method of Test for Measurement of Permeability of Bituminous Paving Mixtures Using a Flexible Wall Permeameter." In accordance with this method the cylindrical asphalt specimens were vacuum-saturated at a residual pressure of 90 ± 2 mm (28 in.) of Hg for 15 minutes with each specimen remaining under water until the permeability testing began. When a specimen was ready for testing it was removed from the water and a thin layer of petroleum jelly was applied to outside diameter to fill the voids and achieve a seal between the specimen and the testing apparatus. Next, the specimen was placed in the permeameter with a confining pressure of 68.9 ± 3.4 kPa (10 ± 0.5 psi) and water was placed in the graduated cylinder. The time required for water to fall from the specified upper mark on the graduated cylinder to the lower mark was recorded to the nearest second. The test was repeated at least three times for each specimen and the percent difference between the first and third tests was limited to less than 4% to ensure the specimens were actually in a saturation condition. All tests were performed at 25°C (77°F); a temperature correction factor of 0.89 was used to adjust the water viscosity.

4.2.1 Permeability Testing Results

The saturated permeability (K) was calculated using Darcy's equation (Eq. 2-10) for all specimens of the three mixtures. The results are shown in Table 4-3.

Table 4-3 Permeability results

Mixture Type	Sample No.	Air Voids, %	Ave. Air Voids, %	Permeability (K) (cm/sec)	Ave. K (cm/sec)
9.5-mm dense-graded	1	6.7	6.2	9.31E-05	8.60E-05
	2	5.6		7.88E-05	
19.0-mm open-graded	3	12.6	13.2	3.64E-02	5.29E-02
	4	13.8		6.94E-02	
19.0-mm dense-graded	5	7.4	6.9	6.45E-04	7.62E-04
	6	6.4		8.78E-04	

4.3 Filter Paper Testing Method Procedure

The WCC of the three asphalt mixtures were obtained using the method by Kim et al. (2015) to measure matric suction of compacted subgrade soils which is based on ASTM D5298, as previously described. In accordance with this method, the mass of each fully saturated asphalt specimen was measured, and a Whatman No. 42 filter paper placed on the top and bottom of the specimen. Each specimen was then quickly covered by two layers of plastic cling wrap, to prevent evaporation (Figure 4-2). Since the surface of each specimen and the filter papers must be in good contact to get the best result, a small contact stress was applied by placing another core specimen on top of each test specimen during the equilibration time. During equilibration, the specimens were stored in a confined space for seven days (Figure 4-3a). After the seven days equilibrium period, each specimen was unwrapped, and the filter papers removed and weighed (Figure 4-3b). The filter papers were quickly placed in separate previously weighed containers and oven-dried for 16 hours. At least three experimental points were used to develop the matric suction-saturation curve for each specimen. Each experimental point represents a percent saturation of the specimen with the average water content of filter papers.

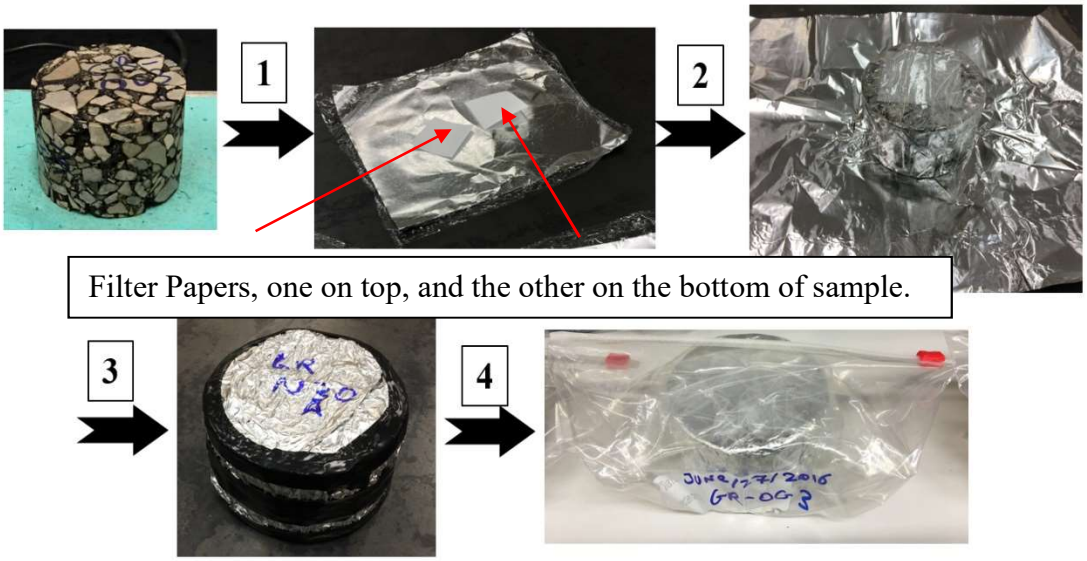

Figure 4-2 Filter-paper test sample preparation

a **b**

Figure 4-3 Filter-paper test a) stored samples with extra cores on top, b) opening samples after the seven-day equilibrium period

The calibration suction-water content curve from ASTM D 5298 was used to estimate the matric suction from the moisture content of the filter papers. From the Whatman No. 42 filter paper calibration curve, the following equations are suggested for determining the amount of suction:

$$h=5.327 - 0.0779W_f,\ W_f < 45.2640 \quad (4.1a)$$

$$h=2.412 - 0.0135W_f,\ W_f > 45.2640 \quad (4.1b)$$

where:

h is suction (log kPa); and

W_f is the filter paper water content (%).

4.3.1 Filter Paper Testing Method Results

The filter paper method results, including matric suction, percent saturation and volumetric water content for all specimens are given in Tables 4-4 and 4-5.

Table 4-4 Paper testing results for asphalt mixtures

Mixture Type	9.5-mm dense-graded						19.0-mm open-graded					
Sample No.	1			2			3			4		
Air Voids, %	6.7			5.6			12.6			13.8		
K, cm/s	9.30E-05			7.80E-05			3.60E-02			6.90E-02		
Saturation, %	100	63	45	100	76	52	100	55	17	100	62	10
Volumetric Water Content	0.067	0.042	0.03	0.056	0.043	0.029	0.126	0.069	0.022	0.138	0.085	0.014
Suction, kPa	0	12.4	694	0	10.6	900	0	1.5	4.9	0	0.98	5.1

Table 4-5 Paper testing results for 19.0-mm dense-graded asphalt mixture

Mixture Type	19.0-mm dense-graded					
Sample No.	5			6		
Air Voids, %	7.4			6.4		
K, cm/s	6.50E-04			8.78E-04		
Saturation, %	100	65	34	100	62	33
Volumetric Water Content	0.074	0.048	0.025	0.064	0.040	0.021
Suction, kPa	0	0.58	790	0	0.78	800

4.3.2 Water Characteristic Curve Analysis

The results from the filter paper method represent only a few data points, which include the measured values of suction at corresponding values of the VWC of asphalt mixtures. Therefore, it is important to determine the values of suction at other VWC values. There are several parametric models which can predict and fit a curve to the data points using a single function (Brooks & Corey, 1964; Fredlund & Xing, 1994; Van Genuchten, 1980). For this work, WWC data from the filter paper tests were fitted the closed form van Genuchten (1980) model (Eq. 4.2) using the SWRC program (Seki, 2007). The results are shown in Table 4-6.

$$\theta = \theta + (\theta_s - \theta_r).\frac{1}{(1+[\alpha.h]^{nvg})^m} \quad (4.2)$$

where:

θ is the volumetric moisture content;

θ_r is the residual moisture content;

θ_s is the saturated moisture content;

α and n_{vg} are curve fitting parameters;

$m=1-1/n_{vg}$; and

h is pressure head.

In the analysis of water characteristic curves, the residual moisture content (θ_r), the asymptotic value of moisture when a material becomes drier, was considered equal to zero.

Table 4-6 Drying Curve-fitting Parameters for the Van Genuchten (1980) Model

Mixture Type	Sample No.	θ_s	α	n	R^2	m	Ksat, m/sec
9.5-mm dense-graded	1	0.067	1.89	1.09	1.00	0.08	9.31E-07
	2	0.056	1.35	1.09	1.00	0.08	7.88E-07
19.0-mm open-graded	3	0.126	0.09	2.12	1.00	0.53	3.64E-04
	4	0.138	0.12	2.27	1.00	0.56	6.94E-04
19.0-mm dense-graded	5	0.074	20.61	1.09	1.00	0.08	6.45E-06
	6	0.064	18.3	1.09	1.00	0.09	8.78E-04

CHAPTER 5. EVALUATION OF FLEXIBLE PAVEMENT DRAINAGE-SEEPAGE ANALYSIS

As stated previously, the main objective of this research was to evaluate the effectiveness of the INDOT's current flexible pavement drainage systems, given the changes to pavement cross-sections, materials, or both that have occurred since INDOT adopted the open-graded drainage layer. Therefore, flexible pavement seepage analysis was performed to see if a drainage layer acts to reduce pavement subgrade moisture. Also, the effect of filter material type was examined to determine its effect on the pavement subgrade moisture. Additionally, the effectiveness of edge drains in flexible pavements without a drainage layer was studied. Finally, the effectiveness of INDOT's current and past flexible pavement drainage designs (Superpave vs. Marshall) was compared and investigated to see if still there is the need for a drainage layer in flexible pavements.

5.1 Evaluation of Pavement Drainage Effectiveness Using DRIP

Based on the 1993 American Association of State Highway and Transportation Officials (AASHTO) pavement design guide (AASHTO, 1993), excellent pavement drainage occurs when moisture can be removed from a pavement within two hours of the end of a rain event. The more quickly moisture can drain from the pavement structure, the better the drainage effectiveness. The design guide rates drainage quality based on a "time-to-drain" approach, defined as the time required for a specific percentage of the moisture, typically 50%, to drain from a pavement's drainable base layer. Depending on the time, the drainage is rated from excellent to very poor. Excellent drainage occurs when 50% of drainable moisture can be removed within two hours. Good, fair, and poor refer to situations where 50% of drainable moisture can be removed within

one day, seven days, and one month respectively. Very poor indicates the drainage layer cannot remove moisture from the pavement structure.

To assist in determining pavement drainage effectiveness during the pavement design phase, the FHWA developed the DRIP software for use in analyzing pavement subsurface drainage (NCHRP, 2004). Given the proper input data, including permeability and effective porosity of the drainable base material, the software analyzes moisture flow within a pavement, predicting time-to-drain and thereby a drainage rating.

A typical INDOT flexible pavement section (Figure 5-1), including a drainage layer, was modeled in the DRIP program to evaluate the drainage efficiency of the pavement with various base materials. An extensive range of potential base course materials was selected for the drainage layer, a layer modeled as 4 in thick and 28 ft wide. The cross slope of the drainage layer was 2 percent. The drainage quality of the different materials was determined using a constant infiltration coefficient of 0.5 and a 1.4 in/hour rainfall rate. The various base course materials used in the analyses, along with their properties, are shown in Table 5-1.

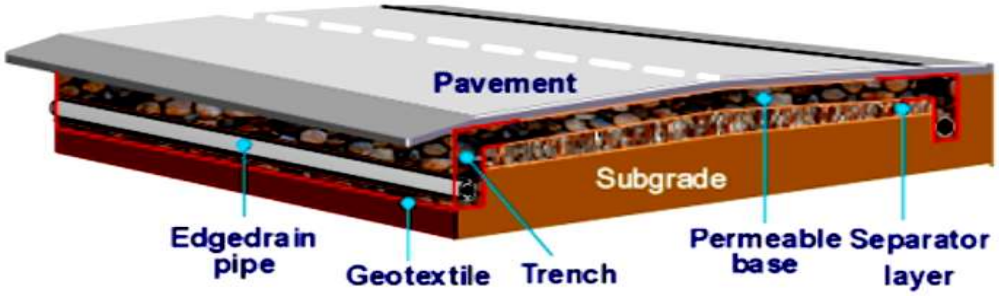

Figure 5-1 Typical asphalt pavement section with drainage layer in the DRIP program (NCHRP, 2004).

Table 5-1 DRIP results for various base courses.

Base Material	K_{sat} (ft/day)	K_{sat} (cm/s)	Porosity	Quality of Drainage	Time to 50% Drainage
#5C Base asphalt mixture [a]	77.4	2.73E-02	0.16	Good	Less than a day (5 hours)
#2 Base (open-graded asphalt mix) [a]	36.3	1.28E-02	0.05	Good	Less than a day (11 hours)
Dense-graded coarse aggregate [b]	0.7	2.31E-04	0.21	Poor	Less than a month
Well-graded sand [b]	36.9	1.30E-02	0.24	Fair	Less than a week (65 hours)
Uniform, coarse-graded sand [b]	1304	0.46	0.25	Excellent	Within 2 hours
Clean, uniform stone [b]	28346.5	10	0.25	Excellent	Within 2 hours
AASHTO #57 aggregate [c]	26560.6	9.37	0.24	Excellent	Within 2 hours
Uniform sand (permeable base) [d]	283.5	0.1	0.25	Good	Less than 1 day (9 hours)
Reclaimed asphalt pavement [e]	5.2	1.85E-03	0.25	Poor	Less than a month (366 hours)
19.0-mm Open-graded asphalt mixture [f]	150	5.29E-02	0.138	Good	Less than a day (10 hours)
25.0-mm dense-graded asphalt [g]	1.0	3.28E-04	0.07	Poor	Less than a month (570 hours)

a-(Hassan & White, 1996), b-(Stormont, Henry, & Roberson, 2009), c- (Liang, 2007), d-(Ariza, 2002), e-(Nokkaew, Tinjum, & Benson, 2012), f-(Lab Experiments in Chapter 4), g-(Tarefder & Bateman, 2009).

5.1.1 DRIP Program Results

Table 5-1 contains the DRIP results based on the time-to-drain approach and shows drainage performance ranging from excellent to poor, depending on the material. As expected, those materials with higher K_{sat} values provide for better drainage quality, when drainage quality is defined by time to drain 50% of the moisture from a pavement. The open-graded asphalt materials tend to give good drainage quality, although none of them exhibit excellent drainage quality, while the dense-graded materials and reclaimed asphalt pavement (RAP) exhibit poor drainage quality.

It is important to remember that while DRIP can estimate pavement drainage quality, the program always assumes a fully saturated conditioned with a constant hydraulic conductivity for the drainable base. The program is therefore useful for quickly estimating drainage quality in a pavement section that will always remain in a saturated condition, but for the more realistic case of an unsaturated or partially saturated pavement, DRIP overestimates the flow quantity; it assumes the same rate of flux for both unsaturated and saturated sections.

5.2 Finite Element Analysis of Unsaturated Water Flow Through Flexible Pavements

An unsaturated flow condition in the pavement occurs when some, but not all pores in a pavement layer are filled with moisture, causing matric suction (negative pore pressure). This condition leads to a variable hydraulic conductivity that is a function of pore pressure; the hydraulic conductivity quickly decreases as pore water content decreases (Tindall et al., 1999). Rabab'ah (2007) recommended considering unsaturated flow principles in the analysis of pavement subsurface drainage. This requires careful consideration of the boundary and initial conditions, as well as the material hydraulic properties, including water characteristic curves (WCC) and the unsaturated hydraulic conductivity functions.

Previous studies have indicated that finite element methods can be a helpful tool in analyzing water flow through pavement in either a saturated or unsaturated conditions (Hassan & White, 1996; Ji et. al., 2013-1; Ji et. al., 2013-2; Rabab'ah, 2007). ABAQUS is an FE software package that can analyze seepage (water flow) for both saturated and unsaturated flow conditions. It can perform both transient and steady-state analyses of pavement sections that include several layers, each having different hydraulic properties, water retention curves, and hydraulic conductivity functions. In the ABAQUS software, the analysis of water flow through pavement

under the unsaturated and transient condition is called “pore fluid flow analysis” (ABAQUS, 2016).

The first task in the unsaturated flow experiment was to rebuild and verify the FE model developed by Hassan and White (1996) using their pavement cross-section, materials properties, and rainfall event. This rebuilt model is referred to Model 1 (Figure 5-4). After confirming that the rebuilt model yielded results consistent with the original FE analysis, which had been validated using field data, the pavement cross-section was modified to remove both the drainage and filter layers. Specifically, the modification included replacement of 12 inches of drainage layer and 8.5 inches of filter layer with 20.5 inches of #8 dense graded asphalt layer (see Figure 5-4 and 5-5). In addition, the edge drain presented in Model 1 was remained in Model 2. These 2 models were compared to determine if there are any differences in the degree of saturation in various pavement layers.

After completing the comparison of Models 1 and 2, Models 3, 4, 5, and 6 were developed using current INDOT flexible pavement cross-section design and materials to evaluate the effect of the drainage layer material types and edge drain (see Figure 5-2). Models 3 and 4 have the same drainage layer material over different filter layer materials, while Models 5 and 6 do not have drainage and filter layers. Models 3, 4 and 5, each has an edge drain. However, an edge drain was excluded in Model 6. The schematic cross-sections of all the pavement models were shown in Figure 5-2, and the Models geometries were presented in Figures 5-4 to 5-9.

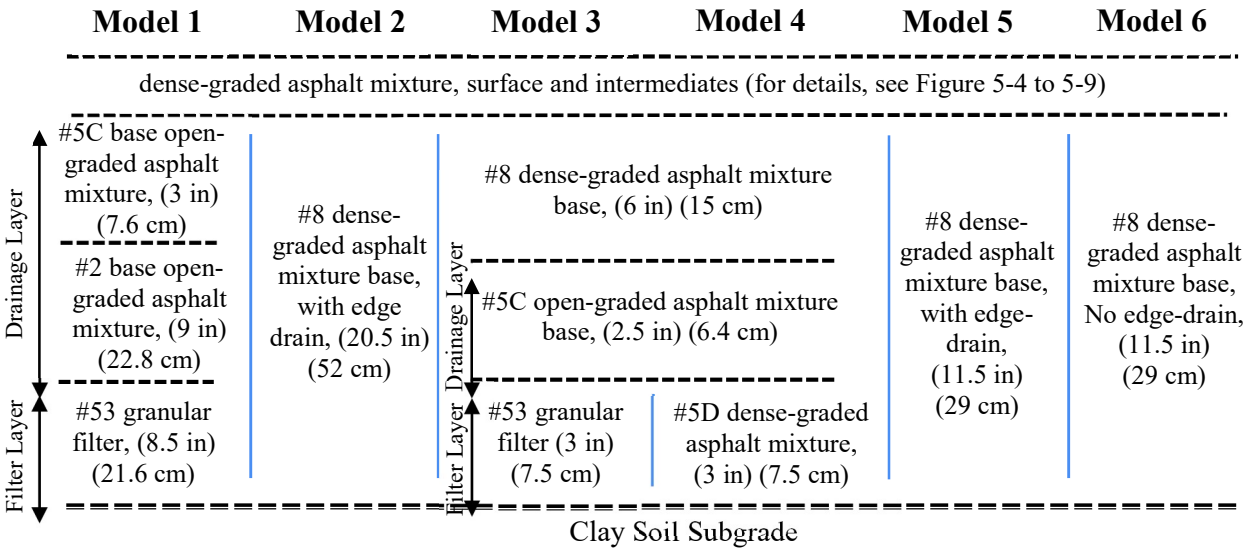

Figure 5-2 Schematic cross-sections of pavement models

5.2.1 Materials

Table 5-2 shows the pavement material types and hydraulic properties, including saturated permeability, used for the study. The numbers assigned to the various layers in Figures 5-4 to 5-9 are presented in Table 5-2. The WCC for all materials were presented in Figure 5.3. For modeling purposes, the WCC and saturated permeability are then used to estimate the unsaturated permeability functions of the materials using the Fredlund and Xing (1994) estimation method.

Table 5-2 Flexible pavement material types and hydraulic properties (Hassan & White, 1996)

Layer No.	**Material Type**	**Max Aggregate Size, (mm)**	**K_{sat} (cm/sec)**	**K_{sat} (ft/day)**
1	#11 Surface (dense-graded asphalt)	12.5	1.01E-04	0.29
2	#9 Intermediate (dense-graded asphalt)	19.0	9.50E-05	0.27
3	#8 Intermediate/base (dense-graded asphalt)	25.0	9.70E-05	0.27
4	#5C Base (open-graded asphalt)	37.5	2.73E-02	77.39
5	#2 Base (open-graded asphalt)	63.0	1.28E-02	36.28
6	#53 Granular aggregate (unbound aggregate)	37.5	3.56E-02	100.91
7	#5D dense-graded asphalt mixture	37.5	1.43E-04	0.41
8	#8 Coarse aggregate (edge drain)	25.0	1.18	3344.88
9	Clay soil subgrade	-	7.70E-8	2.1E-04

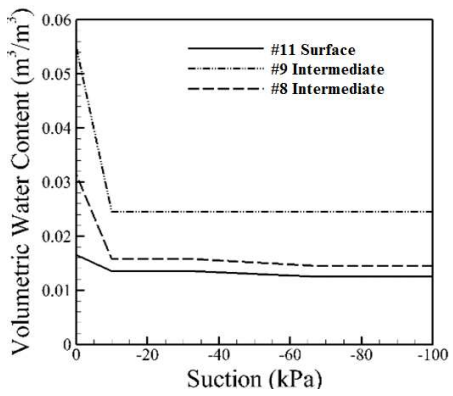

a) #11 surface, #9 and #8 intermediate
(dense-graded asphalt mixture)

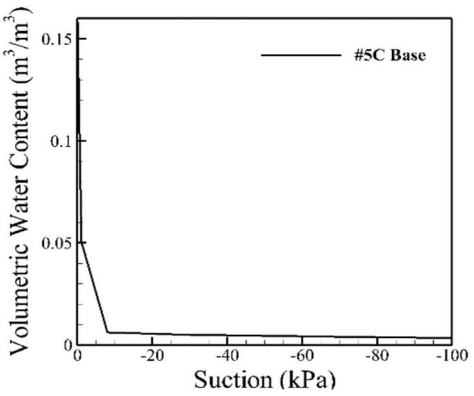

b) #5C base
(open-graded asphalt)

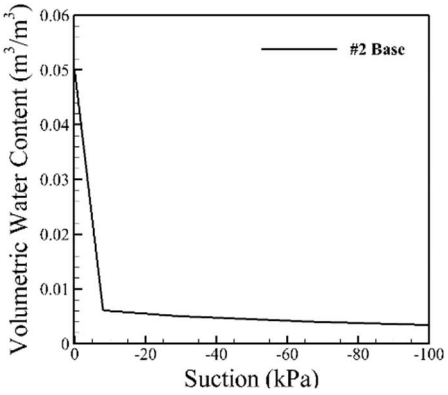

c) #2 base

(open-graded asphalt mixture)

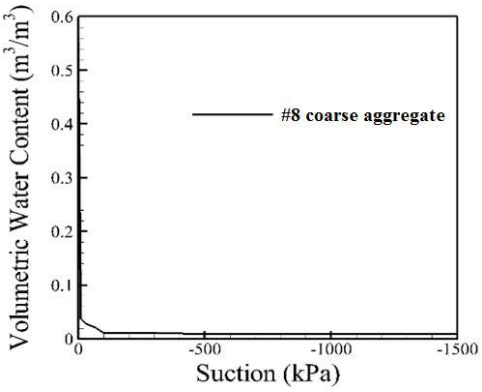

d. #8 coarse aggregate

Figure 5-3 Water characteristic curves of pavement materials (Hassan & White, 1996)

5.2.2 Model Parameters

A flexible pavement cross-section consisting of a 3.65 m (12 ft) pavement lane with a 0.60 m (2 ft) paved shoulder was used for the pavement geometry in the study. The shoulder covers both trench and collector pipe. The 2D FE model geometries for the all 6 Models are shown in Figures 5-4 to 5-9. The material properties assigned to the various layers shown in Figures 5-4 to 5-9 are presented in Table 5-2.

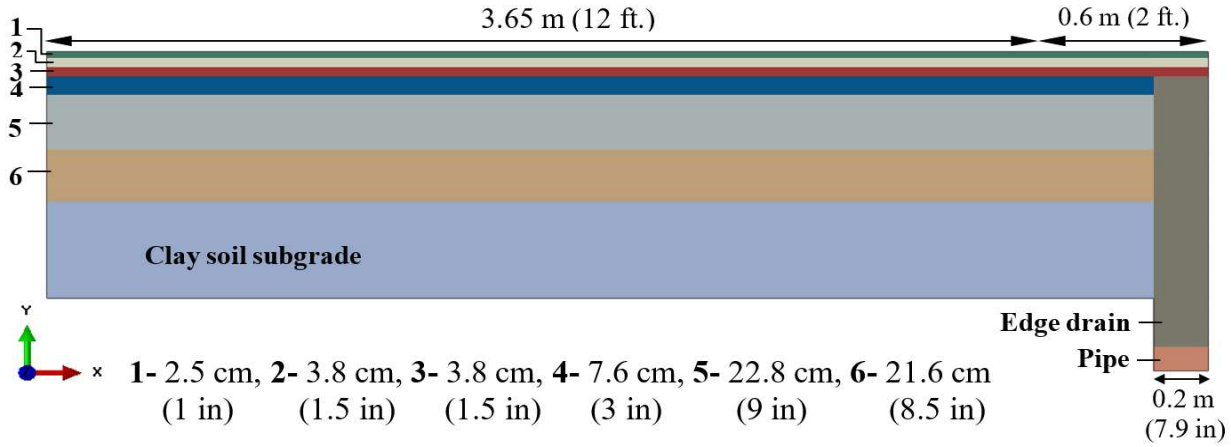

Figure 5-4 Model 1 geometry based on (Hassan & White, 1996)

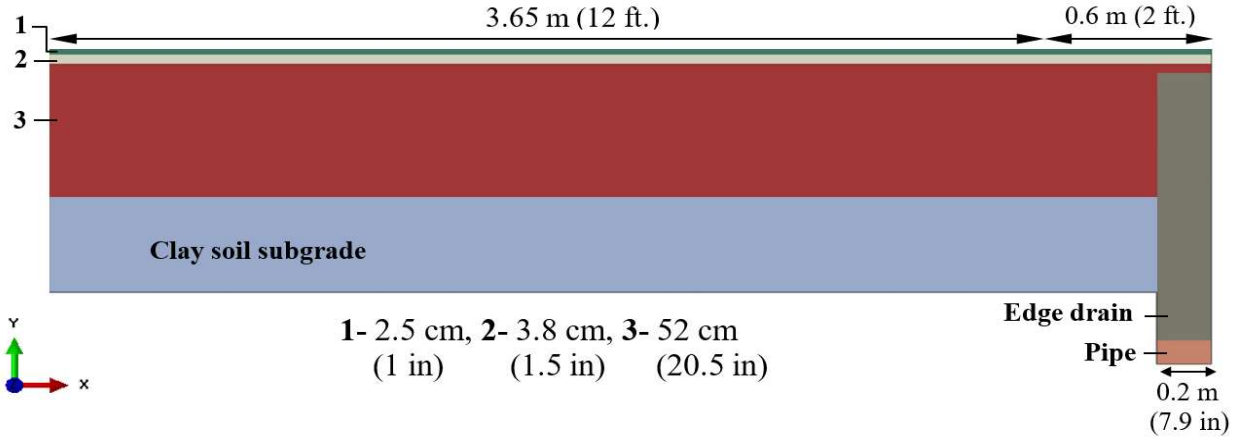

Figure 5-5 Model 2 geometry

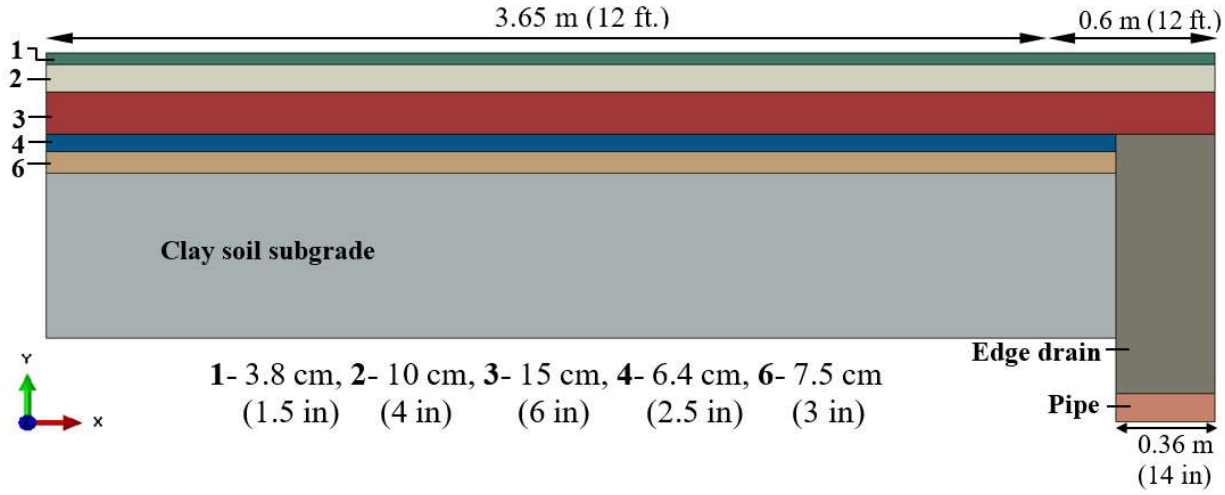

Figure 5-6 Model 3 geometry

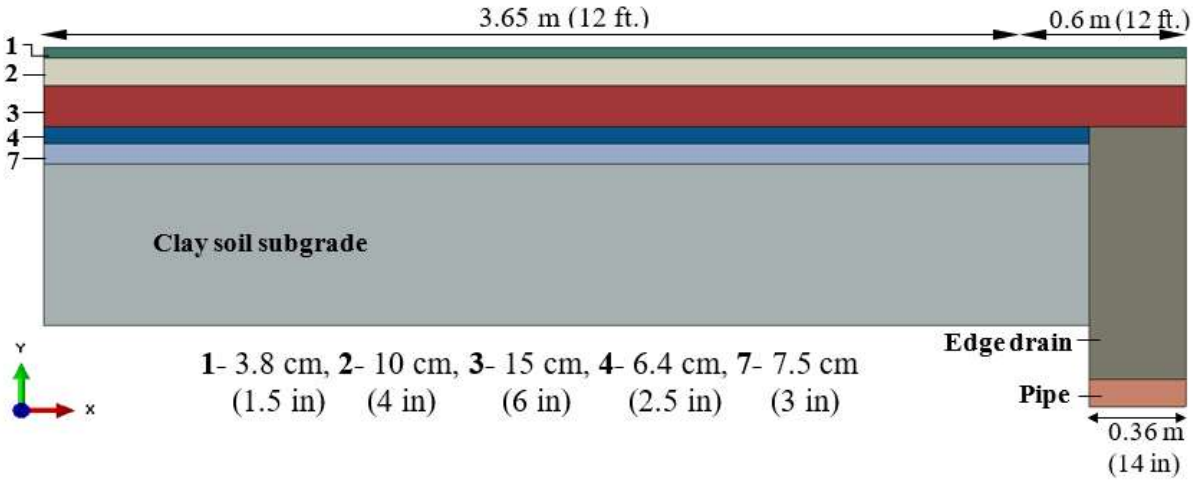

Figure 5-7 Model 4 geometry

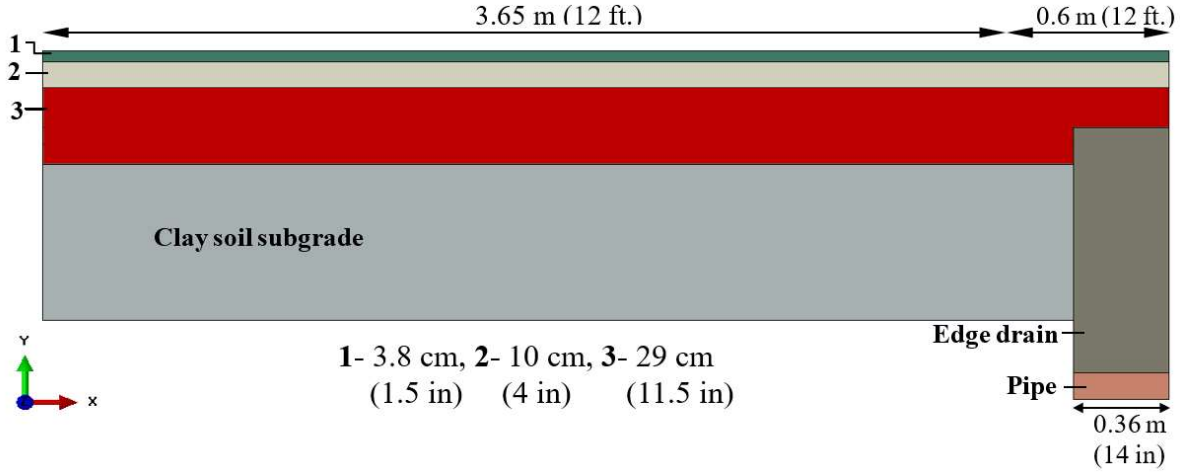

Figure 5-8 Model 5 geometry

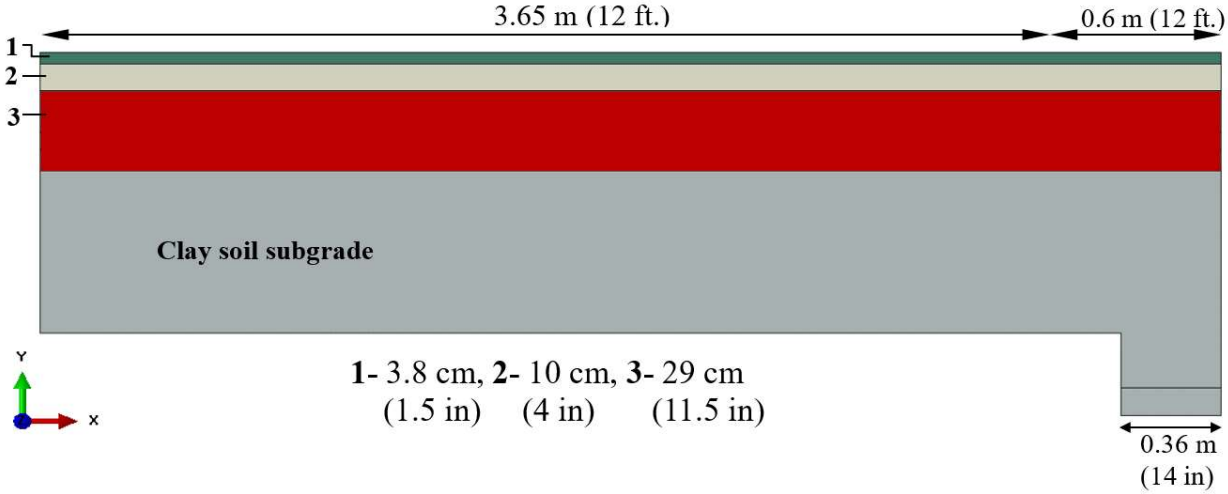

Figure 5-9 Model 6 geometry

The outer edges of the pavement cross-sections were assumed impermeable and a constant zero pore pressure was assumed around the pipe (permeable). During a rainfall event, surface infiltration was modeled by assigning a zero-pore pressure to the pavement surface. Initial saturation for the layers were: Subgrade soil, 90 %; filter layer, 40 %; #2 base, 70 %; and #5C base, 80 percent. These were the field conditions reported by Hassan and White (1996).

Before applying a "rainfall event" to the FE-modeled pavement, the pavement was first brought to equilibrium by applying a gravity load using a "GEOSTATIC" step in ABAQUS, then allowing a 28-hour draining period, as was suggested by Hassan and White (1996), in order to achieve a steady state condition. Once a steady state condition had been reached, a rainfall event was applied in five successive steps as shown in Table 5-3. The rainfall was modeled so that any rainfall intensities of 0.2 cm/hour (0.08 in./hour) or less were ignored (pavement surface assumed to be impervious), as it is unlikely that such light rainfall would penetrate into the pavement surface. Such a period allows for pavement drainage without the accumulation of additional moisture in the pavement.

All the FE models contain 8-noded biquadratic displacement, bilinear pore-pressure (CPE8P) element types. Models 1 and 2 each contain a total of 1,827 of CPE8P elements, while Models 3, 4, 5, and 6 each has a total of 1,894 of CPE8P elements.

Table 5-3 Rainfall modeling (Hassan & White, 1996)

Rainfall time period (hours)	Rainfall intensity (cm/hour)	Modeled pavement surface condition
2	less than 0.2	Impervious
6	more than 0.2	Zero pore pressure
9	less than 0.2	Impervious
2	more than 0.2	Zero pore pressure
51	less than 0.2	Impervious
70	Total time	

5.2.3 Model Validation and Drainage Effectiveness

In order to determine that the recreated FE drainage model was consistent with the model used by Hassan and White (1996), the previously described rainfall event was applied to the Model 1 pavement cross-section and the resulting pore water pressure at the bottom of the drainage pipe trench determined and compared to the original results. The comparison is plotted in Figure 5-10 and shows that indeed Model 1 results closely resemble the original Hassan and White model. Differences in the two results are due to the pipe inlet capacity. In their work, Hassan and White did not provide complete information on the pipe inlet capacity, but by varying the pipe inlet capacity of the recreated model, it appears Hassan and White (1996) assumed the pipe inlet was at least partially clogged. Model 1 makes no such assumption, thus the variation between the two models. Nevertheless, though there are slight variations from the original results, Model 1 appears to reasonably reproduce the Hassan and White results. It was therefore concluded that the recreated model (Model 1) can successfully predict the moisture flow (seepage) in a flexible pavement during a given rainfall event.

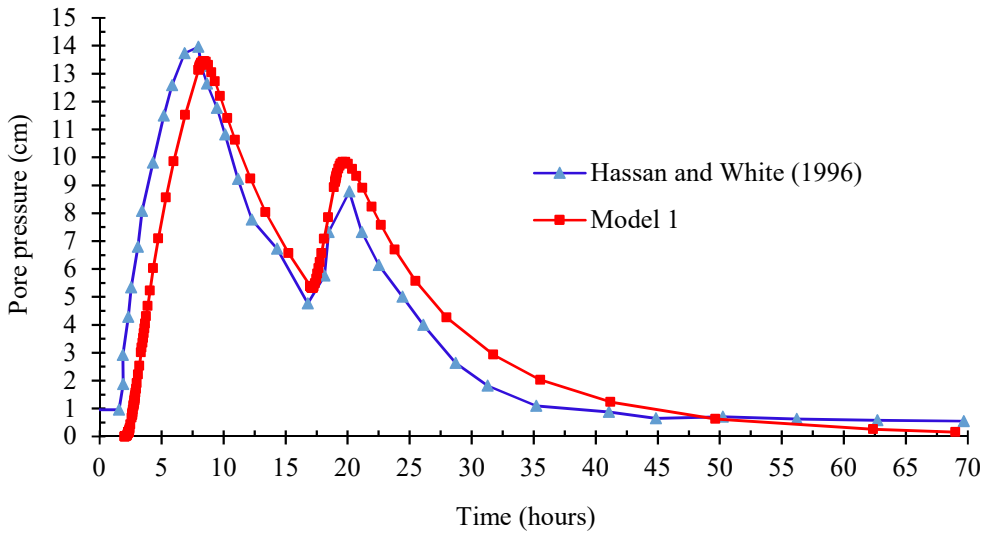

Figure 5-10 Pore water pressure variation at the bottom of the drainage trench

One method to determine the need for, or effectiveness of a pavement drainage system is to establish the degree of subgrade saturation that occurs during a rainfall event. The variation in subgrade saturation during the 70-hour rainfall event for Models 1 and 2 are shown in Figure 5-11. The results indicate the subgrades of both pavements begin to approach full saturation (above 90%) immediately after the rainfall begins. The subgrade in Model 1, the pavement model that includes a drainage layer, quickly begins to lose moisture during drainage periods and reaches approximately 80 percent saturation by the end of the 70-hour period. Model 2, the pavement model without a drainage layer, has a relatively high subgrade saturation level, about 94 percent, at the end of the 70-hour period.

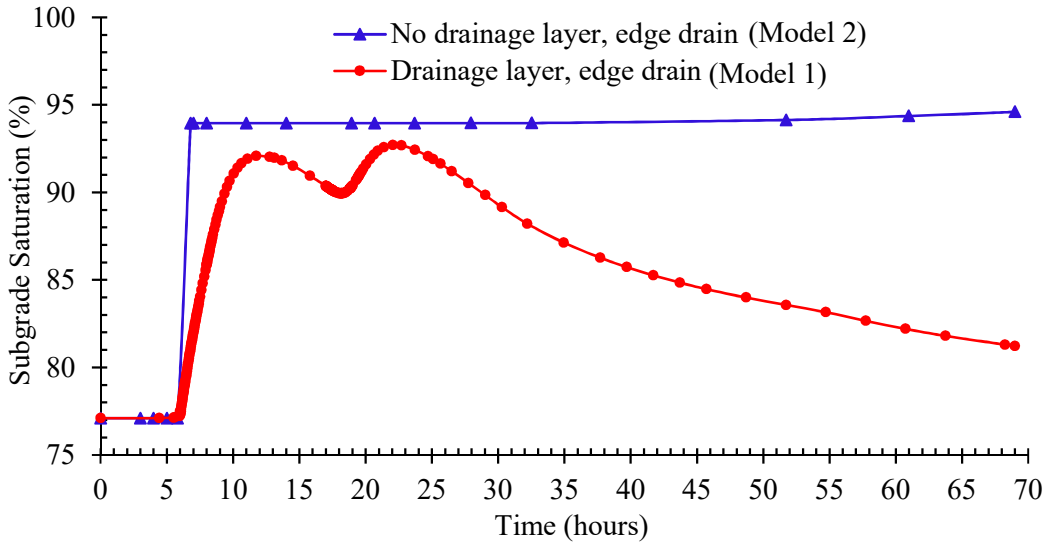

Figure 5-11 Subgrade saturation comparison of Models 1 and 2

The degree of saturation in the various pavement layers at the end of the 70-hour rainfall event for Models 1 and 2 are shown in Figures 5-12 and 5-13. These results are consistent with the subgrade saturation results, in that the degree of saturation for all pavement layers appears to be lower for Model 1 than for Model 2. It is therefore concluded that drainage layer and edge drain systems, as used by INDOT, do effectively lower the moisture content throughout the pavement and subgrade, an effect that should produce increased pavement life. This conclusion is consistent with the findings of Hassan and White (1996).

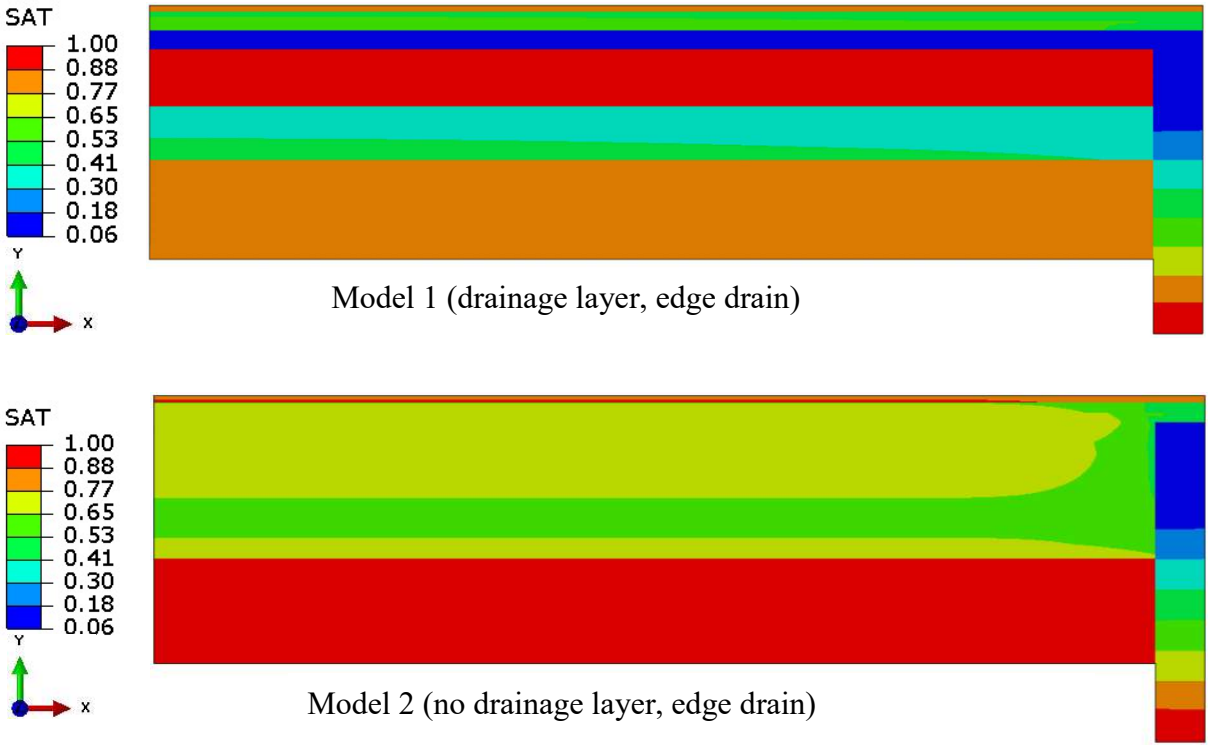

Figure 5-12 Pavement saturation results for Models 1 and 2

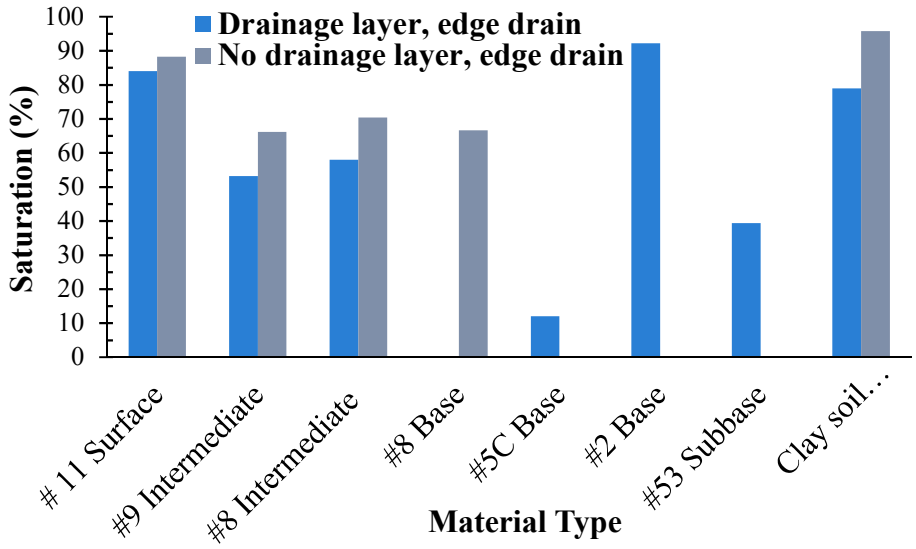

Figure 5-13 Pavement layers saturation results for Models 1 and 2

5.2.4 Effect of Filter Material Types and Edge-drain on Drainage performance

Additional analyses were performed to investigate the drainage effectiveness of INDOT's current flexible pavement cross-sections and assess the effects of filter material types and edge drains. Again, the previously described rainfall event of two peak rainfall periods and three drainage periods was applied. However, for these analyses, the final drainage time was extended to help evaluate the effect of edge drains. These analyses used Models 3, 4, 5, and 6; the resulting degrees of subgrade saturation were determined and compared, as shown in Figure 5-14. The results indicate that subgrades in pavements without a drainage layer become more fully saturated immediately following the initiation of the rainfall and tend to stay near full saturation for a longer period of time (minimum 120 hours) than do subgrades in pavements with drainage layers (maximum 5 hours). However, the pavement with no drainage layer, but with an edge drain begins to lose moisture sooner (around 120 hours after rainfall initiation) than does the similar pavement section without an edge drain (around 150 hours after rainfall initiation). This phenomenon likely represents the effectiveness of the edge drains in flexible pavements that do not contain drainage layers.

The results shown in Figure 5-14 also illustrate the difference in subgrade saturation depending on which filter layer material is used in the pavement section. For both the granular and dense-graded asphalt filter materials, the subgrade saturation levels increase as the rainfall begins, but the pavement with the dense-graded asphalt filter reaches a higher subgrade saturation level (almost fully saturated) than does the subgrade in the granular filter layer pavement. Indeed, the subgrade saturation levels in the pavement with the granular filter layer always remain below that of the pavement with dense-graded asphalt filter layer. However, both pavements successfully drain the excess moisture from the system at the end of the rainfall event.

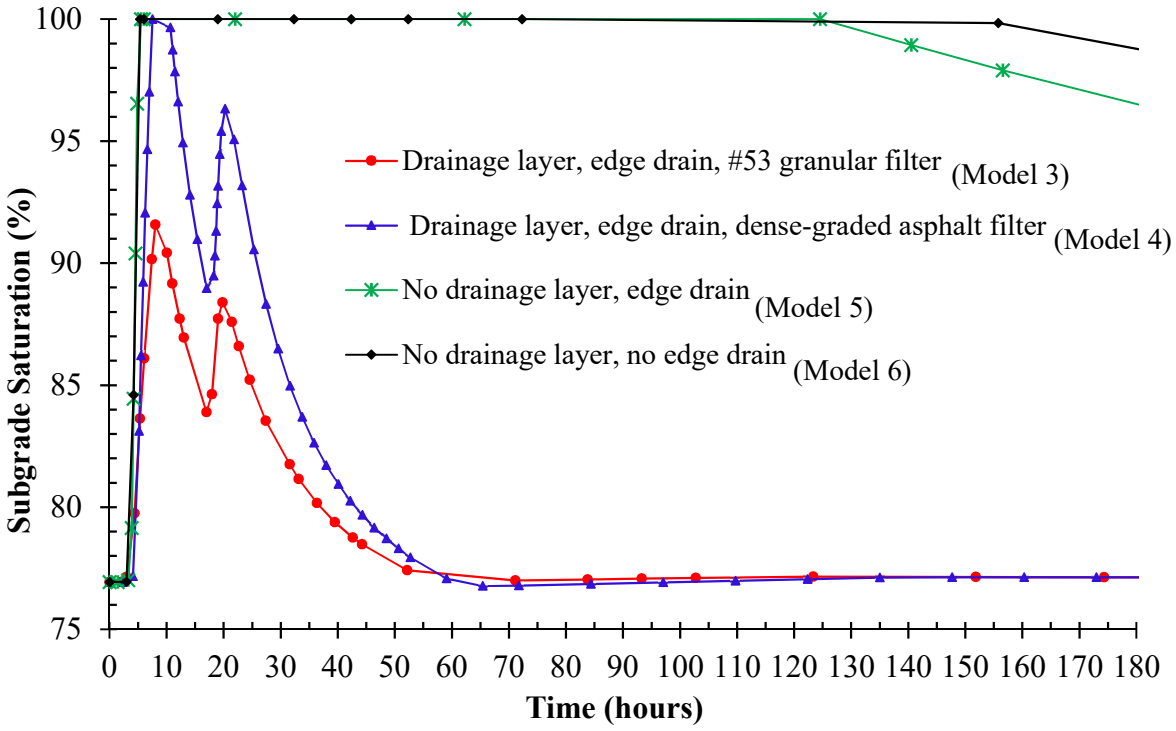

Figure 5-14 Subgrade saturation comparison of Models 3, 4, 5, and 6

5.2.5 Drainage System Effectiveness Using Current INDOT Specified Materials

To evaluate INDOT's currently specified pavement drainage system, Models 7 and 8 were built and tested, similar to the previous analysis. These two models use current INDOT pavement cross-sections and materials properties, as reported in Chapter 4 of this report. Model 7 included a drainage layer, while Model 8 did not (See Figure 5-15). Thus, not only could drainage system effectiveness be compared between the 1996 and current specifications, but the drainage system effectiveness of the current pavement cross-section could be compared with and without a drainage system.

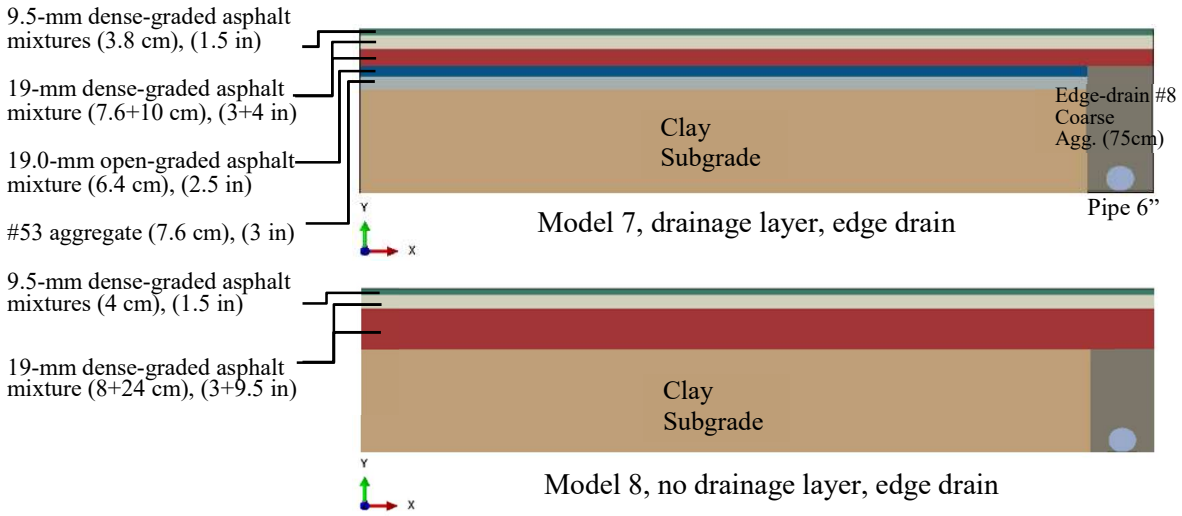

Figure 5-15 Finite element geometries of Models 7 and 8.

The variation in subgrade saturation during the rainfall event for Models 7 and 8 are shown in Figure 5-16. The results indicate the subgrades of both pavements begin to approach full saturation level immediately after the rainfall begins. However, the subgrade in Model 7, the pavement model that includes a drainage layer, quickly begins to lose moisture during drainage periods and reaches approximately 77 percent saturation by the end of the rainfall event, equal to initial subgrade saturation before the rainfall event began. However, Model 8, the pavement model without a drainage layer remains fully saturated until about 280 hours, then begins losing moisture. Again, the results appear to confirm the positive effect a drainage layer can have in lowering the moisture content of flexible pavement subgrade.

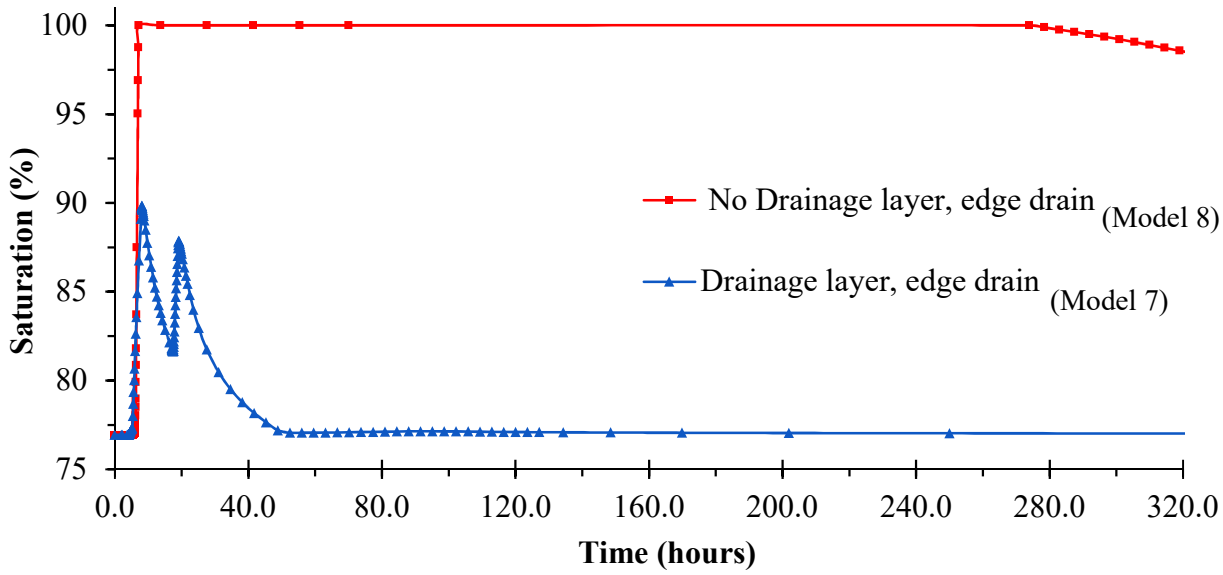

Figure 5-16. Subgrade saturation comparison of Models 7 and 8

By comparing the subgrade saturation at the end of 70 hours rainfall event for Models 1 and 7 (Figure 5-17), it is concluded that the subgrade of the pavement in Model 7 reaches a lower saturation than the subgrade of the pavement in Model 1. Thus, the pavement modeled using the current INDOT materials and construction specifications results in lower subgrade moisture than the pavement modeled using the older INDOT materials and construction specifications. It appears that INDOT's current standard flexible pavement cross-section, including a drainage system, along with current pavement materials and construction specifications has better drainage performance than did previously built flexible pavements using older (1996) materials and construction specifications.

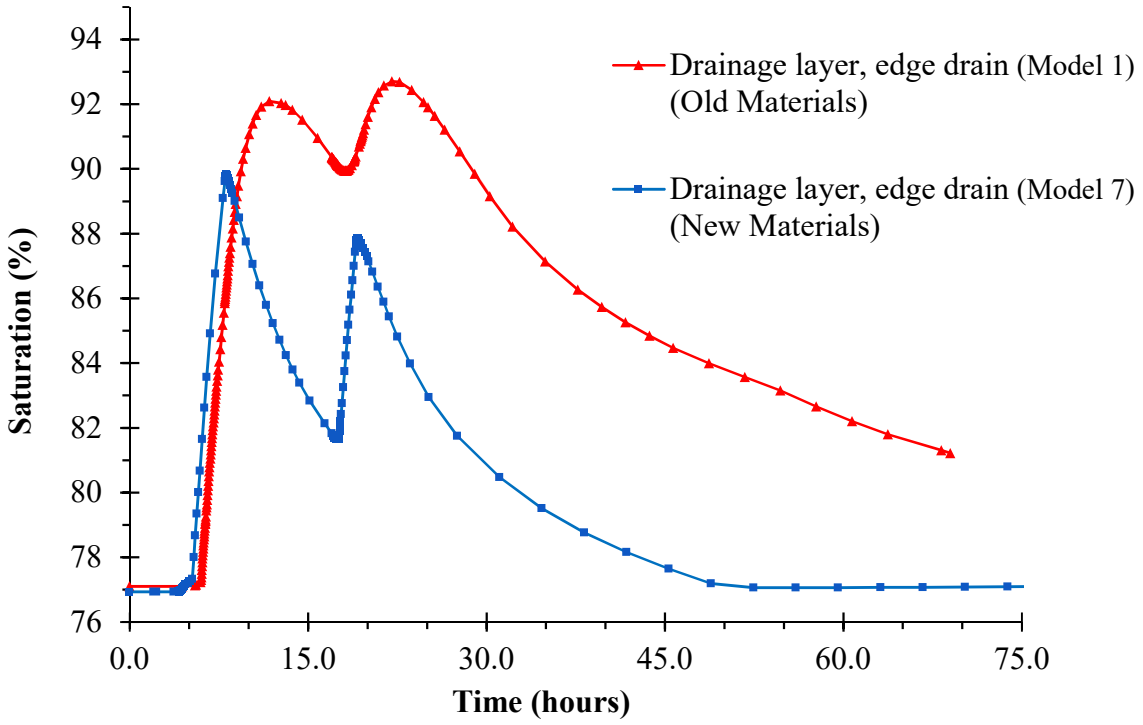

Figure 5-17. Subgrade saturation comparison of Model 7 (new materials) and Model 1 (old materials)

CHAPTER 6. EVALUATION OF FLEXIBLE PAVEMENT DRAINAGE-MECHANISTIC PAVEMENT ANALYSIS

Excessive permanent deformation (rutting) in flexible pavements can cause pavement cracking and thereby increase pavement deterioration. Flexible pavement deformation is caused by plastic flow in the asphalt mixture (usually the surface mixture), loss of subgrade support, or some combination of the two. Plastic flow of the asphalt mixture is a material related distress, while the loss of subgrade support can be caused by poor subgrade materials, poor subgrade compaction during construction, lack of proper pavement design, subgrade weakening by moisture intrusion, or some combination of these factors. The work reported herein investigates pavement distress caused by a combination of asphalt mixture plastic flow and loss of subgrade support due to moisture intrusion. This combination has the potential to cause catastrophic permanent deformation and cracking in flexible pavement systems. Therefore, the study of drainage system effectiveness, how to keep moisture out of the pavement, especially the subgrade, combined with the mechanical pavement performance under various traffic loads becomes an important consideration.

As confirmed by many studies (Feng et al., 1999; Hua, 2000; Huang, 1995; Pan, 1997; Sivasubramaniam & Haddock, 2005), finite element analysis is an excellent tool for mechanistic pavement analyses. Often, the ABAQUS software is the finite element analysis tool of choice because it has the mechanical constitutive models, including the extended Drucker-Prager and the Power-law creep models, suitable for analyzing flexible pavements. Additionally, the ABAQUS software can couple the mechanical constitutive models with water flow analysis to perform unsaturated or saturated analyses of flexible pavements under traffic loads.

The first task was to develop a three-dimensional (3D) finite element model based on the pavement cross-section and material properties adopted by Feng et al. (1999) to predict the section rutting., The result was then compared with the field and finite element results reported by Feng et al. (1999) in order to verify the 3D mechanistic model. Once it had been determined that the model (Model 9) results were consistent with the field results, the rutting analyses of pavements under various traffic and subgrade moisture conditions were performed. Coupled pore fluid flow diffusion and stress analyses were conducted to predict the amount of rutting for a pavement section placed on either a fully saturated, or partially saturated subgrade (Model 10).

6.1 Materials

The material properties (Table 6-1) used for the models were adopted from Feng et al. (1999), and resulted from laboratory triaxial testing for bound (#11, #9, #8, #5D, #5C and #2 asphalt mixtures) and unbound (#53 and #8 aggregates) materials, and a clay subgrade soil. Additionally, the asphalt mixtures' creep rate model parameters (A, M, and N) used are shown in Table 6-2. The asphalt mixture parameters were determined in the test temperature range of 32.8 to 41.1C (91 to 106 F) to simulate the field, seven-day average high temperature of the pavement.

Table 6-1 Pavement material mechanical properties (Feng et al., 1999)

Layer No.	Material Type	Density (kg/m^3)	Cohesion (kPa)	Friction Angle (Degrees)	Poisson's Ratio	Young's Modulus (MPa)
1	#11 Surface (dense-graded asphalt)	2210	95	40	0.35	4000
2	#9 Intermediate (dense-graded asphalt)	1980	120	40	0.35	4000
3	#8 Intermediate (dense-graded asphalt)	2160	80	40	0.35	4000
4	#5C Base (open-graded asphalt)	2030	85	40	0.35	3500
5	#2 Base (open-graded asphalt)	2240	80	46	0.35	3500
6	#53 Subbase (dense-graded aggregate)	2300	15	53	0.3	500
7	Clay soil subgrade	1910	27.6	23	0.3	35
8	#8 Trench (coarse aggregate)	1260	15	33	0.3	400

Table 6-2 Creep rate model parameters (Feng et al., 1999)

Layer No.	Material Type	A (10^{-5})	M	N
1	#11 Surface (dense-graded asphalt)	0.21	-0.34	0.8
2	#9 Intermediate (dense-graded asphalt)	0.62	-0.75	0.8
3	#8 Intermediate (dense-graded asphalt)	0.38	-0.84	0.8
4	#5C Base (open-graded asphalt)	0.38	-0.91	0.8
5	#2 Base (open-graded asphalt)	0.40	-0.78	0.8

6.2 Geometry and Finite Element Mesh

Due to axisymmetric, half of a flexible pavement cross-section was modeled, consisting of a 1.8 m (6 ft) pavement lane with a 0.60 m (2 ft) paved shoulder. The shoulder covers both trench and collector pipe. The longitudinal pavement length modeled was 4.88 m (16 ft); this length is solely for ease of modeling, as longitudinally, a pavement is really considered infinite. The pavement cross-section geometry is shown in Figure 6-1.

Figure 6.2 presents the 3D meshes for Models 9 and 10. An eight-node linear brick, reduced integration (C3D8R) element type was used for Model 9 and an 8-node brick, trilinear displacement, trilinear pore pressure, reduced integration (C3D8RP) element type for Model 10.

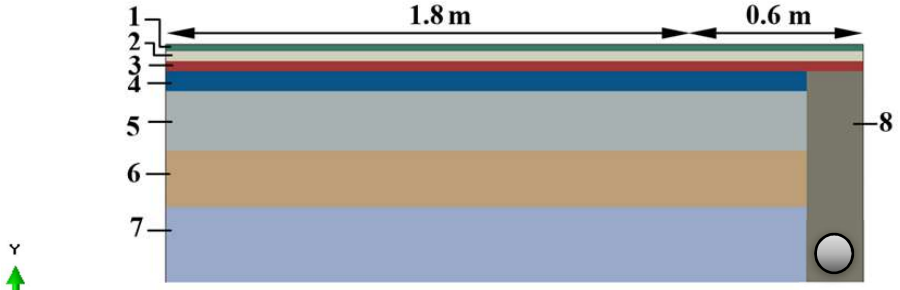

1- 2.5 cm, **2-** 3.8 cm, **3-** 3.8 cm, **4-** 7.6 cm, **5-** 22.8 cm, **6-** 21.6 cm

Figure 6-1 Geometry of the cross-section used in finite element model

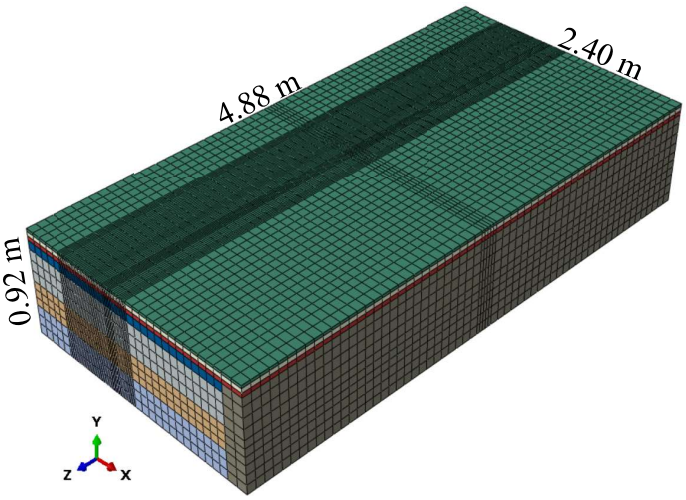

Figure 6-2 Three-dimensional finite element mesh for Models 9 and 10

6.3 Boundary Conditions

The left side of the pavement was fixed in the horizontal direction and also fixed against rotations in two other directions (X-symmetric). The right side boundary was fixed only in the horizontal direction (X direction) due to the pavement continuity. Additionally, both ends were fixed in the Z direction and rotations against X and Y directions (Z-symmetry). Finally, the bottom of pavement was completely fixed against translations and rotations in all the directions. Zero pore-pressure at the top surface was considered whenever moisture was present in the system.

6.4 Model Verification

Pavement rutting accumulates over time under repeated load applications. The traffic loads applied to Model 9 were similar to those used by Feng et al. (1999). The location of the wheel loads are presented in Figures 6-3 and 6-4. A total loading of 140 hours and 1700 trucks per day were assumed in the traffic analysis. The 140 hours loading time represents the three year period (1996-1998) that the pavement surface temperature was equal to or above 40°C (104°F). The equivalent number of loads for this period would be 10,000 trucks, each with two tandem axles and dual tires,

or 40,000 axle loads (see Figure 6-5). The wheel contact area is presented in Figure 6-6. A total loading time was determined based on the time (0.006 sec each truck) needed for 10,000 trucks to travel the length of a wheel contact area 162.6 mm (6.4 in.) moving at a speed of 96 km/hour (60 mph). The total loading time (240 sec) and tire contact pressure 630 kPa (91 psi) were used with the creep rate model to predict rutting. For the simulation of pavement rutting, the ABAQUS "VISCO" step was used.

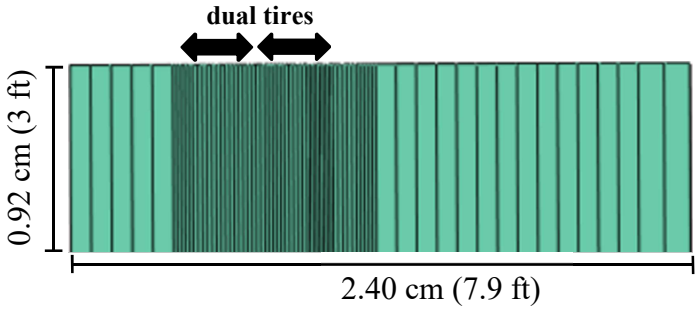

Figure 6-3 Cross-section view of dual tire loading in the models

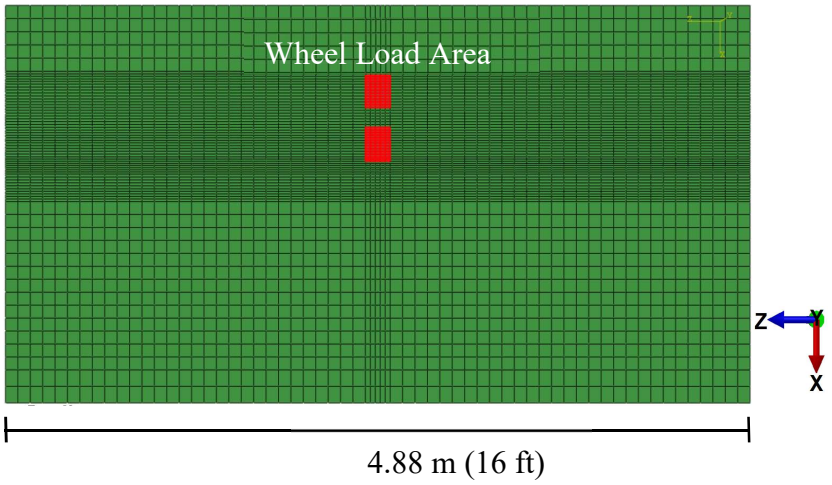

Figure 6-4 Plan view of Models 9 and 10 (z-x plane)

Figure 6-5 Truck, including two tandem axles, each with dual tires

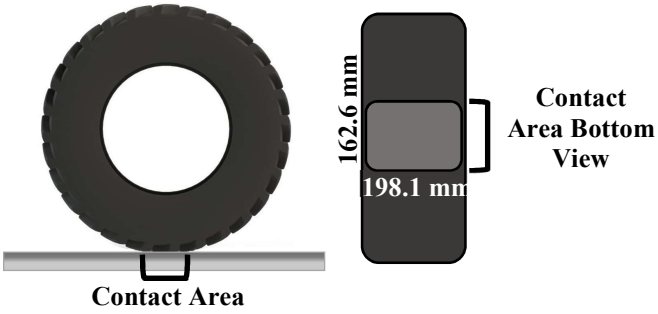

Figure 6-6 Wheel contact area

The permanent deformation (rutting) at the pavement surface predicted by Model 9 is plotted in Figure 6-7 for both the model output and the Feng et al. (1999) field results. Model 9 estimated approximatley 0.6 mm (0.024 in.) of rutting while the field data showed just slightly more than 0.5 mm (0.020 in.). The difference could be due to the effects of “wheel wonder,” which was not considered in the finite element analysis.

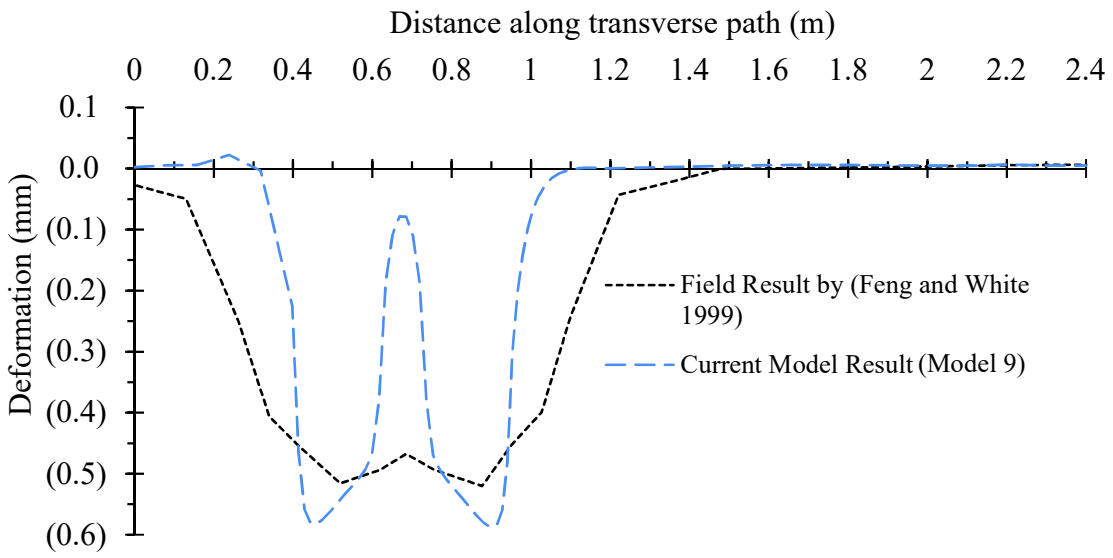

Figure 6-7 Predicted surface deformations after 10,000 truck applications, Model 9.

6.5 Effect of Fully Saturated Pavement Condition

When performing the finite element analysis using Model 9, the effect of moisture was not considered. Therefore, Model 10 was constructed to perform coupled pore fluid flow diffusion and mechanical stress analysis, i.e. to predict the amount of pavement rutting for a fully saturated condition. This represents a condition in which the pavement either does not have a drainage system, or the drainage system cannot efficiently remove the moisture from the pavement, for example when the outlet pipes are clogged. Missing of not functioning drainage system causes the pavement subgrade to become fully saturated.

The Model 9 (dry) and Model 10 (fully saturated) pavement deformation results are presented in Figure 6-8. The fully saturated model (Model 10) predicts an 18 percent increase in the deformation, from 0.6 mm (0.024 in.) to 0.7 mm (0.028 in.), when compared to the dry model.

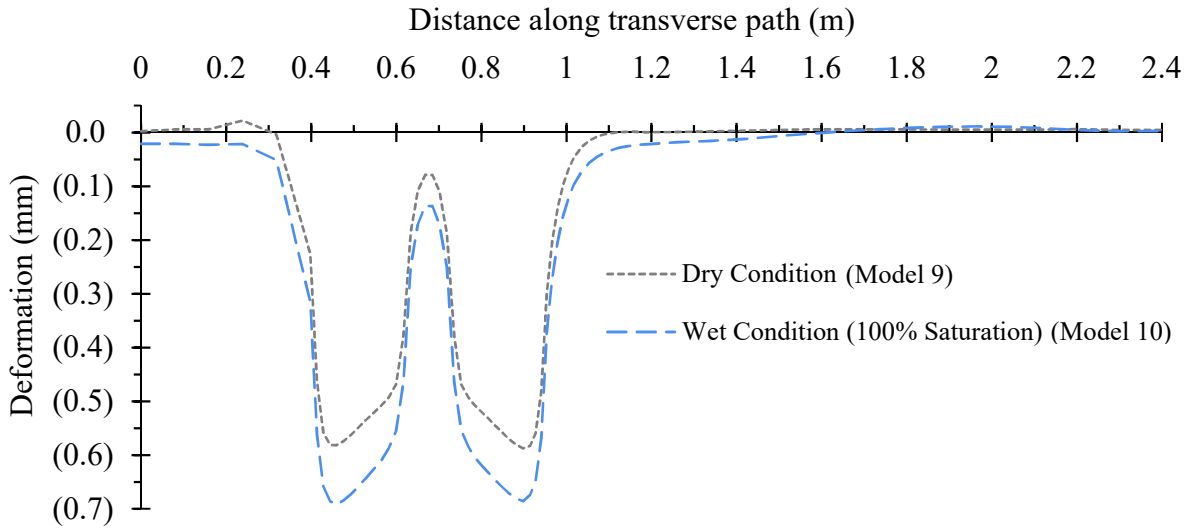

Figure 6-8 Predicted deformations after 10,000 truck applications under dry and fully saturated pavement conditions.

6.6 Effect of Partially Saturated Pavement Condition

Changes were needed in Model 10 in order to be able to perform rutting analysis in partially saturated conditions (70% subgrade saturation). Accordingly, an 8-node brick, trilinear displacement, trilinear pore pressure, reduced integration "C3D8RP" element was used for the subgrade soil, granular aggregate filter, and trench, while element type "C3D8R" an 8-node linear brick, reduced integration element was used for the other pavement layers. Therefore, trilinear pore pressure only was applied to the subgrade soil and unbound aggregates. The model simulation began with a "GEOSTATIC" step, to apply a gravity load to the pavement, then continued with a "SOIL" step, to simulate the coupled transient flow and stress response of the pavement under wheel loads. The model deformation results under various moisture conditions (dry and partially saturated, and fully saturated) and 10,000 truck applications are plotted in Figure 6-9. Partial saturation results in deformations slightly greater than those predicted for dry pavements, but slightly lower than for the fully saturated pavement.

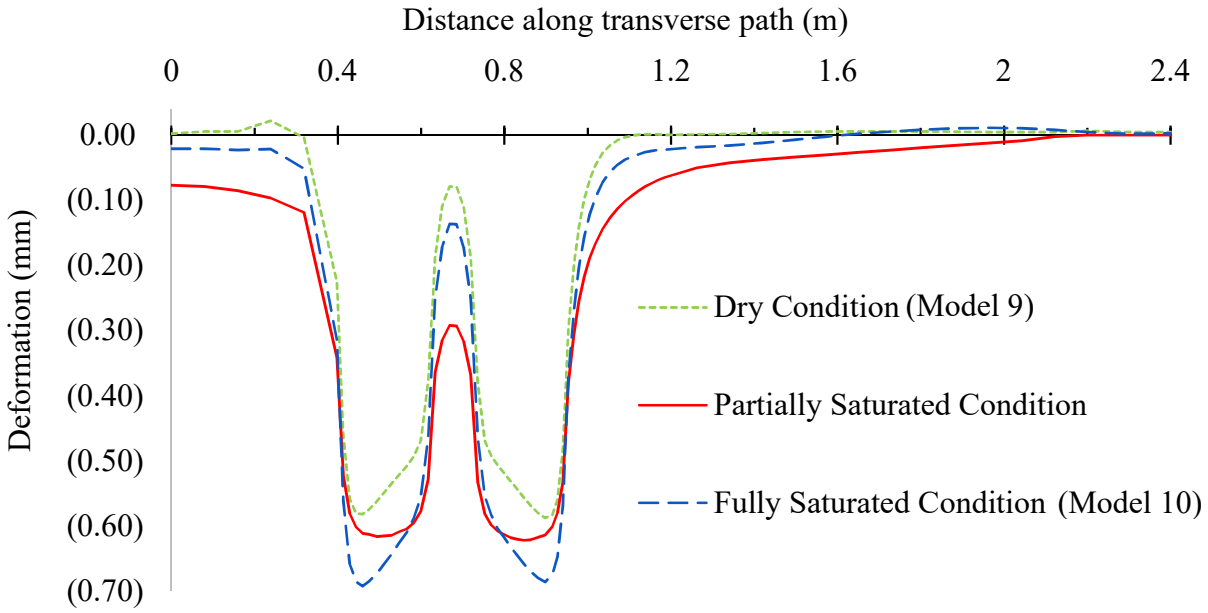

Figure 6-9 Predicted deformations after 10,000 truck applications under dry, partially saturated, and fully saturated subgrade conditions

6.7 Current Typical Indiana Flexible Pavement Sections

Using finite element modeling, additional rutting analyses were performed to estimate the deformation of current typical INDOT pavement sections; their general cross-sections are shown in Figure 6-10. “Drained” and “undrained” refer to the pavement cross-sections with and without a drainage layer, respectively. However, edge drains are included in both. The thickness of pavements layers were adopted from the INDOT design specification as shown in Tables 6-3 and 6-4. The INDOT specification suggests considering six undrained and nine drained flexible pavement sections. The pavement thicknesses were 0.25 m (10 in.) for the undrained sections and 0.32 to 0.42 m (12.5 to 16.5 in.) for the drained sections. The model parameters were similar to those used in the dry model (Model 9). The general finite element meshes and loading condition for the pavement section are presented in Figure 6-11.

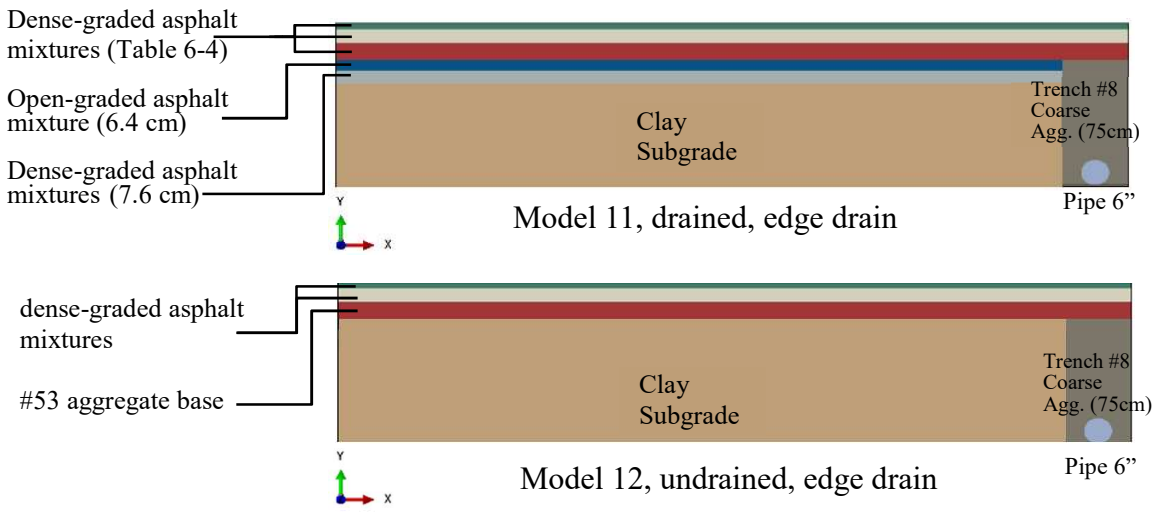

Figure 6-10 Pavements cross-sections

Table 6-3 Recommended thicknesses for undrained flexible pavements (Indiana Department of Transportation, 2013)

Section Number	HMA Pavement Thickness, cm (in)	Layer No.	Course	Lay Rate, lb./yd^2	Mixture Type, mm	Layer Thickness, cm (in)
1	10.2 (4.0)	1	Surface	165	9.5	
		2	Intermediate	275	19.0	
		3	# 53 Aggregate Base	-	-	15.2 (6.0)
2	11.4 (4.5)	1	Surface	165	9.5	
		2	Intermediate	330	19.0	
		3	# 53 Aggregate Base	-	-	14.0 (5.5)
3	11.4 (4.5)	1	Surface	220	12.5	
		2	Intermediate	275	19.0	
		3	# 53 Aggregate Base	-	-	14.0 (5.5)
4	12.7 (5.0)	1	Surface	220	12.5	
		2	Intermediate	330	19.0	
		3	# 53 Aggregate Base	-	-	12.7 (5.0)
5	14.0 (5.5)	1	Surface	220	12.5	
		2	Intermediate	385	19.0	
		3	# 53 Aggregate Base	-	-	11.4 (4.5)
6	15.2 (6.0)	1	Surface	220	12.5	
		2	Intermediate	440	25.0	
		3	# 53 Aggregate Base	-	-	10.2 (4.0)

Table 6-4 Recommended thicknesses for drained flexible pavements (Indiana Department of Transportation, 2013)

Section Number	Full Depth Asphalt Thickness, cm (in)	Layer No.	Course	Lay Rate, lb./yd^2	Mixture Type, mm
1	31.8 (12.5)	1	Surface	165	9.5
		2	Intermediate	275	19.0
		3	Base	330	19.0
		4	Intermediate Open Graded	250	19.0
		5	Base	330	19.0
2	33.0 (13.0)	1	Surface	165	9.5
		2	Intermediate	275	19.0
		3	Base	330	19.0
		4	Intermediate Open Graded	250	19.0
		5	Base	330	19.0
3	34.3 (13.5)	1	Surface	165	9.5
		2	Intermediate	275	19.0
		3	Base	330	19.0
		4	Intermediate Open Graded	250	19.0
		5	Base	330	19.0
4	35.6 (14)	1	Surface	165	9.5
		2	Intermediate	275	19.0
		3	Base	330	25.0
		4	Intermediate Open Graded	250	19.0
		5	Base	330	19.0
5	36.8 (14.5)	1	Surface	165	9.5
		2	Intermediate	275	19.0
		3	Base	330	25.0
		4	Intermediate Open Graded	250	19.0
		5	Base	330	19.0
6	38.1 (15.0)	1	Surface	165	9.5
		2	Intermediate	275	19.0
		3	Base	330	25.0
		4	Intermediate Open Graded	250	19.0
		5	Base	330	19.0
7	39.4 (15.5)	1	Surface	165	9.5
		2	Intermediate	275	19.0
		3	Base	330	25.0
		4	Intermediate Open Graded	250	19.0
		5	Base	330	19.0
8	40.6 (16.0)	1	Surface	165	9.5
		2	Intermediate	275	19.0
		3	Base	330	25.0
		4	Intermediate Open Graded	250	19.0
		5	Base	330	19.0
9	41.9 (16.5)	1	Surface	165	9.5
		2	Intermediate	275	19.0
		3	Base	330	25.0
		4	Intermediate Open Graded	250	19.0
		5	Base	330	19.0

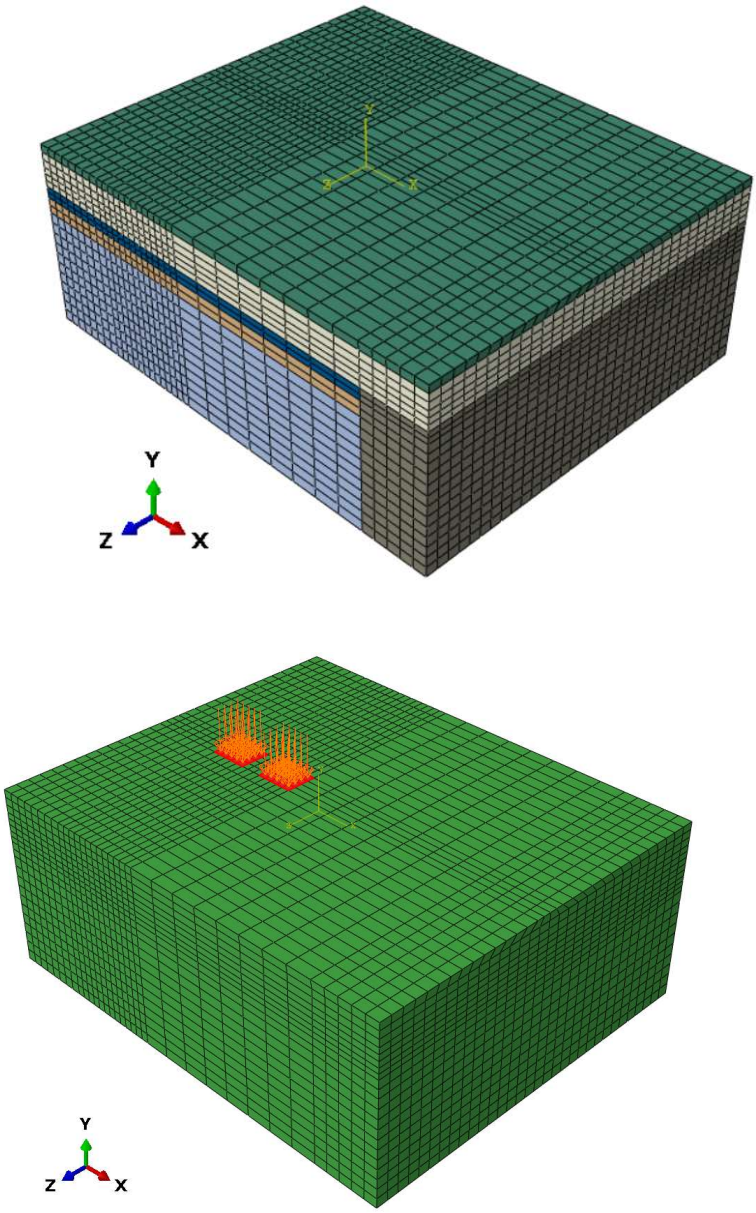

Figure 6-11 Finite element meshes and wheel loading area

The surface deformation of the drained and undrained pavement sections subjected to the various traffic loads are shown in Tables 6-5 and 6-6. It should be noted that in the analyses, the deformations that occur due to the asphalt pavement layers being subjected to traffic loads occur only during the hottest seasons, when the pavement surface temperatures reach or exceed or 40C

(104°F). However, subgrade deformation can occur throughout the pavement life, regardless of pavement surface temperature. This was not accounted for in these models.

Table 6-5 Deformation as a function of daily truck traffic, undrained pavement sections

Traffic (trucks/day)	Deformation (in.)				
	Section 1	Section 2	Section 3	Section 4	Section 5
100	0.02	0.02	0.02	0.02	0.02
200	0.03	0.03	0.03	0.02	0.02
500	0.04	0.04	0.04	0.04	0.03
1000	0.06	0.06	0.05	0.05	0.04
2000	0.08	0.07	0.07	0.06	0.06
5000	0.10	0.09	0.09	0.08	0.07
10000	0.12	0.12	0.12	0.10	0.09
15000	0.14	0.13	0.13	0.12	0.10
20000	0.15	0.14	0.14	0.12	0.11
30000	0.16	0.16	0.15	0.14	0.12
50000	0.18	0.18	0.17	0.16	0.14

Table 6-6 Deformation as a function of daily truck traffic, drained pavement sections

Traffic (trucks/day)	Deformation (in.)								
	Section 1	Section 2	Section 3	Section 4	Section 5	Section 6	Section 7	Section 8	Section 9
100	0.05	0.05	0.05	0.05	0.05	0.05	0.05	0.04	0.04
200	0.06	0.06	0.06	0.06	0.06	0.06	0.06	0.05	0.04
500	0.08	0.08	0.07	0.07	0.07	0.07	0.07	0.06	0.06
1000	0.09	0.09	0.08	0.08	0.08	0.08	0.08	0.07	0.07
2000	0.10	0.10	0.10	0.10	0.10	0.09	0.09	0.08	0.08
5000	0.13	0.13	0.12	0.12	0.12	0.12	0.11	0.11	0.10
10000	0.15	0.15	0.14	0.14	0.14	0.13	0.13	0.12	0.12
15000	0.17	0.16	0.16	0.16	0.15	0.15	0.14	0.14	0.13
20000	0.18	0.18	0.17	0.17	0.16	0.16	0.16	0.15	0.14
30000	0.20	0.20	0.19	0.18	0.18	0.17	0.17	0.16	0.16
50000	0.22	0.22	0.21	0.21	0.20	0.20	0.19	0.18	0.17

CHAPTER 7. EFFECTS OF TRAFFIC LOADINGS ON PAVEMENT SUBGRADES

Subgrade provides the underlying structural support for flexible pavements and thus plays a significant role in flexible pavement performance; excessive subgrade deformation usually results in serious pavement distress. In the analyses presented in Chapter 6, the main goal was to predict the amount of permanent deformation (rutting) for flexible pavements subjected to a simulated, specified number of repeated traffic loads while the pavement surface temperature was at, or above 40°C (104F°). However, the deformation of subgrade due to the traffic loading during the entire pavement design life was not considered. Subgrade deflection can occur during any portion of the pavement design life, while the asphalt mixture plastic creep rutting is insignificant during low-temperature seasons. Therefore, in this chapter, results are presented from the study of drainage system effectiveness by estimating the deformation of typical Indiana subgrade soils combined with asphalt mixture creep rutting, when subjected to the truck traffic applications and moisture variations, allowing subgrade deformations to occur at any time during the pavement life.

Again, the ABAQUS software was used because it can perform coupled pore fluid flow diffusion and stress analysis to simulate subgrade hydromechanical response under wheel loads. The modified Drucker-Prager/Cap and Extended Drucker-Prager mechanical constitutive models were selected to model the subgrade soils and pavement materials respectively, to simulate the nonlinear materials behavior.

7.1 Model Parameters

Three typical Indiana subgrade soils, an A-4, A-6, and A-7-6 were selected and their material properties (see Table 7-1) were adopted from the study of Ji et al. (2014). The modified Drucker-

Prager/Cap parameters for the subgrade materials are presented in Table 7-2 Liu and Muhunthan (2016). Additionally, the cap hardening function for soil materials, which relates the hydrostatic compression yield stress and plastic volumetric strain, used in the finite element analyzes were adopted from Liu and Muhunthan (2016) and are shown for different saturation conditions in Figures 7-1, 7-2, and 7-3.

Table 7-1 Typical Indiana subgrade soil properties (Ji et al., 2014)

AASHTO Soil type	Specific gravity, G_s	Dry unit weight γ_{dry} (kN/m^3)	Saturated unit weight, γ_{sat} (kN/m^3)	Initial void ratio	Saturated permeability K_{sat} (m/sec)
A-4	2.66	18.1	21.1	0.4	3E-10
A-6	2.67	17.8	20.9	0.5	5.5E-10
A-7-6	2.70	16.6	20.3	0.6	2.5E-09

Table 7-2 Modified Drucker-Prager/Cap model parameters for the soil subgrades (Liu & Muhunthan, 2016)

AASHTO Soil Type	Angle of friction, β	Poisson's ratio, v	Cohesion, *C (kPa)*	Aspect ratio of cap surface, *R*	Initial cap yield surface position on the volumetric inelastic strain axis	Transition surface radius parameter, α	Flow stress ratio, K
A-4	36	0.3	13.9	5.57	0	0.01	1
A-6	28	0.3	70.8	5.44	0	0.01	1
A-7-6	36	0.3	58.4	5.57	0	0.01	1

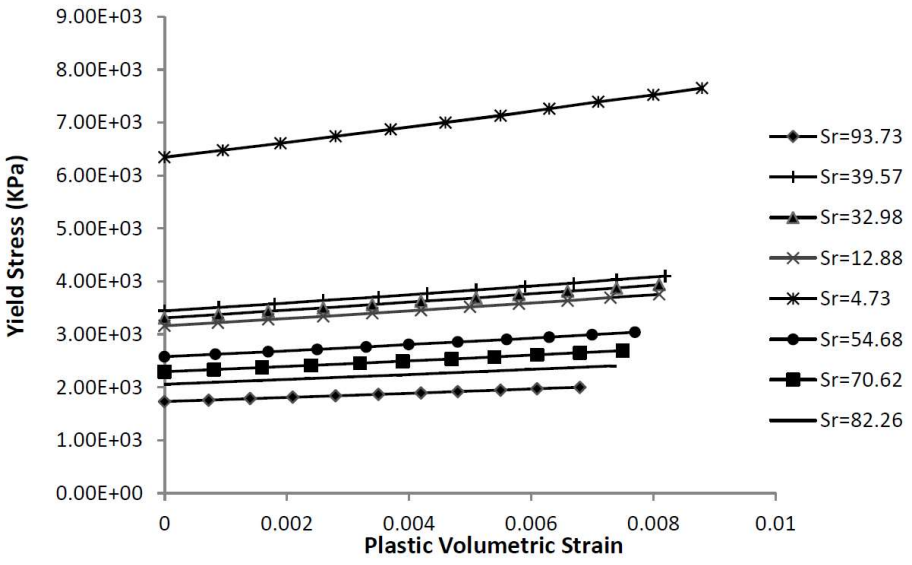

Figure 7-1 A-4 soil cap hardening function for different saturation conditions (Liu & Muhunthan, 2016)

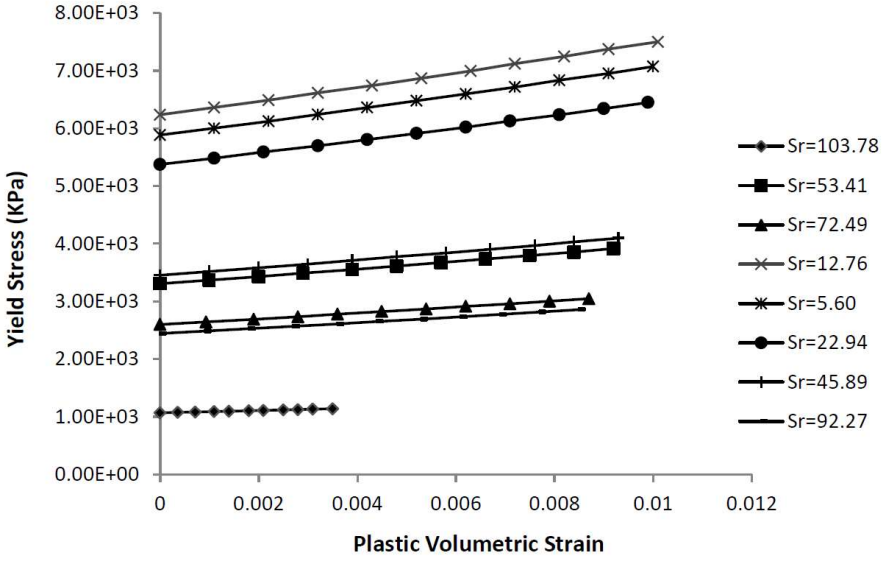

Figure 7-2 A-6 soil cap hardening function for different saturation conditions (Liu & Muhunthan, 2016)

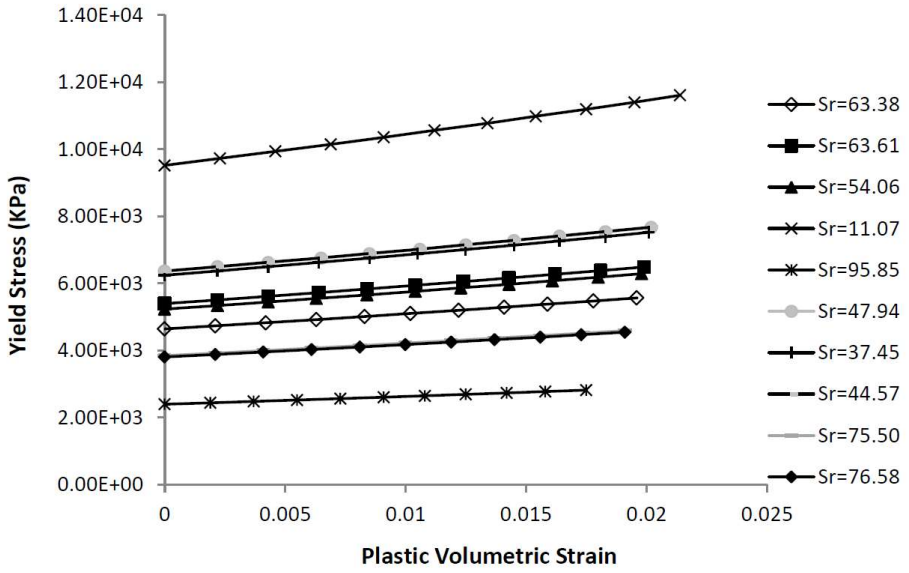

Figure 7-3 A-7-6 soil cap hardening function for different saturation conditions (Liu & Muhunthan, 2016)

7.2 Geometry and Finite Element Mesh

Typical INDOT flexible pavement cross-sections (drained and undrained) consisting of a 4.25 m (14 ft.) wide section placed over the three different soil subgrades (A-4, A-6, A-7-6) were used for the study. As already mentioned in section 6.7, the current INDOT specification suggest consideration of six undrained and nine drained asphalt pavement sections, as shown in Tables 6-5 and 6-6. The pavement thicknesses were considered 0.25 m (10 in.) for the undrained sections and 0.32 to 0.42 m (12.5 to 16.5 in.) for the drained sections. The geometry of the pavement cross-sections used for the computer models is shown in Figure 7-4.

The two-dimensional (2D) computer mesh used in theses models is presented in Figure 7-5. In the computer analyss, an 8-node plane-strain quadrilateral, biquadratic displacement, bilinear pore pressure, reduced integration (CPE8RP) element was used for the soil subgrade, and an 8-node biquadratic plane stress quadrilateral, reduced integration (CPS8R) element for the asphalt layers.

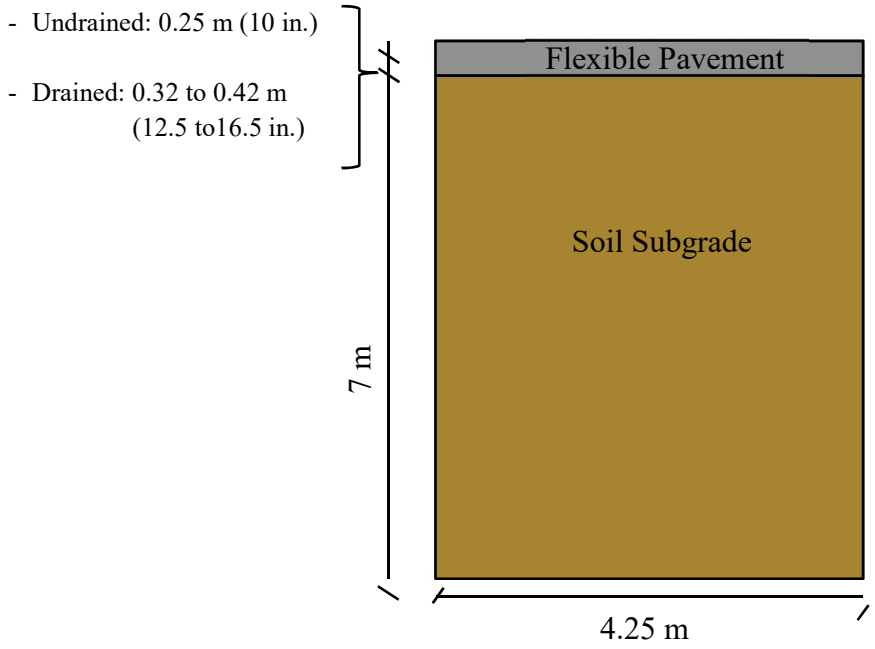

Figure 7-4 Flexible pavement cross-section geometry

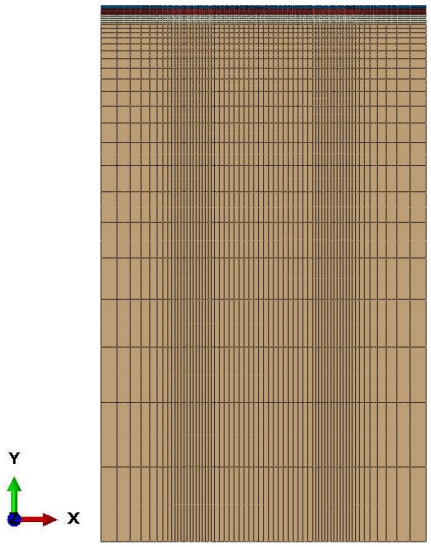

Figure 7-5 Two-dimensional mesh of computer models

7.3 Boundary Conditions

Both the right and left side boundaries are fixed only in the horizontal direction ($u_x = 0$). Additionally, the bottom side is fixed in the vertical and horizontal directions ($u_x = u_y = 0$). Zero pore-pressure at the bottom of pavement is considered to simulate perfect drainage.

7.4 Loading

Various traffic loads were applied to the models, similar to the assumption by Feng et al. (1999). The location of the applied wheel loads is shown in Figure 7-6. A total loading time of 20 years and various number of trucks per day (100 to 50000 trucks/day) were assumed in the traffic analysis. Wheel contact area is shown in Figure 6-6. Total loading time was determined based on the time (0.0061 sec) for the number of trucks to travel the length of a wheel contact area moving at a speed of 96 km/hour (60 mph); a tire contact pressure 630 KPa (91 psi) was used in the model.

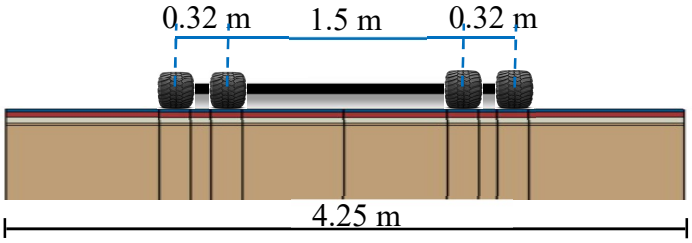

Figure 7-6 Cross-section view of dual tire loading in the computer models

7.5 Finite Element Analysis

Simulations began by applying initial stress conditions along with the effective self-weight of the pavement section to assure equilibrium was satisfied within the subgrade soil. In this step, no drainage was allowed at the bottom of the section and the zero-pore pressure was not considered. The analysis continued by simulating the coupled transient flow and stress response of the pavement under wheel loads. First, the 630 kPa (91 psi) wheel loads were applied to generate a

nonuniform pore pressure throughout the soil layer, specifically near the applied load. All applied stress was carried entirely by the pore water pressure and no stress was taken by the soil skeleton. In this condition, the zero-pore pressure at the bottom of the section was considered to allow drainage, and the consolidation was performed during the specified loading time.

The model results of vertical subgrade deformation underneath the drained and undrained pavements obtained for various traffic loads and three subgrade soil types as shown in Appendix A, Tables A-1 to A-14. Additionally, the results for the saturated (100% saturated) and partially saturated (70% saturation) subgrade soils for the pavement Sections 4 (undrained) and 5 (drained) are plotted in Figure 7-7. The results for the other sections are plotted in Figures 7-8 and 7-9. The results indicate that in each case, the removal of moisture from the subgrade soil, resulted in reduced deformation.

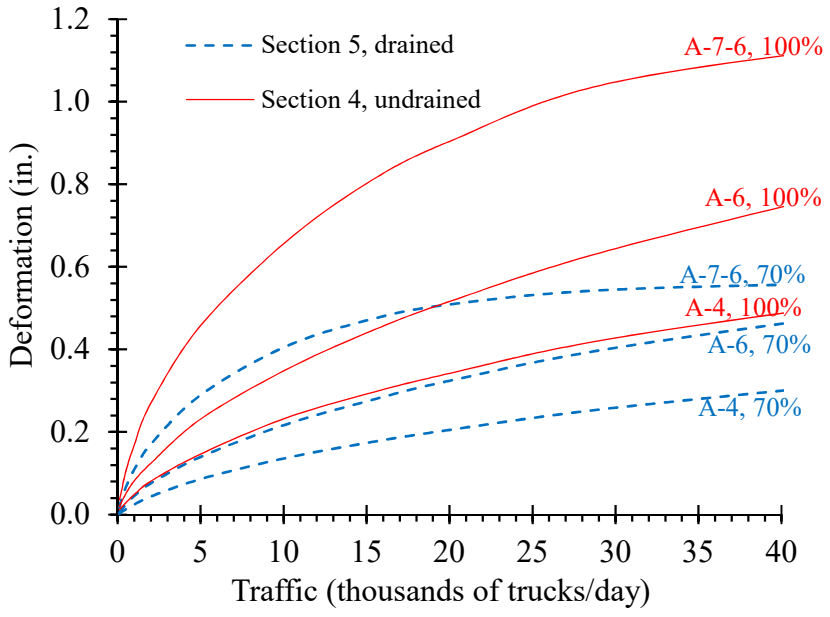

Figure 7-7 Subgrade soil deformation as a function of traffic

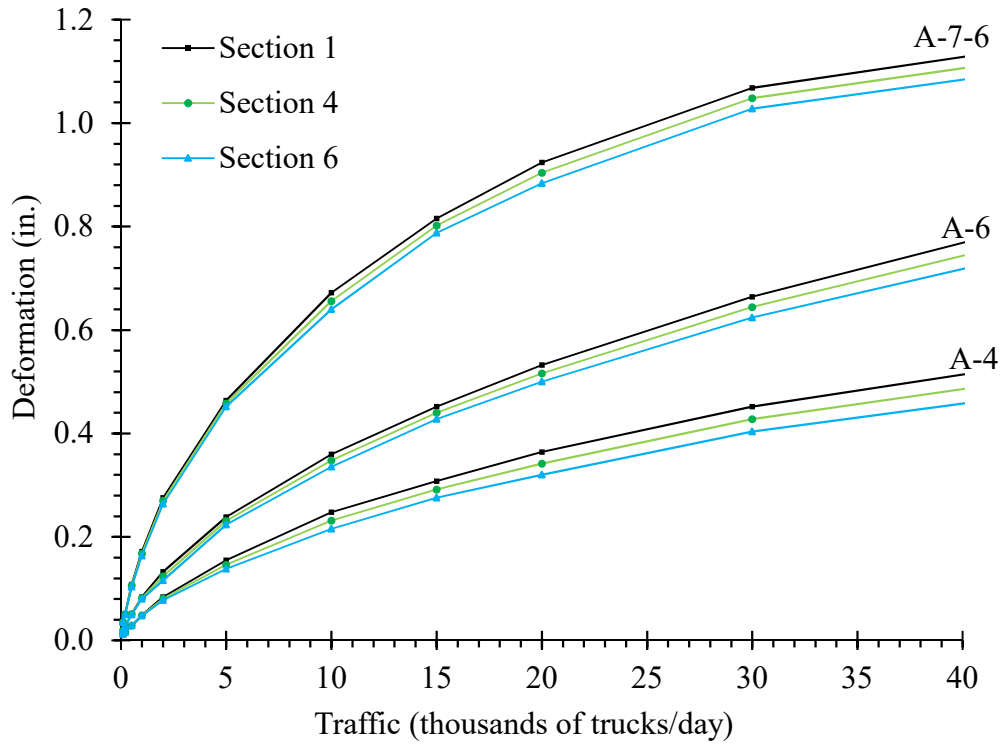

Figure 7-8 Saturated subgrade soil deformation as a function of traffic

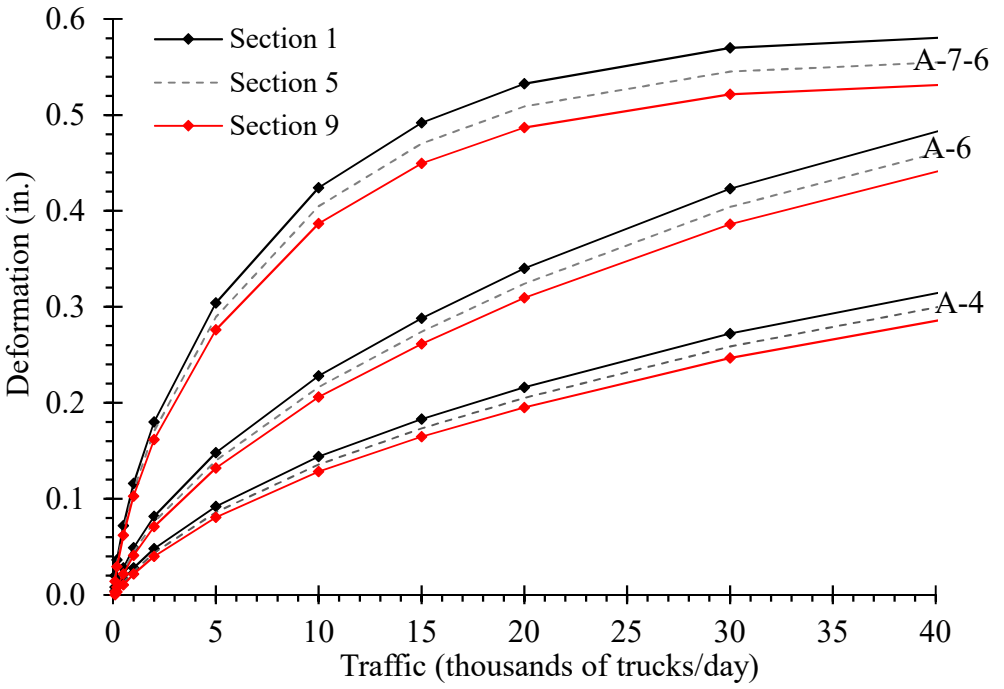

Figure 7-9 Partially saturated subgrade soil deformation as a function of traffic

7.6 Assessing the Need for Pavement Drainage

While subgrade deformation can happen at any point during pavement life, deformation caused in the asphalt mixture mostly occurs during warmer seasons. To account for both deformation types, the estimated flexible pavement asphalt mixture deformation was added to the estimated subgrade deformation, over 20 years of pavement life. The results are in Appendix A, Tables A-15 to A-28 and are shown plotted in Figures 7-10 and 7-11.

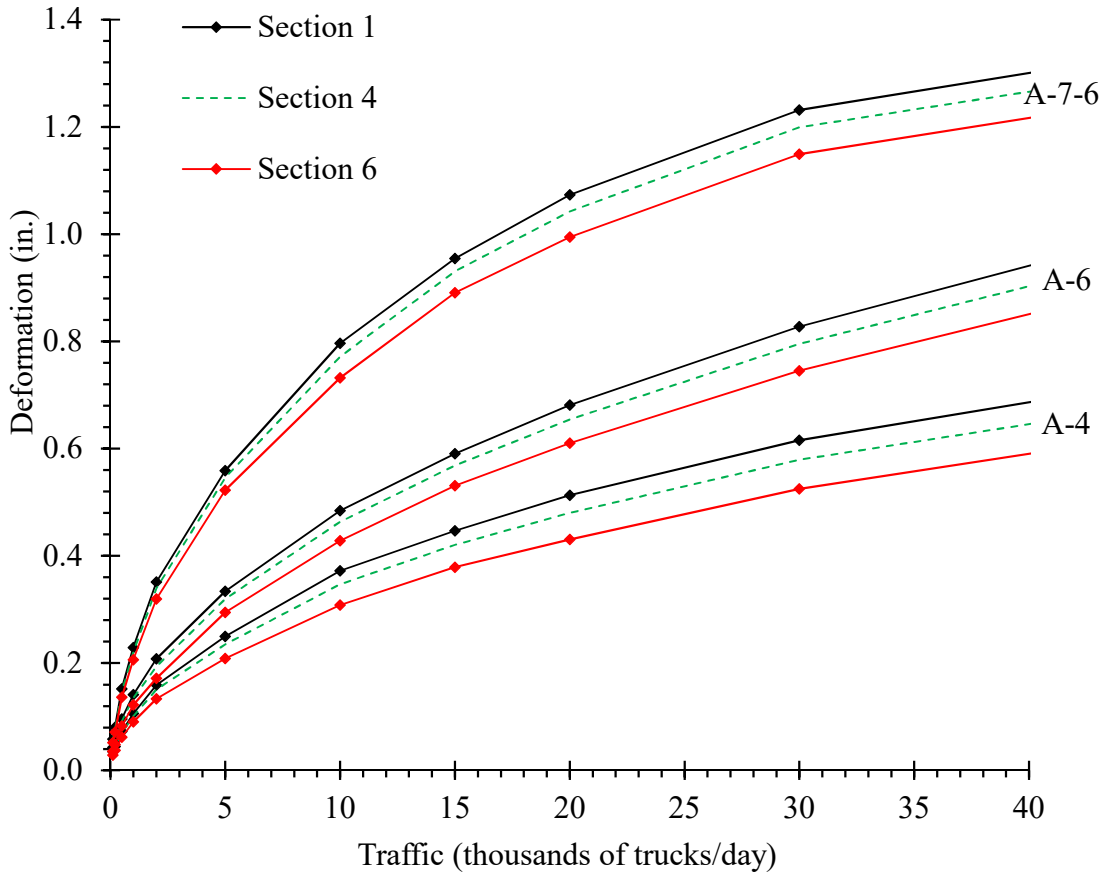

Figure 7-10 Estimated 20-years of total pavement deformation as a function of truck traffic with fully saturated subgrade

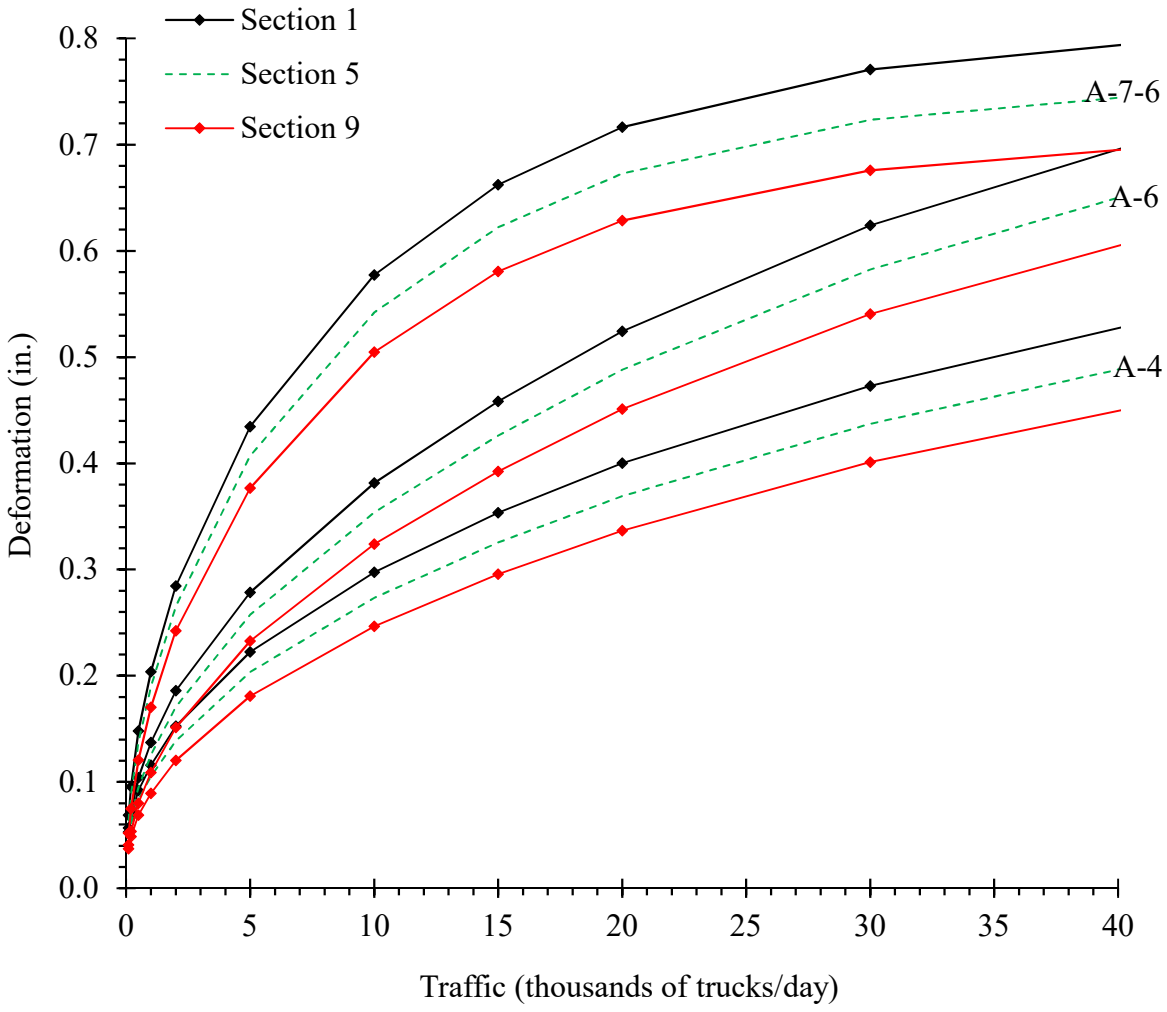

Figure 7-11 Estimated 20-years of total flexible pavement deformation as a function of truck traffic with partially saturated subgrade

For the flexible pavements, those sections without drainage systems that result in a fully saturated subgrade condition, if the total pavement deformation value stays below the INDOT limit of 10 mm (0.4 in.) for the expected truck traffic, then a drainage system is likely not required.

CHAPTER 8. FIELD VALIDATION AND LONG-TERM MONITORING PLAN

8.1 Monitoring Plan

To further validate the findings of this study, an experimental field study is proposed to examine the as-built performance of flexible pavement drainage systems. Such a study will involve selecting, instrumenting, and collecting data from various flexible pavements in Indiana. Study factors and levels will include: subgrade type (A-4, A-6, A-7-6), pavement drainage layer (drainage layer, no drainage layer), drainage layer type (granular, bound), edge drains (edge drains, no edge drains), and truck traffic (low, medium, high). It would be good to complete a full factorial experiment but is likely that some of the factor combinations are not used by INDOT. For example, finding sections with high traffic and no drainage is unlikely, since INDOT currently incorporates drainage into all high traffic flexible pavements.

The pavements identified for inclusion in the study will be instrumented and status and performance data collected. Environmental and precipitation data including moisture content through a pavement section, temperature, groundwater elevation, frost penetration, rainfall and outflow from edge drains can be monitored. Pavement data such as stress and strain responses along with performance data such as rutting (deformation) and cracking can be collected as well. This combined data set can be used to validate the findings of the current study.

8.2 Field Instrumentation

The field instrumentation will include strain gauges, moisture and temperature sensors for all pavement layers, and weather stations. Additionally, the pavements in the study will be periodically monitored using a falling weight deflectomer (FWD) and the pavements' in-situ layer

modulii determined. Finally, surface profile measurements will be used to determine pavement surface rutting as well as individual layer rutting.

8.2.1 Strain Gauges

Strain gauges (Figure 8-1) are designed to measure horizontal or vertical strains in the pavement structure and can be installed at each pavement layer interface. It is suggested that horizontal strain gauges be placed at the bottom of each bound layer and vertical strain gauges at the top of the subgrade, to measure the critical tensile and compressive strains under traffic loading. Additionally, strain gauges should be placed at the top and bottom of the open-graded drainage layers, to evaluate the behavior of these layers under traffic loads.

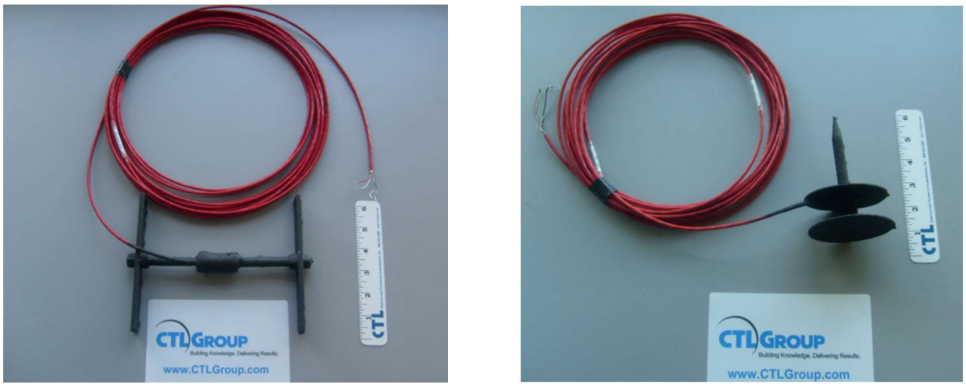

a. Horizontal strain gauge b. Vertical strain gauge

Figure 8-1 Asphalt horizontal and vertical strain gauges (CTLGroup Inc.)

8.2.2 Earth Pressure Cells

Earth pressure cells or total stress cells (Figure 8-2) can measure the vertical stresses in soil structure that can be used in the determination of soil behavior under loads. Earth pressure cells can be installed along with the strain gauges within the pavement structure. Cells respond to both soil pressure and pore water pressure, resulting in total stress (σ). Thus effective stress can be determined based on Terzaghi's principle of effective stress (Geokon, 2017):

$$\sigma = \sigma' + u \tag{8.1}$$

where σ' is the effective stress and u is the pore water pressure.

Figure 8-2 Geokon model 3500 - Earth pressure cell (Geokon, 2017)

8.2.3 Thermocouple and Integrated Soil Moisture and Temperature Sensors

Thermocouples and moisture probes can be used separately to measure the temperatures and moisture respectively, or integrated soil moisture and temperature sensors (Figure 8-3) can be used to measure and record both temperature and moisture at various locations in the pavements.

Figure 8-3 Integrated soil moisture-temperature sensor (METER Group Inc.)

8.2.4 Pavement Surface Profile Measurement Using Laser Profiler

An automatic laser profiler can automatically measure the total pavement rutting by scanning the pavement surface, while pavement surveys can be done to gather other data such as cracking.

8.2.5 Weather Station

A weather station (Figure 8-4) with the capability of monitoring air temperature, and rainfall can be installed to record rainfall events and temperature.

Figure 8-4 Weather station with wireless capability (RainWise Inc.)

CHAPTER 9. SUMMARY, CONCLUSIONS, AND RECOMMENDATIONS

9.1 Summary and Conclusion

The main objective of the study was to evaluate the effectiveness of the flexible pavement drainage system currently specified by INDOT, and determine if such systems are necessary for current INDOT flexible pavement cross-sections, given contemporary materials and construction specifications. Specifically, the effect of a pavement drainage layer was investigated to see if such a layer acts to reduce pavement subgrade moisture. Also, the effect of filter material type (unbound #53 granular aggregate versus bound #5D dense-graded asphalt mixture) was examined to determine its impact on the pavement subgrade moisture. Moreover, the effectiveness of edge drains in flexible pavements without a drainage layer was studied. Finally, the rutting characteristics of the open-graded drainage layers were examined under various traffic loads and subgrade moisture conditions.

These objectives were addressed by determining the hydraulic properties of asphalt mixture samples in the laboratory, including saturated permeability and water characteristic curves, using the results in flexible pavement finite element modeling of sections with and without drainage layers. Additionally, the DRIP program was used to determine which materials might perform better as drainable base materials in a saturated state. Finally, finite element analysis was conducted to investigate the rutting performance of flexible pavement drainage layers under various traffic loads and subgrade moisture conditions. Additionally, typical Indiana subgrade soils (A-4, A-6, A-7-6) subjected to the various truck traffic were analyzed.

Laboratory experiments were performed to determine the hydraulic properties of asphalt mixtures produced using current INDOT design specifications. Accordingly, saturated

permeability testing and filter paper testing were conducted to determine the hydraulic properties of dense- and open-graded asphalt mixtures, result in determining their saturated permeability and water characteristic curve functions for use in the numerical analysis of unsaturated water flow in flexible pavements.

The modeling results indicate that flexible pavement drainage systems can affect the amount of moisture in the pavement subgrade, as well as the various pavement layers. A proper drainage system is able to effectively lower the moisture content throughout the pavement layers and subgrade. These lower moisture contents should translate to improved pavement performance. Specific findings from the project are that INDOT's current flexible pavement drainage system, combining an open-graded drainage layer with edge drains, can be an effective tool in preventing the pavement subgrade from staying saturated for extended periods of time. Additionally, the use of a dense-graded granular filter layer beneath the open-graded drainage layer more effectively prevents the pavement subgrade from reaching fully saturated levels than does a dense-graded asphalt filter layer. Therefore, in the areas with a higher rainfall or high-water tables, the use of a dense-graded granular filter layer should be considered. Moreover, results indicate the positive effect of using edge drains in flexible pavements, especially when no drainage layer is included in the pavement. In general, the results of the finite element analyses suggests that INDOT's current flexible pavement drainage systems that make use of Superpave designed asphalt mixtures are more effective in preventing moisture from reaching the subgrade than was the older system which used asphalt mixtures designed with the Marshall mixture design method. However, while the current INDOT materials and construction specifications appear to do a better job than the older materials and construction specifications of protecting the subgrade from moisture intrusion, the modeling indicated that a drainage system is still needed to protect the subgrade from moisture.

The FE Models also could successfully predict the rutting in the flexible pavement that includes drainage layer. The effect of moisture on pavement rutting was considered under fully and partialy saturated conditions. Results showed an increase in rutting whenever moisture was presented. Thus, the effectiveness of pavement drainage system was confirmed, and from the FE analysis results, the need for pavement drainage system was identified.

9.2 Recommendations

Given the results of the finite element modeling, it appears that INDOT's current use of drainage systems in flexible pavements is warranted. However, it is essential for pavement designers to understand that while an adequate drainage system can extend the life of the pavement, the cost-effectiveness of such a system must be determined and weighed against the extended pavement life it might provide. For example, flexible pavements built on better subgrades and carrying relatively low amounts of truck traffic will usually not warrant drainage layers; it would not be cost effective. As seen in Figure B-3, using the INDOT trigger of 10 mm (0.4 in.) of rutting, on average, the undrained pavement sections can withstand approximately 15,000 trucks per day.

Given the results of this study, it is recommended that INDOT implement better design guidance on when flexible pavement drainage layers must be used. Additionally, such guidance can be used to determine if, and when drainage systems should be installed in existing pavements.

Finally, a field validation study should be completed in order to verify the results of this study. Instrumenting flexible pavement field sections will provide data to lend additional guidance to the findings of this study.

APPENDIX A: FINAL RESULTS-TABLES

Table A-1 Saturated subgrade soil deformation as a function of traffic, Section 1

Traffic (trucks/day)	Subgrade Deformation (in.)		
	A-4	A-6	A-7-6
100	0.01	0.02	0.04
200	0.02	0.03	0.05
500	0.03	0.05	0.11
1000	0.05	0.08	0.17
2000	0.08	0.13	0.28
5000	0.15	0.24	0.46
10000	0.25	0.36	0.67
15000	0.31	0.45	0.82
20000	0.36	0.53	0.92
30000	0.45	0.66	1.07
50000	0.58	0.87	1.19

Table A-2 Saturated subgrade soil deformation as a function of traffic, Sections 2 and 3

Traffic (trucks/day)	Subgrade Deformation (in.)		
	A-4	A-6	A-7-6
100	0.01	0.02	0.04
200	0.02	0.03	0.05
500	0.03	0.05	0.11
1000	0.05	0.08	0.17
2000	0.08	0.12	0.27
5000	0.15	0.23	0.46
10000	0.23	0.35	0.66
15000	0.29	0.44	0.80
20000	0.34	0.52	0.90
30000	0.43	0.64	1.05
50000	0.54	0.84	1.16

Table A-3 Saturated subgrade soil deformation as a function of traffic, Section 4

Traffic (trucks/day)	Subgrade Deformation (in.)		
	A-4	A-6	A-7-6
100	0.01	0.02	0.04
200	0.02	0.03	0.05
500	0.03	0.05	0.11
1000	0.05	0.08	0.17
2000	0.08	0.12	0.27
5000	0.15	0.23	0.46
10000	0.23	0.35	0.66
15000	0.29	0.44	0.80
20000	0.34	0.52	0.90
30000	0.43	0.64	1.05
50000	0.56	0.86	1.18

Table A-4 Saturated subgrade soil deformation as a function of traffic, Section 5

Traffic (trucks/day)	Subgrade Deformation (in.)		
	A-4	A-6	A-7-6
100	0.01	0.02	0.04
200	0.02	0.03	0.05
500	0.03	0.05	0.10
1000	0.05	0.08	0.17
2000	0.08	0.12	0.27
5000	0.14	0.23	0.46
10000	0.22	0.34	0.65
15000	0.28	0.44	0.80
20000	0.33	0.51	0.90
30000	0.42	0.64	1.04
50000	0.53	0.83	1.15

Table A-5 Saturated subgrade soil deformation as a function of traffic, Section 6

Traffic (trucks/day)	Subgrade Deformation (in.)		
	A-4	A-6	A-7-6
100	0.01	0.02	0.04
200	0.02	0.03	0.05
500	0.03	0.05	0.10
1000	0.05	0.08	0.16
2000	0.08	0.12	0.26
5000	0.14	0.22	0.45
10000	0.22	0.34	0.64
15000	0.28	0.43	0.79
20000	0.32	0.50	0.88
30000	0.40	0.62	1.03
50000	0.51	0.81	1.14

Table A-6 Partially saturated subgrade soil deformation as a function of traffic, Section 1

Traffic (trucks/day)	Subgrade Deformation (in.)		
	A-4	A-6	A-7-6
100	0.00	0.01	0.02
200	0.01	0.01	0.04
500	0.02	0.03	0.07
1000	0.03	0.05	0.12
2000	0.05	0.08	0.18
5000	0.09	0.15	0.30
10000	0.14	0.23	0.42
15000	0.18	0.29	0.49
20000	0.22	0.34	0.53
30000	0.27	0.42	0.57
50000	0.36	0.54	0.59

Table A-7 Partially saturated subgrade soil deformation as a function of traffic, Section 2

Traffic (trucks/day)	Subgrade Deformation (in.)		
	A-4	A-6	A-7-6
100	0.00	0.01	0.02
200	0.01	0.01	0.04
500	0.02	0.03	0.07
1000	0.03	0.05	0.12
2000	0.05	0.08	0.18
5000	0.09	0.14	0.30
10000	0.14	0.22	0.42
15000	0.18	0.28	0.49
20000	0.21	0.34	0.53
30000	0.27	0.42	0.56
50000	0.35	0.54	0.58

Table A-8 Partially saturated subgrade soil deformation as a function of traffic, Section 3

Traffic (trucks/day)	Subgrade Deformation (in.)		
	A-4	A-6	A-7-6
100	0.00	0.01	0.02
200	0.01	0.01	0.04
500	0.02	0.03	0.07
1000	0.03	0.05	0.11
2000	0.04	0.08	0.18
5000	0.09	0.14	0.30
10000	0.14	0.22	0.42
15000	0.18	0.28	0.48
20000	0.21	0.33	0.52
30000	0.26	0.41	0.56
50000	0.35	0.53	0.58

Table A-9 Partially saturated subgrade soil deformation as a function of traffic, Section 4

Traffic (trucks/day)	Subgrade Deformation (in.)		
	A-4	A-6	A-7-6
100	0.00	0.00	0.02
200	0.00	0.01	0.03
500	0.01	0.02	0.07
1000	0.02	0.04	0.11
2000	0.04	0.08	0.17
5000	0.09	0.14	0.29
10000	0.14	0.22	0.41
15000	0.18	0.28	0.48
20000	0.21	0.33	0.52
30000	0.26	0.41	0.55
50000	0.34	0.52	0.57

Table A-10 Partially saturated subgrade soil deformation as a function of traffic, Section 5

Traffic (trucks/day)	Subgrade Deformation (in.)		
	A-4	A-6	A-7-6
100	0.00	0.00	0.02
200	0.00	0.01	0.03
500	0.01	0.02	0.07
1000	0.02	0.04	0.11
2000	0.04	0.08	0.17
5000	0.08	0.14	0.29
10000	0.14	0.22	0.40
15000	0.17	0.28	0.47
20000	0.20	0.32	0.51
30000	0.26	0.40	0.54
50000	0.34	0.52	0.56

Table A-11 Partially saturated subgrade soil deformation as a function of traffic, Section 6

Traffic (trucks/day)	Subgrade Deformation (in.)		
	A-4	A-6	A-7-6
100	0.00	0.00	0.02
200	0.00	0.01	0.03
500	0.01	0.02	0.06
1000	0.02	0.04	0.11
2000	0.04	0.08	0.17
5000	0.08	0.14	0.29
10000	0.13	0.21	0.40
15000	0.17	0.27	0.46
20000	0.20	0.32	0.50
30000	0.26	0.40	0.54
50000	0.34	0.51	0.56

Table A-12 Partially saturated subgrade soil deformation as a function of traffic, Section 7

Traffic (trucks/day)	Subgrade Deformation (in.)		
	A-4	A-6	A-7-6
100	0.00	0.00	0.02
200	0.00	0.01	0.03
500	0.01	0.02	0.06
1000	0.02	0.04	0.10
2000	0.04	0.07	0.16
5000	0.08	0.14	0.28
10000	0.13	0.21	0.40
15000	0.17	0.27	0.46
20000	0.20	0.32	0.50
30000	0.25	0.40	0.53
50000	0.33	0.51	0.55

Table A-13 Partially saturated subgrade soil deformation as a function of traffic, Section 8

Traffic (trucks/day)	Subgrade Deformation (in.)		
	A-4	A-6	A-7-6
100	0.00	0.00	0.02
200	0.00	0.01	0.03
500	0.01	0.02	0.06
1000	0.02	0.04	0.10
2000	0.04	0.07	0.16
5000	0.08	0.13	0.28
10000	0.13	0.21	0.39
15000	0.17	0.26	0.46
20000	0.20	0.31	0.49
30000	0.25	0.39	0.53
50000	0.33	0.50	0.55

Table A-14 Partially saturated subgrade soil deformation as a function of traffic, Section 9

Traffic (trucks/day)	Subgrade Deformation (in.)		
	A-4	A-6	A-7-6
100	0.00	0.00	0.02
200	0.00	0.01	0.03
500	0.01	0.02	0.06
1000	0.02	0.04	0.10
2000	0.04	0.07	0.16
5000	0.08	0.13	0.28
10000	0.13	0.21	0.39
15000	0.16	0.26	0.45
20000	0.20	0.31	0.49
30000	0.25	0.39	0.52
50000	0.32	0.50	0.54

Table A-15 Estimated 20-years of total flexible pavement deformation as a function of truck traffic with fully saturated subgrade, Section 1

Traffic (trucks/day)	Pavement Deformation (in.)		
	A-4	A-6	A-7-6
100	0.04	0.04	0.06
200	0.04	0.06	0.08
500	0.07	0.10	0.15
1000	0.10	0.14	0.23
2000	0.16	0.21	0.35
5000	0.25	0.33	0.56
10000	0.37	0.48	0.80
15000	0.45	0.59	0.96
20000	0.51	0.68	1.07
30000	0.62	0.83	1.23
50000	0.76	1.06	1.37

Table A-16 Estimated 20-years of total flexible pavement deformation as a function of truck traffic with fully saturated subgrade, Section 2 and 3

Traffic (trucks/day)	Pavement Deformation (in.)		
	A-4	A-6	A-7-6
100	0.03	0.04	0.06
200	0.04	0.06	0.08
500	0.07	0.09	0.15
1000	0.10	0.14	0.22
2000	0.16	0.20	0.34
5000	0.24	0.33	0.55
10000	0.36	0.47	0.78
15000	0.43	0.58	0.94
20000	0.50	0.67	1.06
30000	0.60	0.81	1.22
50000	0.74	1.03	1.35

Table A-17 Estimated 20-years of total flexible pavement deformation as a function of truck traffic with fully saturated subgrade, Section 4

Traffic (trucks/day)	Pavement Deformation (in.)		
	A-4	A-6	A-7-6
100	0.03	0.04	0.06
200	0.04	0.06	0.08
500	0.07	0.09	0.15
1000	0.10	0.14	0.22
2000	0.15	0.20	0.34
5000	0.24	0.32	0.55
10000	0.35	0.46	0.77
15000	0.42	0.57	0.93
20000	0.48	0.66	1.04
30000	0.58	0.80	1.20
50000	0.71	1.01	1.33

Table A-18 Estimated 20-years of total flexible pavement deformation as a function of truck traffic with fully saturated subgrade, Section 5

Traffic (trucks/day)	Pavement Deformation (in.)		
	A-4	A-6	A-7-6
100	0.03	0.04	0.06
200	0.04	0.05	0.08
500	0.06	0.09	0.14
1000	0.10	0.13	0.21
2000	0.14	0.18	0.33
5000	0.22	0.31	0.54
10000	0.33	0.44	0.75
15000	0.40	0.55	0.91
20000	0.46	0.63	1.02
30000	0.55	0.77	1.18
50000	0.68	0.98	1.31

Table A-19 Estimated 20-years of total flexible pavement deformation as a function of truck traffic with fully saturated subgrade, Section 6

Traffic (trucks/day)	Pavement Deformation (in.)		
	A-4	A-6	A-7-6
100	0.03	0.04	0.05
200	0.04	0.05	0.07
500	0.06	0.08	0.14
1000	0.09	0.12	0.21
2000	0.13	0.17	0.32
5000	0.21	0.30	0.52
10000	0.31	0.43	0.73
15000	0.38	0.53	0.89
20000	0.43	0.61	1.00
30000	0.52	0.74	1.15
50000	0.66	0.96	1.28

Table A-20 Estimated 20-years of total flexible pavement deformation as a function of truck traffic with partially saturated subgrade, Section 1

Traffic (trucks/day)	Pavement Deformation (in.)		
	A-4	A-6	A-7-6
100	0.05	0.06	0.07
200	0.07	0.07	0.10
500	0.09	0.10	0.15
1000	0.12	0.14	0.20
2000	0.15	0.19	0.28
5000	0.22	0.28	0.44
10000	0.30	0.38	0.58
15000	0.35	0.46	0.66
20000	0.40	0.52	0.72
30000	0.47	0.62	0.77
50000	0.58	0.77	0.82

Table A-21 Estimated 20-years of total flexible pavement deformation as a function of truck traffic with partially saturated subgrade, Section 2

Traffic (trucks/day)	Pavement Deformation (in.)		
	A-4	A-6	A-7-6
100	0.05	0.06	0.07
200	0.06	0.07	0.09
500	0.09	0.10	0.14
1000	0.11	0.14	0.20
2000	0.15	0.18	0.28
5000	0.22	0.27	0.43
10000	0.29	0.38	0.57
15000	0.35	0.45	0.65
20000	0.39	0.52	0.70
30000	0.46	0.61	0.76
50000	0.57	0.76	0.80

Table A-22 Estimated 20-years of total flexible pavement deformation as a function of truck traffic with partially saturated subgrade, Section 3

Traffic (trucks/day)	Pavement Deformation (in.)		
	A-4	A-6	A-7-6
100	0.05	0.06	0.07
200	0.06	0.07	0.09
500	0.09	0.10	0.14
1000	0.11	0.13	0.20
2000	0.14	0.18	0.28
5000	0.21	0.27	0.42
10000	0.28	0.37	0.56
15000	0.34	0.44	0.64
20000	0.38	0.50	0.70
30000	0.46	0.60	0.75
50000	0.56	0.74	0.79

Table A-23 Estimated 20-years of total flexible pavement deformation as a function of truck traffic with partially saturated subgrade, Section 4

Traffic (trucks/day)	Pavement Deformation (in.)		
	A-4	A-6	A-7-6
100	0.05	0.05	0.06
200	0.06	0.07	0.09
500	0.08	0.10	0.14
1000	0.11	0.13	0.19
2000	0.14	0.18	0.27
5000	0.21	0.26	0.41
10000	0.28	0.36	0.55
15000	0.33	0.43	0.63
20000	0.38	0.50	0.68
30000	0.44	0.59	0.74
50000	0.55	0.73	0.78

Table A-24 Estimated 20-years of total flexible pavement deformation as a function of truck traffic with partially saturated subgrade, Section 5

Traffic (trucks/day)	Pavement Deformation (in.)		
	A-4	A-6	A-7-6
100	0.05	0.05	0.06
200	0.06	0.07	0.09
500	0.08	0.10	0.14
1000	0.10	0.12	0.19
2000	0.14	0.17	0.26
5000	0.20	0.26	0.41
10000	0.27	0.35	0.54
15000	0.32	0.43	0.62
20000	0.37	0.49	0.67
30000	0.44	0.58	0.72
50000	0.54	0.72	0.76

Table A-25 Estimated 20-years of total flexible pavement deformation as a function of truck traffic with partially saturated subgrade, Section 6

Traffic (trucks/day)	Pavement Deformation (in.)		
	A-4	A-6	A-7-6
100	0.05	0.05	0.06
200	0.06	0.06	0.09
500	0.08	0.09	0.14
1000	0.10	0.12	0.19
2000	0.14	0.17	0.26
5000	0.20	0.25	0.40
10000	0.27	0.35	0.53
15000	0.32	0.42	0.61
20000	0.36	0.48	0.66
30000	0.43	0.57	0.71
50000	0.53	0.71	0.75

Table A-26 Estimated 20-years of total flexible pavement deformation as a function of truck traffic with partially saturated subgrade, Section 7

Traffic (trucks/day)	Pavement Deformation (in.)		
	A-4	A-6	A-7-6
100	0.05	0.05	0.06
200	0.06	0.06	0.08
500	0.08	0.09	0.13
1000	0.10	0.12	0.18
2000	0.13	0.16	0.26
5000	0.20	0.25	0.40
10000	0.26	0.34	0.52
15000	0.31	0.41	0.60
20000	0.36	0.47	0.65
30000	0.42	0.56	0.70
50000	0.52	0.70	0.74

Table A-27 Estimated 20-years of total flexible pavement deformation as a function of truck traffic with partially saturated subgrade, Section 8

Traffic (trucks/day)	Pavement Deformation (in.)		
	A-4	A-6	A-7-6
100	0.04	0.04	0.06
200	0.05	0.06	0.08
500	0.07	0.08	0.13
1000	0.10	0.12	0.18
2000	0.13	0.16	0.25
5000	0.19	0.24	0.38
10000	0.26	0.33	0.52
15000	0.30	0.40	0.59
20000	0.34	0.46	0.64
30000	0.41	0.55	0.69
50000	0.51	0.68	0.73

Table A-28 Estimated 20-years of total flexible pavement deformation as a function of truck traffic with partially saturated subgrade, Section 9

Traffic (trucks/day)	Pavement Deformation (in.)		
	A-4	A-6	A-7-6
100	0.04	0.04	0.05
200	0.05	0.05	0.08
500	0.07	0.08	0.12
1000	0.09	0.11	0.17
2000	0.12	0.15	0.24
5000	0.18	0.23	0.38
10000	0.25	0.32	0.50
15000	0.30	0.39	0.58
20000	0.34	0.45	0.63
30000	0.40	0.54	0.68
50000	0.50	0.67	0.72

APPENDIX B: FINAL RESULTS-GRAPHS

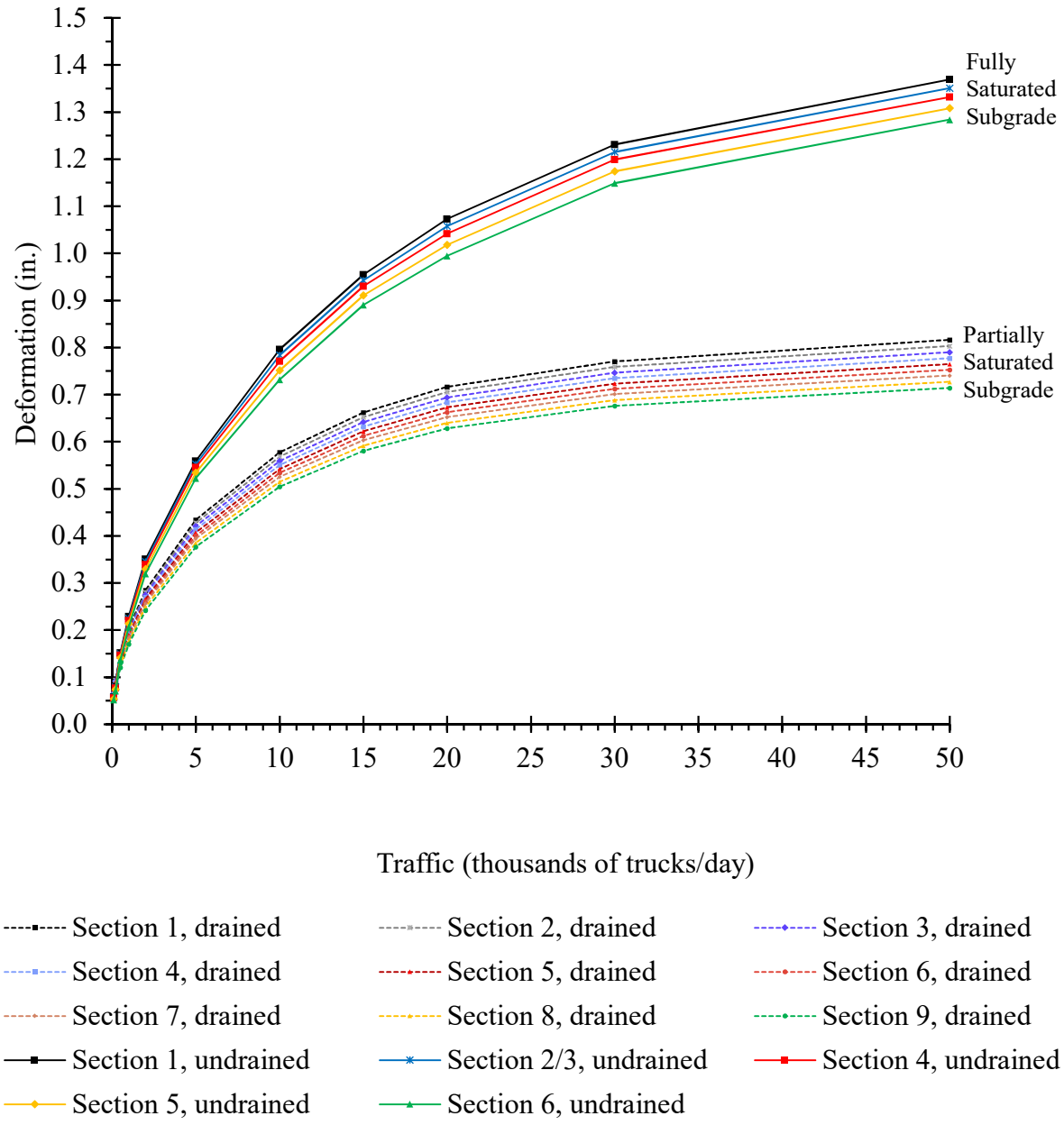

Figure B-1 Estimated 20-years of total pavement deformation as a function of truck traffic, A-7-6 subgrade

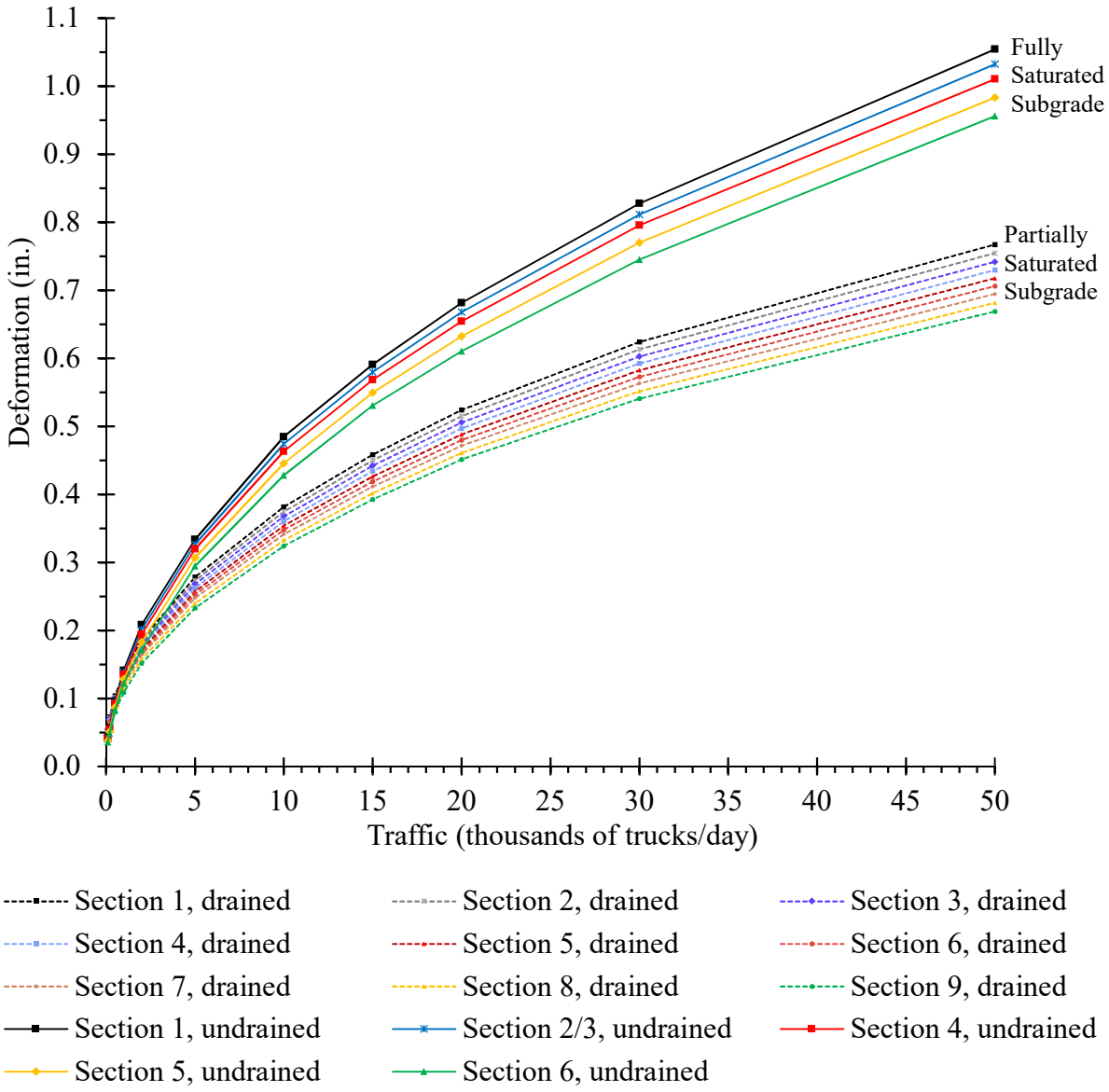

Figure B-2 Estimated 20-years of total pavement deformation as a function of truck traffic, A-6 subgrade

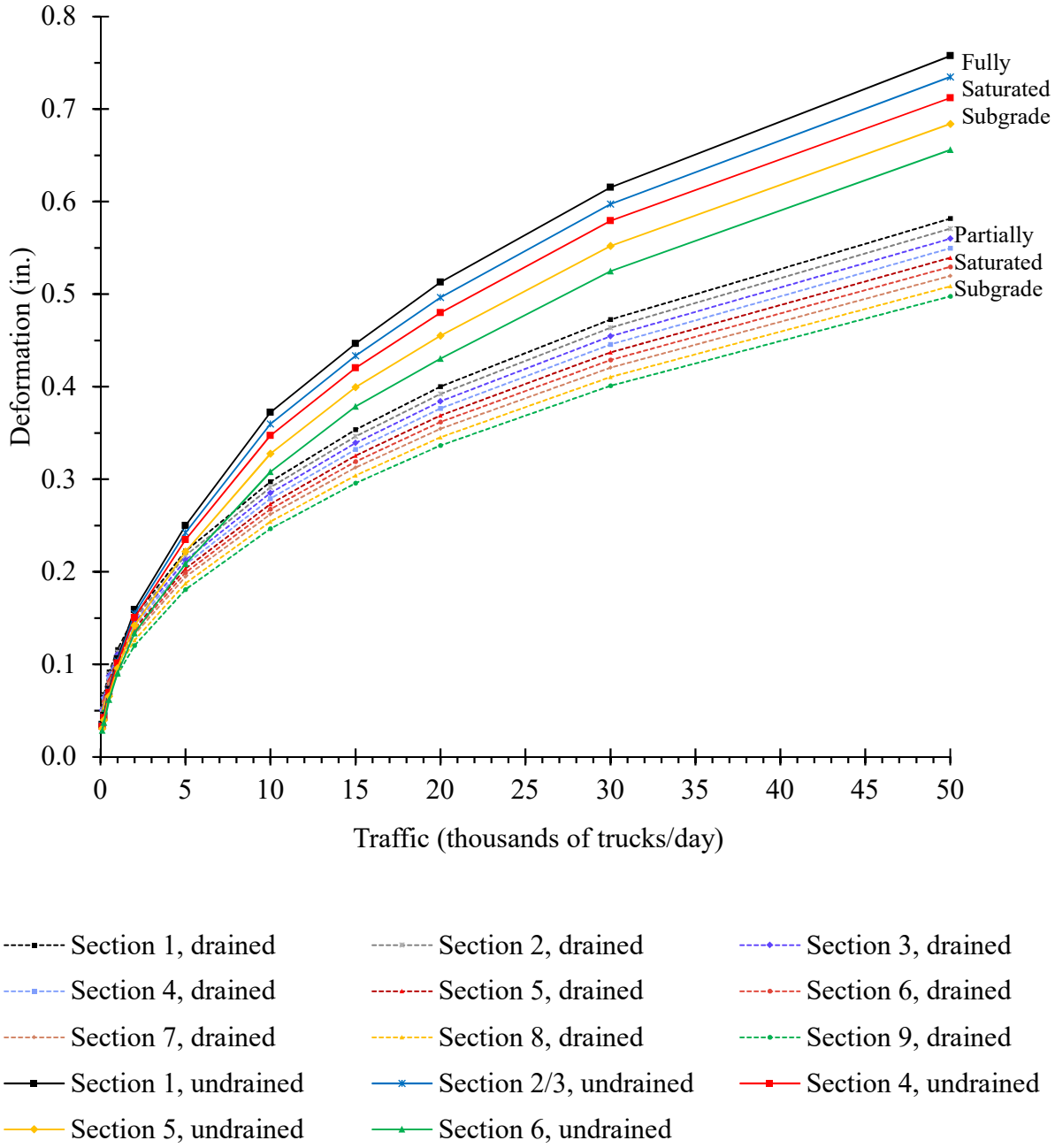

Figure B-3 Estimated 20-years of total pavement deformation as a function of truck traffic, A-4 subgrade

REFERENCES

AASHTO, G. (1993). *Guide for Design of Pavement Structures.* American Association of State Highway and Transportation Officials, Washington, DC.

ABAQUS. (2016). *Abaqus Analysis User's Manual.* USA: SIMULIA Inc.

Ahmed, Z., White, T. D., & Bourdeau, P. L. (1993). *Pavement Drainage and Pavement-Shoulder Joint Evaluation and Rehabilitation.* Joint Highway Research Project, Indiana Department of Transportation and Purdue University, West Lafayette, Indiana, FHWA/IN/JHRP-93/02-2.

Apul, D. S., Gardner, K., Eighmy, T., Benoit, J., & Brannaka, L. (2002). *A Review of water movement in the highway environment: Implications for recycled materials use.* Recycled Materials Resource Center, University of New Hampshire, Durham, New Hampshire.

Arika, C. N., Canelon, D. J., & Nieber, J. L. (2009). *Subsurface Drainage Manual for Pavements in Minnesota.* University of Minnesota, Minnesota Department of Transportation. MN/RC 2009-17.

Ariza, P. (2002). *Evaluation of water flow though pavement systems.* MSc dissertation, University of Florida.

ASTM, D. (1995). 5298-94. *Standard Test Method for Measurement of Soil Potential (Suction) Using Filter Paper*. 4, 154–159.

Bejarano, M., & Harvey, J. (2002). *Accelerated Pavement Testing of Drained and Undrained Pavements Under Wet Base Conditions.* Transportation Research Record, 1816(510), 137–147.

Brooks, R. H., & Corey, A. T. (1964). *Hydraulic properties of porous media and their relation to drainage design.* Transactions of the ASAE, 7(1), 26–28.

Cedergren, H. R. (1988). *Why all important pavements should be well drained.* Transportation Research Record, (1188), 56–62.

Cedergren, H. R., O'Brien, K. H., & Arman, J. A. (1972). *Guidelines for the design of subsurface drainage systems for highway structural sections.* No. FHWA-RD-72-30. United States.

Chandler, R. J., & Gutierrez, C. I. (1986). *Filter Paper Method of Suction Measurement.* Geotechnique, 36(2), 265–268.

Ching, R., & Fredlund, D. (1984). *A small Saskatchewan town copes with swelling clay problems.* 5th International Conference on Expansive Soils, Institution of Engineers, Australia, pp.1–7.

CTLGroup Inc. website at: http://www.ctlgroup.com/uploadedfiles/file_assets/pdfs/other/a10a2278-a248-46b1-a0cc-5ce4ec91199b.pdf

Daniel, D., Hamilton, J., & Olson, R. (1981). *Suitability of thermocouple psychrometers for studying moisture movement in unsaturated soils.* ASTM International, Vol. 746, pp. 84–100.

Vivar, E. & Haddock, J. E. (2006). *HMA Pavement Performance and Durability*. Joint Transportation Research Program, Indiana Department of Transportation and Purdue University, West Lafayette, Indiana, FHWA/IN/JTRP-2005/14.

Diefenderfer, B., Galal, K., & Mokarem, D. (2005). *Effect of subsurface drainage on the structural capacity of flexible pavement.* Virginia Transportation Research Council, No. VTRC 05-R35.

Feng, A., Hua, J., & White, T. D. (1999). *Flexible Pavement Drainage Monitoring, Performance, and Stability.* Publication FHWA/IN/JTRP-99/02. Joint Transportation Research Program, Indiana Department of Transportation and Purdue University, West Lafayette, Indiana.

Fetter, C. W. (2001). *Applied Hydrogeology (4 th)*, Upper Saddle River, NJ, Prentice Hall, 598.

FHWA, D. (1992). Drainable Pavement Systems, FHWA-SA-92-008. FHWA, United States Department of Transportation, Washington, DC.

Fleckenstein, L., & Allen, D. (1996). *Evaluation of pavement edge drains and their effect on pavement performance.* Transportation Research Record: Journal of the Transportation Research Board, (1519), 28–35.

Florida Department of Transportation (FDOT). (2014). Florida Method of Test for Measurement of Water Permeability of Compacted Asphalt Paving Mixtures. Fm 5-565. Florida Department of Transportation.

Fredlund, D. G., Xing, A., Fredlund Xing, A., D., & Fredlund Xing, A., D. (1994). *Equations for the soil-water characteristic curve*. Canadian Geotechnical Journal, 31(3), 521–532. https://doi.org/10.1139/t94-120

Geokon. (2017). *Instruction Manual Model 3500 Series Earth Pressure Cells.* www.geokon.com

Ghavami, M. S. M. (2014). *Evaluation of asphalt pavements construction practice in West Virginia*. West Virginia University.

Ghavami, M., Hosseini, M. S., Zavattieri, P. D., & Haddock, J. E. (2018). *Evaluation of Flexible Pavement Drainage,* No. 18-01537.

Ghavami, M., Hosseini, M. S., Zavattieri, P. D., & Haddock, J. E. (2019). *Flexible Pavement Drainage System Effectiveness,* Construction and Building Materials.

Hall, K. T., & Correa, C. E. (2003). *Effects of subsurface drainage on performance of asphalt and concrete pavements.* Transportation Research Board, NCHRP report 499.

Harrigan, E. (2002). *Performance of pavement subsurface drainage.* NCHRP Research Results Digest, (268), 15, http://trid.trb.org/view.aspx?id=729472

Hassan, H. F., & White, T. D. (1996). *Locating the Drainage Layer for Bituminous Pavements in Indiana*, FHWA/IN/JHRP-96/14, Joint Highway Research Project, Indiana Department of Transportation and Purdue University, West Lafayette, Indiana.

Helwany, S. (2007). *Applied Soil Mechanics: with ABAQUS Applications.* John Wiley & Sons.

Hua, J. (2000). *Finite element modeling and analysis of accelerated pavement testing devices and rutting phenomenon.* Ph.D Dissertation, Purdue University, West Lafayette, IN.

Huang, H. (1995). *Analysis of accelerated pavement tests and finite element modeling of rutting phenomenon.* Ph.D Dissertation, Purdue University, West Lafayette, IN.

Huang, Y. H. (1993). *Pavement analysis and design*. Pearson Education, Inc.

Indiana Department of Transportation. (2013). *Indiana Design Manual.* Indianapolis, IN 46204. http://www.in.gov/indot/design_manual/design_manual_2013.htm

Ji, R., & Nantung, T. (2015). *Quantification of Benefits of Subsurface Drainage on Pavement Performances in Indiana.* Transportation Research Board, TRB 94th Annual Meeting Compendium of Papers, Paper No. 15-3206.

Ji, R., Siddiki, N., Nantung, T., & Kim, D. (2014). *Evaluation of resilient modulus of subgrade and base materials in indiana and its implementation in MEPDG.* The Scientific World Journal, vol. 2014, Article ID 372838.

Ji, R. Y., Nantung, T., Qi, Q. (2013-1). *Numerical Modeling of Retrofit Underdrains on Pavement Rehabilitation and Reconstruction: A Case Study.* Transportation Research Board, TRB 92nd Annual Meeting Compendium of Papers, Paper No. 13-3704.

Ji, R. Y., Nantung, T., Qi, Q. (2013-2). *Numerical Modeling of Subsurface Drainage under Concrete Pavement.* Transportation Research Board, TRB 92nd Annual Meeting Compendium of Papers, Paper No. 13-3716.

Kanitpong, K., Benson, C., & Bahia, H. (2001). *Hydraulic Conductivity (Permeability) of Laboratory-Compacted Asphalt Mixtures.* Transportation Research Record: Journal of the Transportation Research Board, 1767(1767), 25–32.

Kim, H., Ganju, E., Tang, D., Prezzi, M., & Salgado, R. (2015). *Matric suction measurements of compacted subgrade soils.* Road Materials and Pavement Design, 16(2), 358–378.

Klute, A., & Klute, A. (1986). *Water Retention: Laboratory Methods. Methods of Soil Analysis: Part 1—Physical and Mineralogical Methods*. Agronomy Monograph, 9, 635–662.

Lam, L., Fredlund, D. G., & Barbour, S. L. (1987). *Transient seepage model for saturated–unsaturated soil systems: a geotechnical engineering approach.* Canadian Geotechnical Journal, 24(4), 565–580.

Liang, R. Y. (2007). *Evaluation of Drainable Bases Under Asphalt Pavements*. Department of Civil Engineering, University of Akron, Akron, Ohio, FHWA/OH-2007/10.

Liu, Y., & Muhunthan, B. (2016). *Cap Plasticity Model Parameters under Varying Moisture Contents.* In Transportation Research Board 95th Annual Meeting, pp. 16–4391.

Mallela, J., Larson, G., Wyatt, T., Hall, J., & Barker, W. (2002). U*ser's Guide for Drainage Requirements in Pavements–DRIP 2.0 Microcomputer Program.* Federal Highway Administration, United States Department of Transportation, Washington, DC.

McGennis, R. B., Anderson, R. M., Kennedy, T. W., & Solaimanian, M. (1995). *Background of Superpave Asphalt Mixture Design and Analysis.* FHWA-SA-95-003.

METER Group Inc. website at: https://www.metergroup.com/environment/products/ech2o-5tm-soil-moisture/

NCHRP. (2004). *Guide for Mechanistic-Empirical Design of New and Rehabilitated Pavement Structures.* NCHRP Project 1-37A.

Nokkaew, K., Tinjum, J. M., & Benson, C. H. (2012). *Hydraulic properties of recycled asphalt pavement and recycled concrete aggregate.* GeoCongress 2012, 1476–1485.

Onyango, M. A. (2009). *Verification of mechanistic prediction models for permanent deformation in asphalt mixes using accelerated pavement testing.* PhD dissertation, Kansas State University.

Pan, C. (1997). Analysis of bituminous mixtures stripping/rutting potential, PhD dissertation, Purdue University.

Pease, R. E., Stormont, J. C., Hines, J., & O'Dowd, D. (2010). *Hydraulic properties of asphalt concrete.* Geotechnical Testing Journal, 33(6), pp. 445-452.

Quintus, H. L. Von. (1994). *Performance Prediction Models In the Superpave Mix Design System.* Strategic Highway Research Program, National Research Council, Washington, DC, Vol. 699

Rabab'ah, S. R. (2007). *Integrated Assessment of Free Draining Base and Subbase Materials Under Flexible Pavement.* PhD dissertation, University of Akron.

RainWise Inc. website at: https://www.rainwise.com/

Seki, K. (2007). SWRC fit – *a nonlinear fitting program with a water retention curve for soils having unimodal and bimodal pore structure.* Hydrology and Earth System Sciences Discussions, 4(1), 407–437.

Sivasubramaniam, S. and Haddock, J.E. (2005). *Validation of Superpave mixture design and analysis procedures using the NCAT test track.* Joint Transportation Research Program, FHWA/IN/JTRP-2005/24.

Smith, T., Forsyth, R., & Gray, W. (1970). *Peformance Of An Asphalt-Treated Drainage Blanket In A Flexible Pavement Section.* Highway Research Record, No. 310, pp. 40-51.

Stormont, J., Henry, K., & Roberson, R. (2009). *Geocomposite capillary barrier drain for limiting moisture changes in pavemen*ts: Product application. Contract No. NCHRP-113, Washington, DC, Highway IDEA Project, 82.

Tam, V. W. Y., & Tam, C. M. (2006). *A review on the viable technology for construction waste recycling.* Resources, Conservation and Recycling, Vol. 47.

Tarefder, R. A., & Bateman, D. (2009). *Future design of perpetual pavements for New Mexico.* New Mexico Department of Transportation, Research Bureau, No. NM08MSC-01.

Tindall, J. A., Kunkel, J. R., and Anderson, D. E. (1999). *Unsaturated Zone Hydrology for Scientists and Engineers.* No. 04, GB1197, T5.

van Genuchten, M. T. (1980). *A Closed-form Equation for Predicting the Hydraulic Conductivity of Unsaturated Soils*. Soil Science Society of America Journal, 44(5), 892.

White, T. D., Haddock, J. E., Hand, A. J. T., & Fang, H. (2002). *Contributions of Pavement Structural Layers to Rutting of Hot Mix Asphalt Pavements.* Transportation Research Board, National Research Council, NCHRP Report 468.

Wyatt, T., & Macari, E. (2000). *Effectiveness Analysis of Subsurface Drainage Features Based on Design Adequacy.* Transportation Research Record: Journal of the Transportation Research Board, No. 1709, pp. 69–77.

Zaghloul, S., Ayed, A., Ahmed, Z., Henderson, B., Springer, J., & Vitillo, N. (2004). *Effect of Positive Drainage on Flexible Pavement Life Cycle Cost.* Transportation Research Record: Journal of the Transportation Research Board, 629(1868), pp. 135–141.